Global Journal of Science Frontier Research: D
Agriculture and Veterinary
Volume 15 Issue 5 Version 1.0 Year 2015
Type : Double Blind Peer Reviewed International Research Journal
Publisher: Global Journals Inc. (USA)
Online ISSN: 2249-4626 & Print ISSN: 0975-5896

The Isolation of, and Cytodifferentiation of a *Mucor* Species as Affected by Nitrogen Source and Elevated Temperature

By Omoifo C. O. & Nwajie N.
Ambrose Alli University, Nigeria

Abstract- Vegetative differentiation leading to dimorphic switching by filamentous microorganisms has drawn intense attention from scientists for a long time because of the central role played in the attempt to understand life processes, as well as the serious impacts exhibited in medicine, agriculture and industrial processes. A mucoraceous isolate, *Mucor manihotis* (tentative), from an agricultural niche was found to exhibit dimorphism in minimal medium; induced were thalloarthric-, holothallic-, holoblastic conidia as well as polar budding globose yeast cells when supplemented with ammonium sulphate or peptone as nitrogen source. Boxplot construction showed that peptone enhanced growth, but elevated temperature had profound morphogenetic effect as ovoidal and spindle shaped yeast cells additionally induced.

Keywords: mucor isolate, minimal medium, box plot, cytodifferentiation, cytoplasmic membrane, neoplastic units, binary protoplasts, yeast ontogeny, elevated temp, yeast form variability.

GJSFR-D Classification : FOR Code: 960413p, 670602

Strictly as per the compliance and regulations of :

The Isolation of, and Cytodifferentiation of a *Mucor* Species as Affected by Nitrogen Source and Elevated Temperature

Omoifo C. O. [α] & Nwajie N. [σ]

Abstract- Vegetative differentiation leading to dimorphic switching by filamentous microorganisms has drawn intense attention from scientists for a long time because of the central role played in the attempt to understand life processes, as well as the serious impacts exhibited in medicine, agriculture and industrial processes. A mucoraceous isolate, *Mucor manihotis* (tentative), from an agricultural niche was found to exhibit dimorphism in minimal medium; induced were thalloarthric-, holothallic-, holoblastic conidia as well as polar budding globose yeast cells when supplemented with ammonium sulphate or peptone as nitrogen source. Boxplot construction showed that peptone enhanced growth, but elevated temperature had profound morphogenetic effect as ovoidal and spindle shaped yeast cells additionally induced. The simultaneous induction of different cell wall structures necessitated further examination of the early growth stage. The process of differentiation that resulted in yeast ontogeny rooted in cytodifferentiation, involving vanishing cell wall of germ cells and then sequentially generated cryptic forms, only membrane bound, until reappearance of cell wall in nascent yeast, which at maturity became polar budding. Simultaneous induction of wall-less entities on the one hand, and complex walled entities on the other prompted a re-examination of cell wall geometry as hinge for dimorphic switching. It was suggested that more attention should be given to cytoplasmic membrane as default candidate.

Keywords: mucor isolate, minimal medium, box plot, cytodifferentiation, cytoplasmic membrane, neoplastic units, binary protoplasts, yeast ontogeny, elevated temp, yeast form variability.

I. Introduction

Except for the yeasts, which exist in unicellular form, fungi are filamentous microorganisms which grow by tubular progression and may not or, have cross walls. Tubular coenocytic forms are the more primitive types. They belong to the Phylum Zygomycota which habours 2 classes: Zygomycete and Trychomycete, both of which unlike the higher fungi lack defined fruiting structures (White *et al*, 2006). Zygomycetous fungi reproduce asexually by the production of sporangiospores, arthrospores and chlamydospores. Septation is not a feature of this group of fungi except when aged (Kendrick, 1973), or as response to injury or to cut off older portion of hyphae (Gooday, 1973). In like manner, unicellular existence is not their growth habit. However, in certain conditions some of the genera habour some species which reversibly convert to a unicellular form. Examples include *Mucor, Mycotypha* and *Benjaminiella*. Of these genera, *Mucor* habour more species known to convert to the unicellular phase in modified environments (Ghomade *et al.*, 2012). These include *M. rouxii, M. circinelloides, M. pusilus, M. genevensis, M. hiemalis* and *M. racemosus*.

The alternative form of these species is globose yeast which multiply asexually by multipolar budding. This is perhaps why it is referred to as yeast-like cells. For normal yeast cells like *Saccharomyces cerevisiae* (Class, Ascomycota), or *Rodoturola* (Class, Basidiomycota), exhibit polar budding. For yeast-like cells for example, *M. rouxii*, the globose mothercell, which is multinucleate (Bartnicki-Garcia and Lippman, 1977; McIntyre *et al*., 2002) is comparatively larger than the normal polar budding yeast cells, but produce multiple buds by blastic action. Dimorphic *M. circinelloides* also produces yeastlike cells (Lubbehusen *et al*, 2003, McIntyre *et al*, 2002). This microorganism has also been shown to exhibit polymorphic existence in modified environments, for beside the normal tubular and coenocytic growth habit, forms recorded in defined environment include holoblastic-, holothallic-, thallo-arthric conidia, septate filament/hyphae with vesicular catenate conidia, and terminal budding yeast cells. (Omoifo and Omamor, 2005; Omoifo *et al*., 2006; Omoifo, 2006ab).

There was a preponderance of induced terminal budding yeast cells of *M. circinelloides* when cultivated in strictly defined medium (Omoifo, 2006ab; Omoifo *et al*., 2006). Because of this recurrent observation, a model was developed for its conversion (Omoifo, 2009), an intermediary form, protoplast, formed the central element to the transformative process; this subsequently converted to the yeast form which became terminal budding (Omoifo, 2003). It was also shown that potassium ions was needed in the multiionic medium for the formation of the protoplasts (Omoifo, 2013). Several transient phases were involved in the conversion process that involved intermedial circulation of ions (Omoifo and Awalemhen, 2012).

Author α σ: Department of Crop Science, Ambrose alli University, Ekpoma, Edo State, Nigeria.

Our medium design in which terminal budding yeast cells were induced, was thought to be responsible for the induction from sporangiospores, as it supplies the abiotic regulatory factors that are perceived, and intracellularly transduced so as to permit the genetic and physiological machineries to regulate its dimorphic switching. It has been used for the conversion of 3 different filamentous microorganisms to terminal budding yeasts. Firstly, *Dimorphomyces pleomorphis* (now invalid) was found to transit to terminal budding yeast cells at 15°, 20° and 37°C when the nitrogen source was $(NH_4)_2SO_4$ while preformed nitrogen supply, peptone, induced terminal budding yeast cells primarily at 15° and 20°C but multipolar budding yeastlike cells at elevated temperature, 37°C (Omoifo, 1996). Secondly, *Rhizopus stolonifer*, which was found to be incapable of converting to yeastlike cells under CO_2 atmosphere (Bartnicki-Garcia and Nickerson, 1962) converted to terminal budding yeast cells in a study that underscored the significance of calcium ion as agonist for the conversion process (Omoifo, 2011). Thirdly, several studies have hilighted the possible role of uracil, myoinositol, K^+, Na^+ and H^+ in the transformation of *M. circinelloides*; it was suggested that they play key roles in signal transduction and electrophysiological status in the conversion process (Omoifo, 2006ab; 2013; Omoifo and Awalemhen, 2012).

In the experimental design combining several environmental factors, assessment of the magnitude of growth was attempted using quadratic polymonial model procedure but this was unsuccessful as data obtained were inconsistent with the assumptions made therein. Explanation was therefore anchored on transmembrane-pH-gradient (Omoifo, 1996). This lent some credence to the modifications observed therein and gave full complicity to the growth phases evolved and consequently made possible explanation on the sigmoid growth pattern exhibited (Omoifo, 2011).

The study with *M. circinelloides* gave insight into the transport mechanism between the bulk and intracellular media and hilighted the important role played by Na^+ in stimulating the yeast form induction from protoplast in the timely upshot into the exponential growth phase (Omoifo, 2012). This was further emphasized as absolute congruence exhibited between ionic circulation and the sigmoid growth pattern (Omoifo, 2014).

Our studies have shown that transformation of sporangiospores to terminal budding yeast cells involved complex phenotypic modification exhibiting several transient phases until the stable form, which thereafter proliferate by budding. The present study aims to show how this process is affected by complex and inorganic nitrogen sources on the one hand, and elevated temperature on the other. Absorbance has been used for quantitation since a mixture of morphologies were formed especially as all are distinct from the filamentous growth habit, or the typical unicellular growth form.

II. Materials and Methods

a) Fungal strain isolation

The fungal strain used in this study was isolated from a wasted cassava stump (*Manihot esculenta* L.) in an old farm where cassava tubers were uprooted about 6months earlier. Pieces from sections of the stump, which had turned white, or black, were taken with a sterile forceps and deposited into sterile universal bottles which were then transported to the laboratory. The stripes of root were deposited unto sterile wash glass and further cut with a sterile scalpel and subsequently transferred 3 each unto PDA Petri dishes at equidistant and triangular points. These were incubated on the laboratory side bench and monitored 24 hourly such that outgrowths from samples were promptly isolated and purified on PDA. Pure cultures were stored in McCartney bottle PDA slants.

b) Microscopic examination and Fungal Identification

Slides were prepared from cultures of pure isolates and stained with lactophenol in cotton blue and viewed with AmScope Binocular microscope attached with 1.3MP USB camera. Specific morphological features of the pure isolate were captured. These were used for identification of the fungus based on description in literature including CAB (1971), Ellis (1976), Von Arx (1970) and Samson *et al*., (2000).

c) Inoculum preparation for growth studies

A bent sterile glass rod was used to rob the surface of the PDA culture so as to dislodge the spores into distil deionized water so as to make a suspension in the Petri dish. This was poured into sterile centrifuge tubes and washed at 5000rpm for 7min. After decanting the supernatant, the spores were further washed with 2 changes of sterile deionied distil water. Spore count of the isolate was taken with Neubauer Haemocytomer (BSS No 784 Hawsley, London, Vol. 1/4000) and was adjusted to $1x10^6$ spores per ml with sterile deionized distil water.

d) Reagents and culture media

The synthetic medium of Omoifo (1996) incorporated with uracil (Omoifo, 1997; 2006), myoinositol (Omoifo, 2006a, Omoifo *et al*., 2006), zinc (Omoifo and Omamor, 2005) and calcium chloride (Omoifo, 2011) was used. Briefly, it contained per litre 10g glucose (Fisher Scientiic Coy New Jersey), 5g K_2PO_4 (BDH, England), 5g KH_2PO_4 (Aldrich Chemical), 0.10g $FeSO_4$ (J.T. Phillipsburs), 0.20g $MgSO_4$ (BDH,England), 0.10g NaCl (Kermel), 0.075 $CaCl_2$ (BDH, England), 0.065g $MnCl_2$ (Reidd-DeHaen Ag, Hannover), 0.06g $CuSO_4$ (BDH, England), 0.06g $ZnSO_4$ (BDH, England), 0.10g uracil (Fluka AG Switzerland),

0.250g myoinositol (Sigma), 1.83g Na_2HPO_4 (BDH, England), and 1.07g citrate (Sigma, USA). The nitrogen source was either 5g $(NH_4)_2SO_4$ (BDH) or 5g peptone (Biotech). Medium was prepared in 2000ml beaker and pH adjusted to 5.0 with 2N NaOH or 2N HCl using a hand held pH meter with glass electrode. Duplicate experiment was set up for each test. Each experiment contained 100ml broth in a 250ml conical flask. A 15μl of test isolate was inoculated into prelabelled flask using a micropipette in a sterile hood. After inoculation each broth flask was shaken for 30s and thereafter incubated at the set temperature regimes, viz: 15°, 28° and 37°C. At 24h intervals the broth flasks were brought to the sterile hood and 10ml withdrawn from each one with sterile pipettes one for each flask into factory sterilized universal plastic sample tubes. The broth flasks were thereafter returned to the set incubation regimes. The samples were kept at -18°C until analysis.

e) Biomass determination

Culture samples were thawed up to room temperature before biomass determination. The absorbance was obtained at 600 nm, using a Camspec M105 spectrophotometer Cambridge, UK).

f) Experimental design and analysis

Factors including nitrogen-source, temperature and time effect were incorporated into this design (Fig. 1). Thus absorbance values were subjected to exploratory box plot and to a 3-way analysis of variance to test for significance of factors and comparison between means made at $p < 0.05$ using GenStat Release 8.1 package. Time-course plots were made on Excel format.

III. Results

a) Preliminary morphological description

Fig.2a showed the specific cassava stump from which the initial isolation was made. Root-stalks of harvested cassava tubers, as well as underneath dry and cracked skin of the lower stem of the cassava stem turned black with white patches. Colonial growth of isolate: substrate level mycelium hyaline to white & irregularly circular, with conspicuous strands up to diam. 30mm in 24h with effuse and orange coloured aerial mycelium which lag 3-8mm behind the margin (Fig. 2b). At 72h substrate-level mycelium reach 90mm while 3-5mm of margin compact forming whitish mycelium (Fig. 2c). As from 120h after inoculation, aerial mycelium initially with distinct sporophores on forming compact mycelium reach the roof of the dish; the central diameter turn purplish on the A-side of the dish (Fig. 2d) while the B-side is reddish as blue strands/patches scatter all over the surface (Fig. 2e). The central core become purple with age and the whole mycelium gradually turn black (Fig. 2f). After 3days globose heads reveal as smooth walled sporangia borne on long sporangiophores (Fig.3a) apically septate thus cutting off the double walled sporangium in which spores are directly observed (Fig.3b&c). Spores may be short or long ellipsoidal, cylindrical, sausage roll or crescent shaped, which may also be multicelled (Fig. 3d-h). Apical columellum is globose (Fig. 4a) as sporophores arise from septate substrate level mycelia; the double walled septa irregularly delimit cytoplasm, which may be fragmented or become granular (Fig. 4b-d). Polarized germ cells may give rise to holothallic growth which may subsequently fragment, thus giving rise to arthrospores (Fig.4e).

Fig. 5a showed that sporophores terminating in globose columellum may also be curvy. These originate from septate mycelia that give rise to multiple germ tubes which anchor into the substratum with coenocytic apparent rootlets and subsequently ramify the medium (Fig. 5b,c). Cytoplasmic cleavages could occur in the cellular compartments thus giving rise to glistening bodies; these could be individually released (Fig. 5d,e). Release of such cytoplasmic contents as protoplasts become frequent as the culture aged (Fig.5f,g-h), so also is the formation of arthrospores (Fig.5i) and chlamydospores (Fig. 6). After 9days of growth, the double walled hyphal cells, septa and thick-walled chlamydospore become melanized (Fig. 6a-f).

b) Effect of N-source on Growth

Growth occurred in both inorganic and complex nitrogen sources. Total growth in the N-sources were shown in table 1, which also showed the morphological forms exhibited. These included discrete units and or determinate entities of various shapes and forms. Because of these varied forms, we sought to find out if the population had normal distribution. Parallel boxplots for absorbance values in Amm. sulphate and Peptone broths were shown in Fig. 7a. The Peptone broth median is above the 75th percentile of observations in the Amm. sulphate broth. Furthermore, the boxes which were positively skewed were not associated with outscores. These indicated that the populations which were distinct were normally distributed. On the graphic representation of cummulative estimator at the different temperature levels, performance was enhanced at 28°C but was least at 15oC (Fig. 7b).

When such plots were obtained for each nitrogen source at the different temperature regimes, the pattern display showed differences among the populations. The degree of dispersion among the Amm. sulphate populations at the different temp regimes were quite distinct (Fig. 8). It was optimal at 28°C where growth was symmetrical, an indication of an even dispersion in a normal population and also the first quartile was even more than the median in the 37°C regime, which in turn had its first quartile above the 15°C interquartile range. In contrast to the higher temp. regimes which were positively skewed with no outliers,

the minimal observations at 15°C was negatively skewed and had an outlier at the upper extreme. This indicated that quantitative data in Amm. sulphate broth at this temp level was very low and also had very little dispersion, in contrast to that at higher temp regimes.

Fig 8 also showed group constructs in Peptone broth over the temp. regimes. The range at 15°C showed the least growth estimate. But this was greatly enhanced at 28°C being above the maximum in the aforementioned regime, and was also above the extreme value at 37°C. Thus the group display suggested significant differences in the estimator at the different temp. regimes. The boxes for the Peptone broth were positively skewed, having longer whiskers except for that at the elevated temp. where the negative skew had longer lower whisker, thus increasing the variability downward as most observations were concentrated on the high end; this was reflected in the larger interquartile range, and possibly suggested an interaction between medium type and elevated temperature on the growth estimator.

Now on comparing the Amm. sulphate- and Peptone broth graphics at each temp. regime, median for the former is absolutely lower than that in the Peptone broth. Similar comparison showed that the 2 interquartile ranges do not overlap along the vertical axis. Since half the observations in a distribution are between the upper and lower quartiles, that is, between the 25th and 75th percentiles, we see that half of the observation in Peptone broth is above the 75th percentile of the Amm. sulphate broth at any of the temp. regimes. These distinct characteristics suggested that the two population means (Amm. sulphate- and Peptone broth) differed beyond just random variation. We resorted to the analysis of variance procedure to validate or otherwise, this contention.

A 3-way analysis of variance showed that the impact of the individual factors on growth, including N-source, temp. and time, as well as the combined interactive elements, was significant p0.001 (Supplementary Table 1). Perhaps we should look at the behavioral trend of the microorganism in the cultures which may yield to understanding the specific effects of the factors.

c) Growth profiles

The deterministic nature of the observations evidence the fact that the study was parametrically based. Thus in a time-series manner, it was thought that trends could be established so as to lend data to further evaluation from which physiological relationship could be deduced. Growth profiles in the Amm. sulphate and Peptone broths were therefore obtained. These were shown in Figure 9.

Profiling growth of the microorganism at 15°C in Amm. sulphate medium did not give a sigmoid pattern. The hardly perceptible increase fell after 72h. But marginal increase occurred as from 96h till termination of experiment. This low profile exhibition seem to agree with the weakly presentation of the descriptive graphic earlier observed. Although not also sigmoid, a bell-view profile occurred between 24 and 72h in the Peptone broth, whereafter rapid growth ensued till termination of experiments.

Growth at the 28°C regime purviewed a logarythmic phase without inherent lag or log phase in Amm. sulphate broth. However, in Peptone broth an enhanced rise yielded to a more or less steady growth after 48h; but growth surged after 96h.

Profiling growth at 37°C was oustanding. In either media, a sudden rise in growth occurred but this leveled off after 48h. A resurgence occurred as from 72h and thereafter approached a stationary phase in Peptone broth. On the other hand, a truncated log phase was portrayed in Amm. sulphate broth.

Growth pattern in Peptone broth at all temp levels seem remarkable as a rise in growth up till 48h appeared to break off and a resurgence commenced after 72h. Interestingly, profile exhibition in Amm. sulphate broth at 37°C assumed similar pattern. These were not revealed in the graphic display of the boxplots. Perhaps, microscopic examination may be more revealing.

d) Ammonium sulphate-incorporated minimal medium

Growth occurred in all the broths incorporated with ammonium sulphate and at all temp levels tested. However, morphological expression varied.

e) Temperature 15°C effect on morphology

Commencement inoculum was sporangiospores which were of various shapes and sizes: globose, crescent, cylindrical or sausage roll-like, and ellipsoidal. These differentiated to spherical to germ cells and some had protruding germ tubes by 24h (Fig. 10a); further growth could occur with single or double germ tubes which could be oppositely borne on a single germ sphere and extended on each axis (Fig. 10b). These were however scanty. The predominant morphology was greenish spherical units which appeared to arise from cytoplasmic contents of growth spheres (Fig. 10c). Beside these were innumerable granular units. By the 2nd day clumps of, and dispersing granular units were copiously produced (Fig. 11a) and the hue of greenish spherical units became intensified (Fig. 11b). Similar observations were made after 72h of growth. But the sizes of the spherical units subsequently increased (Fig 12). Gradation in sizes was apparent: from granular units to ultimate spherical units. By day 4, clumps, which appeared to arise from implosion of the cytoplasmic contents were observed (Fig. 13a). These subsequently gave rise to structures, some of which could be short rods or cylindrical (Fig. 13b). Fig. 13c showed numerous formless units which could arise from this implosion. The emerging rods

could be binary (Fig. 13d). The most outstanding morphology here was unicellular globose yeasts, which subsequently acquired budding capabilities (Fig. 13e). The daughter bud could adhere to the mother cell through a short sterigmata (Fig. 13f). By the 5th day, the spherical units were still numerous (Fig. 14a), but globose unicellular yeasts were predominant (Fig. 14b). These coexisted with enterothallic conidia (Fig. 14c) and numerous rod shaped single or binary structures that were protoplast-like.

f) Temperature 28°C effect on morphology

This intermediate temp. level elicited septate filamentous growth and holoblastic conidia in broth after 24h (Fig. 15). By 48h, numerous other morphologies were observed. These included beside the aforementioned types, thallic growth, neoplastic units, and protoplasts-possibles (Fig. 16a-f). These were very numerous at 72h after inoculation (Fig 17ab) and became the predominant morphology 96h after inoculation (Fig. 18a); they were coinduced with yeast cells (Fig. 18b). When walls of holoblastic conida ruptured (Fig. 19), and this was frequent , cytoplasmic contents were release either as granular or neoplastic units (Fig. 19). These were also co-induced with yeast cells.

g) Temperature 37°C effect on morphology

At 24h of growth clusters of differentiating neoplastic units (Fig. 20ai) were conspicuous. Some appeared to increase in size *in situ* (Fig. 20aii). The ultimate neoplastic units co-induced with yeast cells, which were polar budding (Fig. 20cd). Although not the most predominant, holoblastic conidia co-induced with varying sizes (Fig. 21a-c). These coexisted with globose and spindle shaped yeast cells (Fig. 21b,d) at 48h of growth. Spindle shaped and globose yeast cells became the most predominant morphologies at 72h after inoculation. This was shown in figure 22a. Even though holoblastic conidia were observed and appeared to dininsh in size and number, their cytoplasm appeared to differentiate *in situ* (Fig. 22bc) and also coexisted with the predominant globose and spindle shaped yeasts (Fig. 22d). Observation of the aforementioned morphologies continued after 96h from inoculation (Fig. 23a-f) with globose cells dominating (Fig. 23e). Although scantily, when thallic growth occurred and, or fragmented into arthrospores, cytoplasmic contents receded from cellular walls, thereafter differentiating (Fig. 23f) and on cell wall bursting, the cellular contents released as neoplastic units. At 120h after growth, at this elevated temp. regime all the aforementioned morphologies occurred. So also were ovoidal yeast cells encountered (Fig. 24a-f).

h) Peptone-incorporated minimal medium

Growth appeared more enhanced with the complex nitrogen source.

i) Temperature 15°C effect on morphology

After 24h of growth nondescript entities dispersed from the apparently imploded cytoplasm (Fig. 25a). This possibly gave rise to the clusters of protoplasts (Fig. 25b). Prevegetative cells or nascent yeasts were very conspicuous (Fig. 25c). These subsequently became polar budding (Fig. 25d). At 48h after cultivation, the ultimate neoplastic units were very numerous (Fig. 26) and coinduced with the other cryptic forms. When thallic growth co-induced with yeast cells, cytoplasmic contents could be released on rupture of cell wall (Fig. 27a), which assumed the characteristic features of true fungal wall (Fig. 27b). But the most predominant morphology at 72h after inoculation was globose unicellular cells (Fig. 27c). Numerous protoplasts could be seen transiting to nascent yeasts(Fig. 28a) and these abscised but subsequently became terminal budding (Fig. 28b). At 120h after growth, the protoplasts were robust (Fig. 29a). They coexisted with other thallic structures in which the cytoplasmic content also differentiated (Fig. 29bd). Fig. 29e exhibits form as binary protoplasts initiated nascent yeasts, which on disarticulation became prevegetative cell and these at maturity became globose unicellular yeast cells. These thereafter became polar budding (Fig. 29f).

j) Temperature 28°C effect on morphology

Various forms of thallic structures were induced at 24h after growth. These included holoblastic-, and thallloathric conidia (Fig. 30). Numerous neoplastic units and single rod and binary protoplasts co-induced and predominated the broth after 48h of growth (Fig. 31). By 72h, cytoplasm of all germ cells, holoblastic conidia and thalloarthric conidia were conspicuously granular and this on release converted to ultimate neoplastic units (Fig. 32). Protoplasts were also numerous (Fig. 32f) and could be observed even within the cellular compartments. Figure 33 showed that the growth cell cytoplasmic content (a) underwent apparent cytoplasmic differentiation (b) and subsequently lost the cell envelop, thus leaving only the neoplasm (c). This was subjected to apparent implosion (Fig. 33de) and thereafter dispersed as each nondescript entity increased in size (Fig. 33f). Cytoplasmic contents of thalloarthrospores (Fig. 33g), holothallic conidia (Fig. 33h) and fragmented spore (Fig. 33i) underwent similar processes of granulation, implosion, and on release of the individual units after cell wall rupture, nondescriptness and subsequent form development. Thus neoplastic units, protoplasts and yeast cells were abundant (Fig. 33jk). All the aforementioned forms were observed after 120h of growth, but neoplastic units, protoplasts and yeast cells predominated the medium. Fig. 34a showed units clinging to walls of thallic structures, extruded units from conidia (Fig. 34b) and numerous protoplasts (Fig.34c).

k) Temperature 37°C effect on morphology

The morphology after 24h was predominantly yeast form. There were two types of yeasts- globose and spindle shaped (Fig. 35ab). These were of various sizes. Holoblastic-, holothallic- and thalloarthric conidia on the one hand, and transitory phases including neoplastic units and protoplasts on the other hand, as well as yeast forms-globose and spindle shaped- were observed as from 48h of growth (Fig. 36a-f). The observations and variability of forms at 72h after inoculation were not different from that at 48h, but conidia and the yeast cells appeared more robust (Fig. 37a-d). Co-induction of the various forms occurred at 96h. Thallic growth bearing blastospores were observed. True fungal filaments with double walled septa also debuted (Fig. 38b), although these were scanty and in each case, not very extensive. Similar representation occurred 120h after growth (Fig.39a), and further highlighted the variability of forms co-induced at this level. The yeast types occurred in a variety of sizes. Figure 39c showed a well matured spindle shaped yeast cell.

l) Primordial growth phase of Mucor manihotis in minimal medium

Preponderance of neoplastic units at the different temp. levels was outstanding and it was co-induced with the various morphological forms, including globose yeast cells, spindle shaped yeast cells, holoblastic conidia, holothallic conidia, thalloarthrospores. In some instance, neoplastic units appear to pinch off plastic neoplasm (Fig. 40a), or emerge from effused arthrosporal content (Fig. 40b) or after conidial rupture (Fig. 40c). In fig. 40de, the units foreground thalloarthrospores and holoblastic conidia (both out of focus), while Fig. 40f portrayed high numericity in ultimate neoplastic units. The difference in occurrence- from fluid neoplasm (Fig. 41a) or possible size increases of cytoplasmic granular units (Fig. 41b), prompted its re-examination at the primordial phase.

Fig. 42 showed cryptic forms sequential to globose yeast formation after 3h of growth in Amm. sulphate incorporated medium at 28°C. The growth of spore is accompanied with volume changes as it assumed spherical growth with the subsequent appearance of double wall of germ sphere. This yielded the spheroplast as cell wall is lysed. The cytoplasmic membrane subsequently disappear, leaving the intact cytoplasm and thereafter neoplasm which further differentiates, thus appearing as granular units. Therefrom, nondescript entities formed. As these nondescript provencal entities enlarged, individual units eventually asssumed shape, hence emerging as neoplastic units which ultimately appeared spherical. From the ultimate neoplastic units emerged single rod shaped protoplasts and subsequent binary protoplasts. These eventually gave rise to globose yeasts, which appeared in singles or doubles.

Microscopic examination after 6h of growth in Amm. sulphate incorporated medium appear to reveal more details in the formation of neoplastic units. This was shown in fig. 43. After the sphaeroplast formation, several stages were seen in the implosion of neoplasm until individualization of the initially apparently consistent neoplasm. These differrentiated, as granular component, asssumed individual life form *in situ* as provencal entities; therefrom becoming incipient neoplastic units. As they spread out through inherent conventional current, we could see primordial neoplasts changing into midmost neoplastic units. These subsequently assumed spherical shape as the ultimate neoplastic units.

Observation of broth after 9h of cultivation perhaps accord more recognition to the differentiating neoplasm, which yielded more cryptic incipient neoplastic units and the midmost neoplastic units as these became a little more conspicuous, until the ultimate neoplastic units were formed; the latter were spherical in shape. This was shown in fig. 44.

In the exposure of spores to organic nitrogen source, peptone, the process appeared to have been abridged as binary protoplast upshot from provencal entities occurred as early as 3h after growth; the steps: spheroplast-, neoplasm- and neoplastic units formation appeared subsumed. This was shown in fig. 45. Although the count was not obtained, visual observation indicated that protoplast population was higher in the Peptone broth in comparison with Amm. sulphate. However, ultimate neoplastic units were also observed in the Peptone incorporated broth. This was shown in Fig. 45.

Observation at 6h after cultivation in Peptone broth showed the evolving neoplasm undergoing several topological changes: from plastic form it became furrowed and, thereafter fragmentized into provencal entities. When the plastic neoplasm became amorphous, incipient or upshots of neoplastic units could be observed. Thus, midmost neoplastic units and ultimate neoplastic units were abundant. In contrast to cultivation in Amm. sulphate broth, the midmost neoplastic units were more robust and assumed varying shapes, some of which appeared flagellated. This was shown in fig. 46.

Subjective assessment showed that generation of neoplastic units or their upshot from imploded or fragmented neoplasm in Peptone incorporated broth was higher in number as compared to Amm. sulphate incorporated broth. Clusters of primal neoplastic units, midmost neoplastic units and ultimate neoplastic units were also more numerous in Peptone broth at 9h after cultivation (Fig. 47) in contrast to earlier sequential observation. Perhaps, this was as a result of time effect.

In fig.48, we see that protoplasts also emerged from neoplastic units at 37°C in Amm. sulphate broth. This confirmed the fact that at whatever temp level used in this study, and whether inorganic or organic nitrogen source, the same process of differentiation occurred. That protoplast upshot from provencal entities, as shown in fig. 45, possibly meant that the rate of emergence of a particular form could be enhanced, hence a faster growth rate, a fact that could be extrapolated to the other growth entities. The unique effect of this is that the rate of achieving the optimum morphology of a unit is faster in the peptone medium. This could be reflected in the physiology, size, volume and form of the individual units. Fig. 49 illustrated the contrasting robustness of protoplasts induced in media incorporated in Amm. sulphate and Peptone.

It is pertinent to point out that the final morphological form induced in either medium is the same, embellished detail notwithstanding. Fig. 50 showed the topology of a spindle shaped yeast cell. Each javelin-like cell has an expanded central region, which may have several markings, and narrows down the apices. Although pointed at both ends, one apex appeared truncated. The markings may be restricted to one side of the approximately equally divided elongate yeast cell (Fig. 51).

m) Reversion to filamentous growth habit

At termination of experiments culture flasks were shifted to the laboratory side bench, temp. 28°C. Observation showed that mycelia matt formed on broth surface of the shifted cultures. This was shown in fig. 52. This indicated that the induced conidia and yeast cells, being the most predominant, as well as the transient forms including neoplasm, neoplastic units and protoplasts- were re-converted to the original growth habit, which is filamentous. Microscopic examination of such re-growth showed multipore sporangia, multitype sporangiospores, hyphal septation, thalloarthrospore formation, chlamydospore formation, and melanization of hyphal structures. This was shown in Figure 53.

IV. Discussion

That the fast growing isolate, at first whitish, then orange upright effussion of aerial mycelium, reproduce asexually by having large multispored globose sporangium enclosing distinct spheroidal columella borne at the apex of elongate sporangiophore, consign it to the Genus, *Mucor* (Family: Mucoraceae). Here, the smooth double walled sporangium enclosing multi-type aplanospores: globose, ellipsoidal, cylindrical, elongate, sausage roll-like and crescent shaped, which may have more than one cell against the spheroidal columellum with singular cross wall between its base and the coenocytic sporangiophore indicate an advanced species of the primitive Mucoraceae (Alexopoulos and Mims, 1979). This view is supported by the fact that its somatic structure approximates the characteristics of the higher fungi: multiple branching mycelium, the hyphae possessing more or less regular septa. This argument is re-inforced by the presence of thalloarthrospores and chlamydospores, characteristics of the hyphomycetes. In addition, hyphal and septal walls, are characteristically melanized with age. This is in sharp contrast to *M. rouxii* which produces multipolar budding yeastlike cells (in modified environments), coenocytic hyphal structures, but septum, whenever it occurs and sporangiophores that do not contain melanin pigments, except sporangiospores, i.e. 10.35% of spore dry weight (Bartnickii-Garcia, 1968). Although *Mucor* species exist which show cross walls right from commencement of growth (Hesseltine and Ellis, 1973), the presence of multiple type sporangiospores and melanized somal structures, make this a distinct *Mucor* strain. Baring a full taxonomic evaluation, including phylogenetic analysis, this isolate may tentatively be referred to as *Mucor manihotis*, taking into consideration the niche of first isolation (Davenport, 1980) and strictly for the purpose of this report.

The initial stages of growth of *M. manihotis* corresponded to stages 1 and 11 shown in the growth of *M. rouxii* (Bartnicki-Garcia and Lippman, 1977; Bartnicki-Garcia *et al*., 1968). Contrastingly, the primary thallic growth pattern gave rise to septate filaments of four different types, including holoblastic-, holothallic-, thalloarthric- and endoarthric conidia. However, none was extensive nor ramified the medium, but remained as discrete units. Hence it was possible to obtain optical density readings used for boxplot construction or pattern determination.

In thallic endoarthrospores/enterothallic conidia, cell wall appeared be formed within the existing hypha without disruption of existing hypal cell wall during septum formation (Fig. 27ab). This makes it similar to other zygomycete like *M. rouxii* (Barrera, 1983). On the other hand, it could be compared with the hyphomycete *Oidiodendron griseum* which exhibits determinate thallic growth followed by a backward production of spherical or subspherical arthrospores (Fig. 30d, 33g), or truncate arthrospores (Fig. 31, 39a) as found in *O. truncatum* (CAB, 1971; Ellis, 1973). On the other hand, it could be compared with *Geotrichum candidum* as filaments gave rise to oblong-rectangular or subglobose arthrospores (Fig. 30b). Of the holoblastic type, conidia were produced directly and successively from the growth initial by blastic action (Fig. 21ab, 22bc, 23a-d). Here, both the secondary wall and part of the thick primary (outer) wall entirely enclosed the spore, which in turn enclosed the cytoplasmic membrane; thus septum formation was between the outer walls of two conidia borne in succession (Carmichael, 1971; Kendricks, 1971). In the holothallic type, germ initial produced a germ tube; this converts to the short conidiophore as

successive disarticulatable conidia were produced therefrom (Fig. 33hi).

Since dimorphism involves phenotypic switching from one growth habit to another in a culturally controlled situation, we see a change from the environmental mold morphotype to discrete units production in our minimal medium as exhibiting this phenomenon. Herein, conidiogenesis involved both persistent and nonpersistent conidia production. Persistent conidiogenesis include the various thallic forms (enterothallic-, holothallic-and holoblastic conidia) whereas nonpersistents involved the successive budding and transient discret units. These signify a change in shape from the natural tubular substratal growth and production of fertile aerial sporophores.

In an attempt to ellucidate the mechanism regulating hyphal tip growth, and hence responsible for dimorphic switching, Bartnicki-Garcia and colleagues (Bartnicki-Garcia *et al*., 1968, 1989) developed the concept of the vesicle supply center (VSC), where cell wall precursors and important enzymes are deposited in the subapical region, that is, at the ring of the cytoplasmic membrane immediately below the apex prior to exchange with the outside of membrane through exocytosis, (Dieguez-Uribeondo, 2003; Ghomade *et al*., 2012). Several workers have deduced that since it involved cell wall metabolism, apical growth, involving the change in integrity and or cell geometry could be attributed to the cell wall polymer deposition pattern (Bartnicki-Garcia, 1987; Orlowskii,1991; Chitnis and Desphade, 2002), wherein the enzymes chitin synthase and chitinase are involved in specific cell wall construction (Bartnicki-Garcia, 1973, 1987). Three such patterns have been suggested for fungi undergoing dimorphic switching: polarized hyphal tip growth for elongation; nonpolarized regulated growth for the yeast form which may appear globose or ellipsoidal, and deregulated polarized deposition pattern for the irregular configuration (Diophode *et al*., 2009).

If we consider the different types of discrete entities in our minimal medium, then the pattern distribution theory calls for further consideration. It is difficult to see how one cell polymer diposition pattern would induce the numerous shapes of this microorganism that occurred simultaneously. Now, take the determinate thallic growth where there is polarized growth, like the strictly prolongation on hyphal axis of *M. rouxii* (Bartnicki-Garcia and Lippman, 1969) resulting in coenocytic tubular filament. In *M. manihotis,* at the end of such growth, a retrogressive conidiogenesis occurs as backward centripetal growth of cytoplasmic membrane is followed by septum formation. What triggers an end to the forwardly directed chitosome - mediated cell wall biogenesis (Bartnicki-Garcia, 1981) and, then directly apposite resort to regressive internal spore formation in this type of conidiation, is not yet clear. As for the holoblastic conidia, is it a case of non-polarized deposition of cell wall materials followed by deregulated polarized deposition, then a repeat of non-polarized deposition with a continued reversion and continuation? This conidial type is a form in which the cytoplasm is encapsulated in its spore wall and this in turn is integumented by the thallic wall such that septum formation is by the inner thallic walls of adjacent conidia. How then is this structure regulated in contradistinction to thalloendoarthrospores where the primary thallic wall is not involved in septum formation? Still, within the same reaction medium are the more predominant populations of non-persistent conidia- polar budding yeast cells. If this falls within the non-polarized category, what about the other types of yeast shapes and the numerous transitory stages which were without geometry or shape?

The cell wall is integument of the cytoplasm and confers mechanical stability and shape. We find in this study numerous nondescript entities being released after conidial rupture. Unless by intussusception, these discernable entities could not have acquired an encompassing cell wall while within the conidium. Indeed microscopic examination at a magnification of 2500x showed granular units that only acquired cellular membrane with time, after several hop-stages. The germ cell was prime ontogeny for nondescript units, often after spheroplasting. From cleavages of neoplasm, a sequence of cryptic forms, with inherent changes in volume, additionally align in the differentiation process of this microorganism, each form different from its immediate precursor, but none appeared to be enclosed by a cell wall until the nascent yeast is initiated by the evolved binary protoplast. Thus, in our consideration the cell wall material deposition patterns do not explain the inherent cytoplasmic granulation and primeval entities emergent from the conidial structures nor the germ cell, neither the occurrence of neoplastic units or protoplasts which were considered only bounded by membrane. This implied that at this primordial phase sequential units no carbon moieties were being converted into mannans, glucans or chitin/chitosan, which are the polysaccharide structural components of the yeast cell wall (Arnold, 1981; Walker, 1998). The scheme shown in Fig. 54 possibly illustrates the lateral morphogenetic transformation (Omoifo, 2003) that occurred in our minimal medium.

Topological view showed that neoplasm, on differentiating from cytoplasm after lysis of membrane of spheroplast, underwent cleavages of content thus exposed to the medium. This inures population growth. On the other hand, granulation individualized the neoplastic content wherefore biophysical activities, as happens in a dynamic system like a broth, could enforce osmotic relations at its optimal level. This implied succinct development of membrane in order to regulate transverse movement of materials and energy transduction at this primary level. Suppose the fluid

dynamics and stimulating factors permitted various epigenetic expressiveness of the innumerable offspring, what we might have could be reflected in the varying shapes and forms of incipient neoplastic units. Assuming there was vectorial energy transduction in a study conducted within a narrow range of pH, a concept that has been severally called upon in an attempt to explain an possible electrophysiological role in the dimorphic phenomenon (Omoifo, 1996, 2003, 2005, 2011b, 2012, 2014; Omoifo and Awalemhen, 2012; Omoifo *et al*., 2013), there could be a drive for directional physiological relationship that would perhaps give premium to specific biochemical reactions leading to expression of particular morphology. But witness the changing nature of morphological expressiveness, each state different from the precursor. Hence the various forms of neoplastic units and, sequentially differentiated to protoplasts; these initiated the nascent yeasts.

It was shown in the case of *Rhizopus stolonifer*, an organism said not to be dimorphic (Bartnicki-Garcia and Nickerson, 1962), that transformation to terminal budding yeast cells was achieved in synthetic broth at pH5.0 where growth was optimum and sigmoid pattern obtained (Omoifo, 2011b). Subsequent study using *M. circinelloides* showed that the early modifications that gave rise to the ultimate stable but nonpersistent morphology (Omoifo, 2013) were lag phase events during which phenotypic modification occurred in a system that permitted intermedial ionic flux (Omoifo, 2014). Subsequently, the induced proliferating yeast could be subjected to exponential growth (Omoifo, 2011b), only when the physiological process of glycolysis occurred (Omoifo *et al.,* 2013). At such primordial phase, a congruence occurred between the observed transient forms and Na^+-K^+ antiport movement (Omoifo and Awalemhen, 2012). Thus, in a 1.0g/l K^+: 0.10g/l Na^+ incorporated ionic broth, as used in this study, there was a time dependent intracellular K^+ accumulation as intracellular Na^+ simultaneously diminished, as germ cells sequentially transited through neoplasm to protoplasts and subsequently prevegetative cell prior to formation of obpyriform yeast cells of *M. circinelloides* (Omoifo, 2014). However, in the present study in which globose, ovoidal and spindle shaped yeast cells were induced, sigmoid growth pattern was not exhibited. Perhaps this was due to the presence of persistent morphological forms including holothallic-, holoblastic-, and thalloarthric conidia. Since these conidia were encased in geometrical walls of persistent nature, they remained permanently in broth after conidial wall burst and release of their differentiating primeval contents; their stability perhaps resisting the braisive effects of the dynamic reactions within the broth. This could impact strongly on the determined absorbance value of the broth at the early growth phase, although when such cell walls ruptured, which was frequent, the released primeval units were subjected to similar differentiating steps as those originating from germ cell.

The pathway to differentiation exhibited by the microorganism in both Amm. sulphate and Peptone incorporated broths was the same. The nature of vanishing and reappearance of the cell wall at the primordial phase of growth was unique. The two biophysical events were separated by a span where the intervening stretch domiciled numerous distinct forms, each of which was without a cell wall. The first event starts with spheroplast formation from the germ cell; then the cytoplasmic membrane disintegrates and only the cytoplasm is left. This converts to neoplasm, which occurs in various topological forms. This is followed by granulation and, or multiple cleavages subsequently viewed as nondescript entities. These provencal entities, in modified form, which then become incipient or pinched off as they change sizes/volume and shape, then changing through numerous and variously shaped middling stages become ultimately discernable as spherical neoplastic units. From these rod-shaped protoplasts form; they become binary through a denticle. A round protrusion appear to blast out from one end of the binary protoplast; it sutbsequently enlarges. Its integument contrasts sharply with the membranous protoplast that mothers it and its staining hue distinct from the protoplast. This is the nascent yeast initial. When it abscises, it becomes globose. This is the nascent yeast, or prevegetative cell. At maturity, it undergoes budding. Thus, daughter bud could be seen attached to the mother cell through a short denticle. Figures 54& 55 reflect this primordial sequential differentiation process.

In our view, the differentiation process through the sequential wall-less cryptic forms just described for nascent yeast formation originated from germ cell and the possible cytoplasmic membrane initiated conidial types tend to shift the emphasis on cell wall biogenetic possibility from the cell wall *per se*, to the cytoplasmic membrane default. Right from the time of spore inoculation, the bathing medium is the same for all derived growth spheres. Thus whatever changes inherent in the reaction medium, in terms of osmodynamic relationships, equally affect all growth spheres. Therefore, when cell wall of the conidial types ruptured, the primeval entities released into the commonwealth bathing medium subject to the same differentiating mechanism to nascent yeast initial as that arising from the germ cell. This is proof that the intracellular physiology that led to cytoplasmic granulation and ensuing differentiation thereby generating the neoplastic units within the conidial types was similar to what occurred within the germ cell which also generated primeval units. Since the pliable cytoplasmic membrane is the operational platform on which intermedial exchanges occur, especially through exocytotic and other transport activities in cell wall

generation, it is possible that its specific orientation and available materials (substrate and ions) transport through it could detail alterations which streamline different programmes that impacted on the emerging but distinct morphologies. Witness in Fig. 56 the coexistence of a germ cell-generated neoplasm and emergent (young) holoblastic conidia, which were differentiating along two different lines. Similar observation was made by Omoifo and Awalemhen (2012) when it was found that a 1.10 g /l K^+ incorporation into multiionic broth led to induction of higher proportion of thallic conidial subtypes in comparison with 1.0 g /l K^+-medium which predominantly yielded terminal budding yeast cells of *M. circinelloides* Tieghem.

The lateral morphogenetic transformation outlined here presumes a remarkable intracellular coordination of differentiation. The observed sequences would be controlled by diffusable chemicals relaying signals in the long process of differentiation. The rate of reaction would possibly depend on the temperature level. As the graphic presentation above showed, the cummulative growth of transformed *M. manihotis* was higher at 28°C. This was followed by that at the elevated temp. 37°C and it was least at 15°C.

Following cytodifferentiation, the stable morphology was polar budding globose yeast cell. It is interesting to note that elevated temp caused morphological diversity of the yeast form. Thus additionally induced were spindle- and ovoidal shaped yeast cells at 37°C. This diversity probably resulted from the response of the induced form to stress imposed by the sublethal temperature level.

This study has shown how pristine granular units have evolved, then progressed through a sequence of cryptic entities, each different from the preceding one. What this entails is that a series of structural and functional adjustments occurred as one entity transited to the other until the final complex functional stable form occurred. Thus a germ cell converted into spheroplast after disappearance or lysing of the cell wall and, following the loss of the cytoplasmic membrane what we see was the cytoplasm from which neoplasm derived, an exhibition of differing topological changes whence imploding into innumerable neoplastic units in a directional transformation as each unit transited into individual protoplast, a precursor to the prevegetative cell. As we see, the changes that occurred during such differentiation apart from the size and shape, would include inherent metabolic activity, membrane potential as well as signal responsiveness. Thus inherently, each matured stable unicellular form had reproductive capabilities and, hence produced offspring. This trendline of daughter generation and or proliferation is distinct from the previously described germ sphere-derived population growth.

Therefore, primordial phase differentiation exhibited in this study did not involve the conventional mitotic division, which encompasses prophase-nuclear membrane disintegration, chromosome doubling, seggregation, cell division and daughter bud formation-activities which are DNA polymerase alpha mediated at the S-phase. In this study, daughter buds were formed after maturation of the nascent yeast initialized by the binary protoplast. It is reasonable to say that cytodifferentiation as expressed here involved differential gene expression that resulted in the multiple morphologies, though transient. But since the genetic constitution of the *M. manihotis* was not affected, it was possible to revert to the original filamentous growth habit, evidenced by the congruence of characteristics of the re-induced filaments at termination of experiments, with the original state of the isolate. Similar morphogenetic interconversion has been achieved in our laboratory using different microorganisms including the now invalid *Dimorphomyces* strains (Omoifo, 1996,1997), *M. circinelloides* (Omoifo, 2006ab, 2011ab, 2013, 2014; Omoifo and Awalemhen, 2012; Omoifo and Omamor, 2005; Omoifo *et al*., 2006) and *R. stolonifer* (Omoifo, 2011ab; Omoifo *et al*., 2013).

V. Acknowledgements

This work was done in the Agronomy laboratory of the Faculty of Agriculture, Ambrose Alli University, Ekpoma, Edo State, Nigeria. The technical assistance of Bayo Omoikhojie is hereby acknowledged. We express thanks to Dr. C. E. Ikuenobe of the Nigerian Institute for Oil Palm Research, Benin City who helped with the statistical analysis.

- *Contribution.* The concept, design, analysis, literature search and write up was done by COO. NN was a project student who participated physically in this study.

References Références Referencias

1. Alexopoulos C. J. and Mims C. W. (1979) *Introductory Mycology*. 3rd edition. Wiley Eastern Ltd, New Delhi. 631pp
2. Arnold W. N. (1981) *Yeast Cell Envelops: Biochemistry, Biophysics, and Ultrastructure* Vol. 1. CRC Press Inc. Florida, 125pp.
3. Barrera C. R. (1983) Formation and ultrastructure of mucor rouxii arthrospores *J. Bacteriol.* 155(2): 886-895.
4. Bartnicki-Garcia S. (1968) Cell wall chemistry, morphogenesis and taxonomy of fungi. *Annu. Rev. Microbiol*, 22: 87-108.
5. Bartnicki-Garcia S. (1973) Fundamental aspects of hyphal morphogenesis, *In*: Ashworth J. M., Smith J. E. Eds. *Microbial Differentiation*. Cambridge University Press, Cambridge, pp 245-267.

6. Bartnicki-Garcia S (1987) Chitosomes and chitin biogenesis. *Food hydrocolloides*, 1:353-358
7. Bartnicki-Garcia S. and Lippman, E. (1969) Fungal morphogenesis: cell wall construction in *Mucor rouxii. Science*, 165: 302-304
8. Bartnicki-Garcia S. and Lippman, E. (1977) Polarization of cell wall synthesis during spore germinationof *Mucor rouxii*. *Exptl. Mycol*. 1: 230-240.
9. Bartnicki-Garcia S, Hergert F, GierzG, (1989) Computer simulation of fungal morphogenesis and the basis for hyphal (tip) growth. *Protoplasma*, 153: 46-57.
10. Bartnicki-Garcia, S. Nelson, N, and Cota-Robles E. (1968). Electron microscopy of spore germination and cell wall formation in Mucor rouxii. *Arch. of Microbiol*., 63: 242-255.
11. CAB (1971) *Dematiaceous Hyphomycetes*. Commonwealth Agricultural Bureau, Common wealth Mycological Institute, Surrey, England.
12. Carmichael J. W. (1971) Blastospores, Aleurospores, and Chlamudospores. In: *Taxonomy of Fungi Imperfecti,* pp50-70. Edited by B. Kendrick. Toronto University Press.
13. Chitnis M. V. and DesphadeM. V. (2002) Isolation and regeneration of protoplasts from the yeast and mycelial form of the dimorphic zygomycete *Benjaminiella poitrasii*: role of chitin metabolism for morphogenesi during regeneration. *Microbiol Res*. 157: 29-37.
14. Davenport R. R. (1980) *Biology and Activity of Yeasts*, In: Skimmer F. A., S. M Passmore and R. Davenport, eds. Academic Press, London pp 1-27.
15. Di_eguez-Uribeondo,J., Giertz G and Bartnicki-Garcia S (2004) Image analysis of hyphal morphogenesis in Saprolegniaceae (Oomycetes) *Fungal Genetics and Biology* 41: 293–307
16. Diophode N., Joshi C., Ghomde V.,Deshpande M. V. (2009) The biotechnological implications of dimorphic yeasts. In: Satyanarayana T, Kunze G, Deshpande M. V. Eds. *Yeast Biotechnology: Diversity and Applications*, Springer Science + Business Media B. V. pp635-650
17. Ellis M. B. (1976) *More Dematiaceous Hyphomycetes*. CAB, Surrey, England.
18. Ghomade V, Pathan E, and Deshpande M. V. (2012) Yeast-hypha dimorphism in Zygomycetous fungi. In: J. Ruiz-Heerrera Ed. *Dimorphic Fungi: Their Importance as Models for Diffentiation and Fungal Pathogenesis*. Bentham Books, Mexico.
19. Gooday G. W (1973) Differentiation in the Mucorales. In: *Microbial Differentiation*. J. M. Ashworth and J. E. Smith. eds. Cambridge University Press, Cambridge, pp 269-294.
20. Hesseltine C. W. and Ellis J. J. (1973) Mucorales; In: *The Fungi: An Advanced Treatise*, vol. IVB, pp. 187-217. Ed. G. C. Ainsworth. New York Academic Press.
21. Kendricks B (1971) *Taxonomy of Fungi Imperfecti*. 309p, Toronto: University of Toronto Press.
22. Kendrick W. B. (1973) *Fungi: An Advanced Treatise* Vol. IV Ed. G. C. Ainsworth. New York Academic Press
23. Lübbehüsen T.L., Nielsen J. and McIntyre M. (2003) Characterization of the *Mucor circinelloides* life cycle by on-line image analysis Journal of *Appl*. *Microbiol*. 95 (5): 1152 - 1160.
24. McIntyre *et al*., 2002 McIntyre, M., Breum, J., Arnau, J. and Nielsen, J. (2002) Growth physiology and dimorphism of *Mucor circinelloides* (syn. racemosus) during submerged batch cultivation. *Appl. Microbiol. & Biotechnol*. 58, 495–502
25. Omoifo C. O**,** Ohenhen R. E. and Elemonfo R. A. (2013) Induction of yeast cells from sporangiospores of *Rhizopus stolonifer* was inhibited by sodium fluoride. *Afri. J. Microbiol. Res*, 7(19): 1964-1976,
26. Omoifo C. O. (2012) Effect of potassium ions on protoplast generation during yeast induction from *Mucor circinelloides* Tieghem. *ISRN Biotechnology*, vol 2013, Article ID 734612, 12 pages, http://dx.do1 .org/10.5402/2013/734612.
27. Omoifo C. O. and Awalemhen B. I. (2012) Sporangiospore-yeast transformation of *Mucor circinelloides*: Ionic circulation, chemical potential, sodium influx rate and morphogenesis. *Afri. J. Biotechnol*. 11(14): 3217-3442.
28. Omoifo C. O. (2011a). *Rhizopus stolonifer* exhibits dimorphism. *Afri. J. Biotechnol*. 10 (20): 4269-4275
29. Omoifo C. O (2011b). Effect of extracellular calcium chloride on sporangiospore-yeast transformation of *Rhizopus stolonifer*. *Afri. J. Biotechnol*. 10 (20): 4276-4288..
30. Omoifo, C.O. (2006a). Effect of K^+, Na^+ and uracil on sporangiospore-yeast transformation of *Mucor circinelloides* Tieghem. *Afri. J. Biotechnol*. 5 (9): 715-722.
31. Omoifo, C.O. (2006b). Effect of myoinositol and zinc on sporangiospore-yeast transformation of *Mucor circinelloides* Tieghem. *Afri. J. Biotechnol*. 5 (9): 707-714.
32. Omoifo, C.O. (2003). Sequential sporangiospore – yeast transformation hypothesis. *Afri. Scientist* 4 (4) 191-273.
33. Omoifo C. O. (1996) Modeling sporangiospore-yeast transformation of Dimorphomyces strain. *Hind. Antibiot. Bull*., 38: 12-31.
34. Omoifo C. O. (1997) Auxotrophic requirement for sporangiospore-yeast transformation of *Dimorphomyces diastaticus* strain C12. *Hind. Antibiot. Bull*., 39: 11-15.
35. Omoifo C. O. (2009) Sporangiospore-to-yeast conversion: Modeel for morphogenesis. *Afri. J. Biotechnol*. 8(16): 3854-3863

36. Omoifo C. O. (2014) Sodium-potassium ionic ratio correlates with yeast induction from *Mucor circinelloides* Tieghem. *Afri. J. Microbiol. Res.*, 8 (1): 46-65.
37. Omoifo C. O. and Omamor I. B. (2005) Effect of zinc on sporangiospore-yeast transformation of *Mucor circinelloides* Tieghem. *ASSET Series B*, 4 (1): 159-166
38. Omoifo C. O. Aruma M. B. and Omamor I. B. (2006) Effect of myoinositol on sporangiospore-yeast transformation of *Mucor circinelloides* Tieghem cultivated in synthetic broth. *Hind. Antibiot. Bull.* 48: 24-31.
39. Omoifo C. O, Ohenhen R. E, Elemonfo R. A (2013). Induction of yeast cells from sporangiospores of *Rhizopus stolonifer* was inhibited by sodium fluoride. *Afri. J. Microbiol. Res.* 7(19):1964-1976
40. Orlowskii M. (1991) Mucor dimorphism. Microbiological Reviews, 55(2): 345-258.
41. Samson R. A., Hekstra E. S, Frisvad J. C, and Filtenborg O. (2000). *Introduction to Food- and Airboune Fungi.* 6th edn. CBVSC, Utrecht.
42. Von Arx J. A. (1974) *The Genera of Fungi Sporulating in Pure Culture*. J. Cramer, FL-9490 VADUZ
43. Walker G. M, (1998) *Yeast Physiology and Biotechnology*. 350p. John Wiley & Sons New York.
44. White M. M, James T. Y,O'Donnel K, Calfino M. J, Tanabe Y, Sugiyama J.(2006) Phylogeny of the Zygomycota based on nuclear ribosomal sequences data. *Mycologia*, 98: 872-884

Table 1 : Total biomass, mean bomass, standard error and form of growth of *Mucor manihotis* cultivated in synthetic broth incorporated with organic and inorganic nitrogen sources at pH 5.0

Temperature (ºC)	Total biomass	Mean biomass	Standard error	Form of growth
		Ammonium sulphate		
15	0.211	0.021	0.004	Gs, Nu, Tg Yo, P, N, TY, Ec
28	2.088	0.208	0.068	Gs , Nu, Tg, y, Ec, Hc, Fs, P, B, Tg
37	0.808	0.080	0.022	Nu, Yo,Y, Yc, H, Yg, Tc, Yo
		Peptone		
15	0.912	0.091	0.417	Gs , `Nu, Tg, P, Y, N,
28	3.682	0.368	0.073	Tg, Hc, Nu, Tg, P, Pv, Ta
37	2.419	0.242	0.061	Nu, TgYs, Yg, B, Nu, To, Tg, Fs, Ta

Legend: Gs – growth sphere; Nu – neoplastic units; Tg – thallic growth; Yn – nascent yeast; P – protoplast; N – neoplasm; Y – polar budding yeast cells; Ec – enterothallic conidia; Hc – holoblastic conidia; Ta – thalloarthric conidia; Fs – septate filament; Pb – binary protoplast; Ys – spindle yeast cell; Yg – globose yeast cell; Yo – ovoidal yeast cell; Tc – thallic conidia; B – blastospore

Supplementary Table 1 : Analysis of variance of growth data of *Mucor manihotis* cultivated in minimal medium incorporated with Amm.sulphate and Peptone and incubated at different temp.levels at pH 5.0

Variate: Variate					
Source of variation	d.f.	s.s.	m.s.	v.r.	Fpr.
BLOCK stratum	4	0.0000000	0.0000000	0.00	
BLOCK.*Units* stratum					
N-source	1	1.3926453	1.3926453	2113.62	<.001
Temp	2	2.9309735	1.4654867	2224.17	<.001
Time	4	2.0258522	0.5064630	768.66	<.001
N-source.Temp	2	0.1675792	0.0837896	127.17	<.001
N-source.Time	4	0.2373338	0.0593335	90.05	<.001
Temp.Time	8	0.6129923	0.0766240	116.29	<.001
N-source.Temp.Time	8	0.3096117	0.0387015	58.74	<.001
Residual	266	0.1752650	0.0006589		
Total	299	7.8522530			

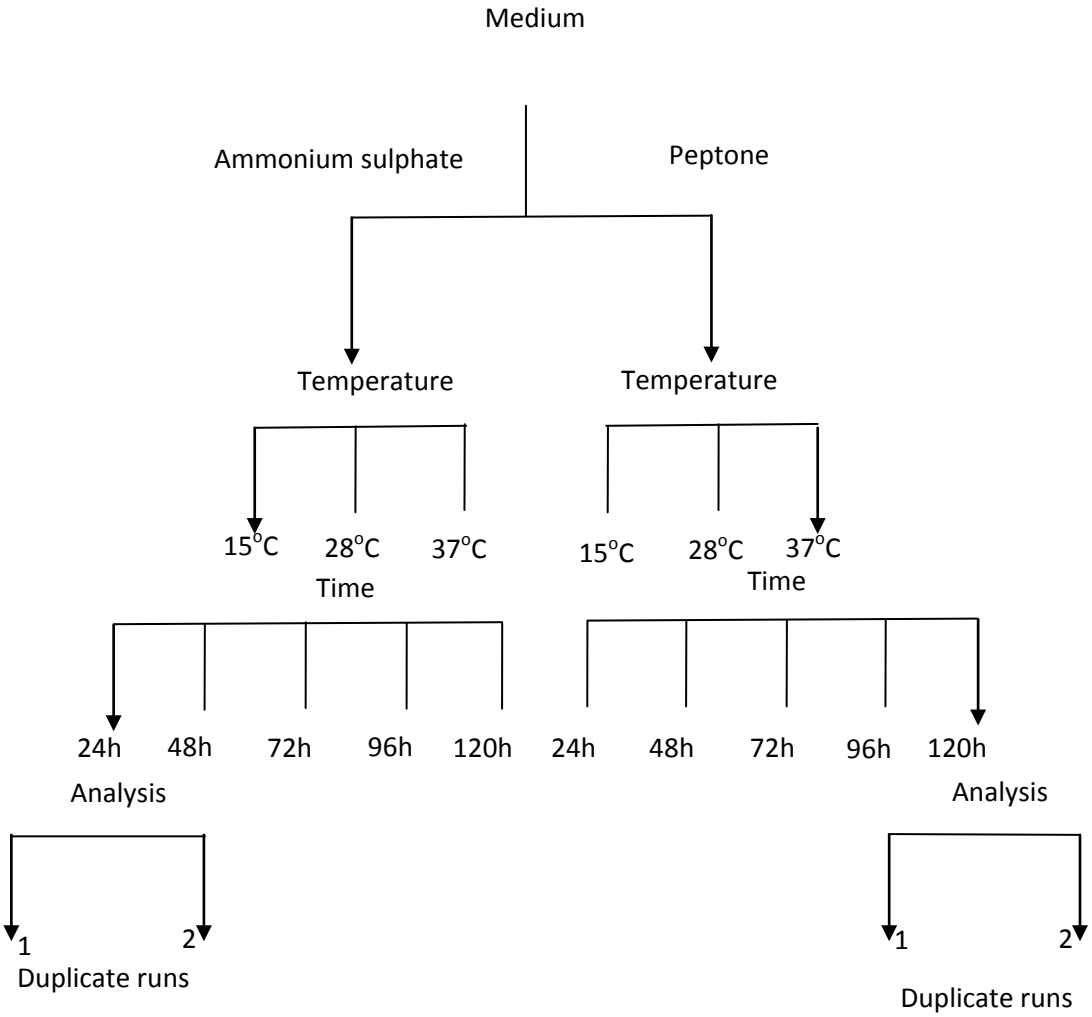

Figure 1 : Experimental design for growth and evaluation of *Mucor manihotis* used in this study

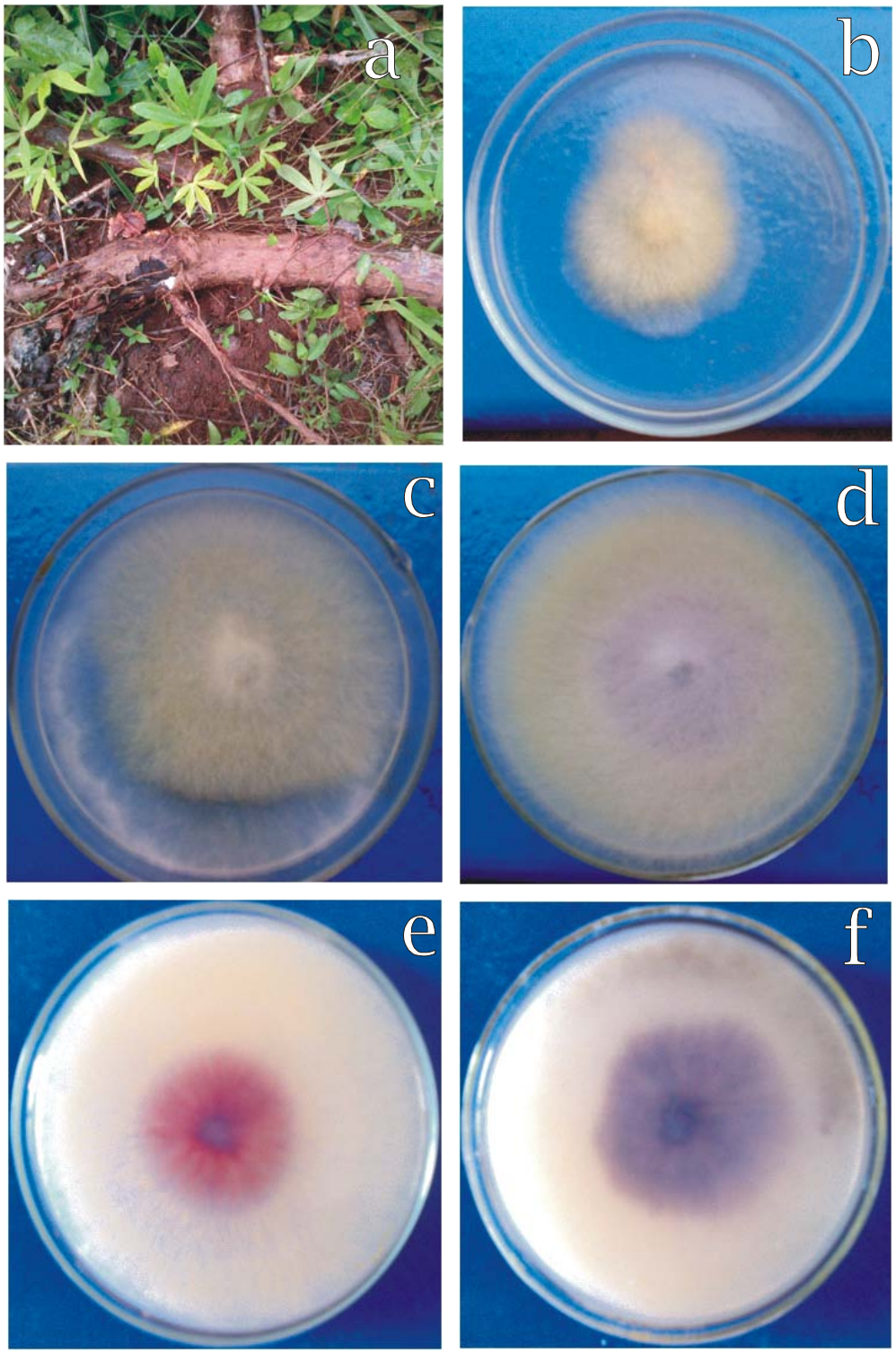

Figure 2 : PDA cultures of *Mucor manihotis;* **a**, specific point of sample isolation in the farm; **b**, culture at 1 day after inoculation; **c**, culture at 3 days from inoculation;, **d**, A-view at 6 days from inoculation, observe the colour change at the central region; **e**, B-view: the central region is reddish; **f**, 45 days from inoculation, the central region is purple while mycelium towards the edge turn black.

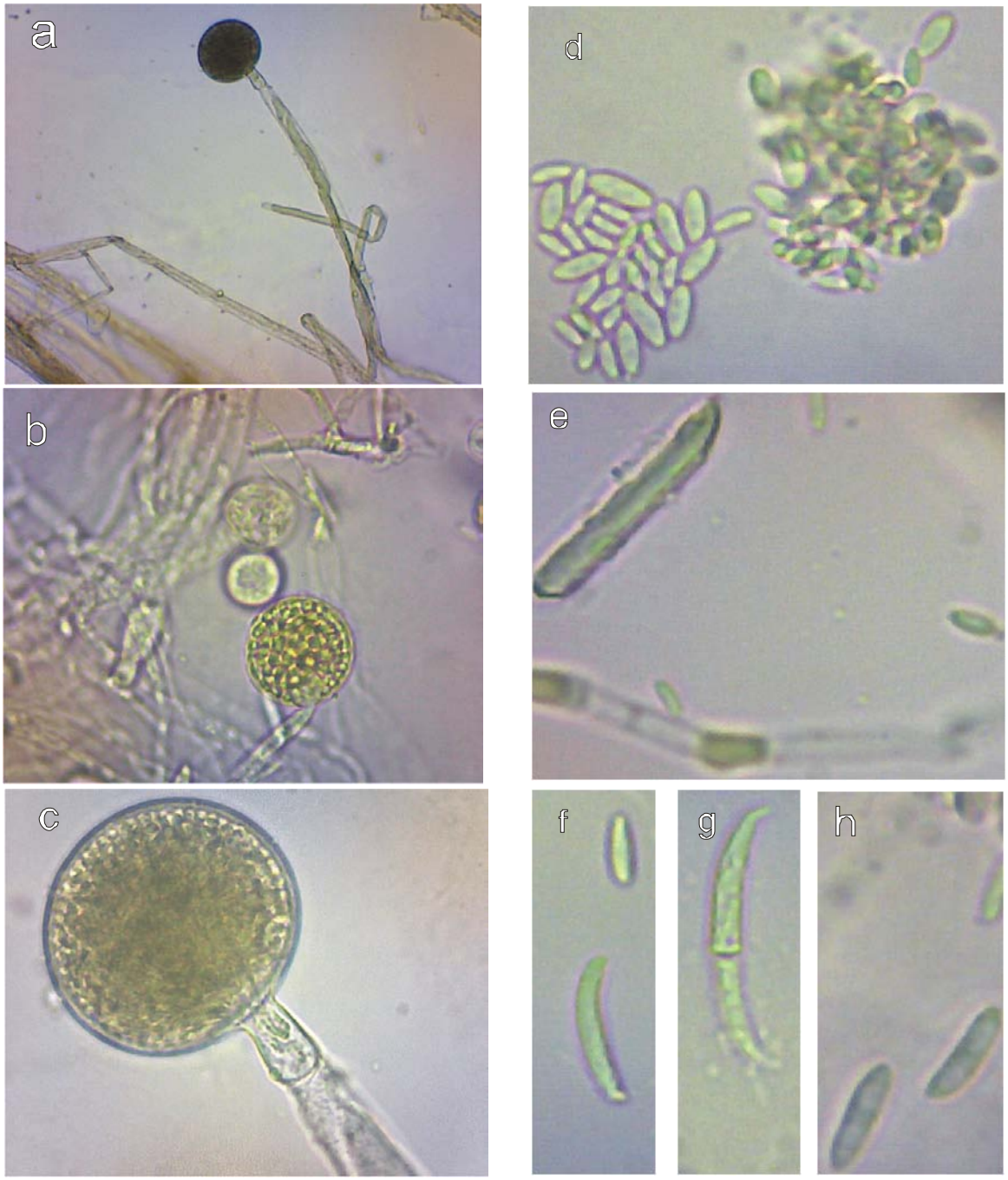

Figure 3 : Aerial mycelia of *Mucor manihotis;* ***a***, sporophore & sporangium; **b**, spores directly observed in the sporangium, x800mag; ***c,*** sporangium: observe septum cutting off columellum from sporophore, x1000mag; ***d,*** clusters of ellipsoid & cylindrical sporangiospores; ***e,*** cylindrical elongate sporangiospore; **f**, crescent shaped sporangiospore; **g**, double-celled crescent sporangiospore; **h**, sausage-roll sporangiospore; d e, f, g, h are at 2500mag.

Figures 1b : The isolation of, and cytodifferentiation of a Mucor species as affected by nitrogen source and elevated temperature

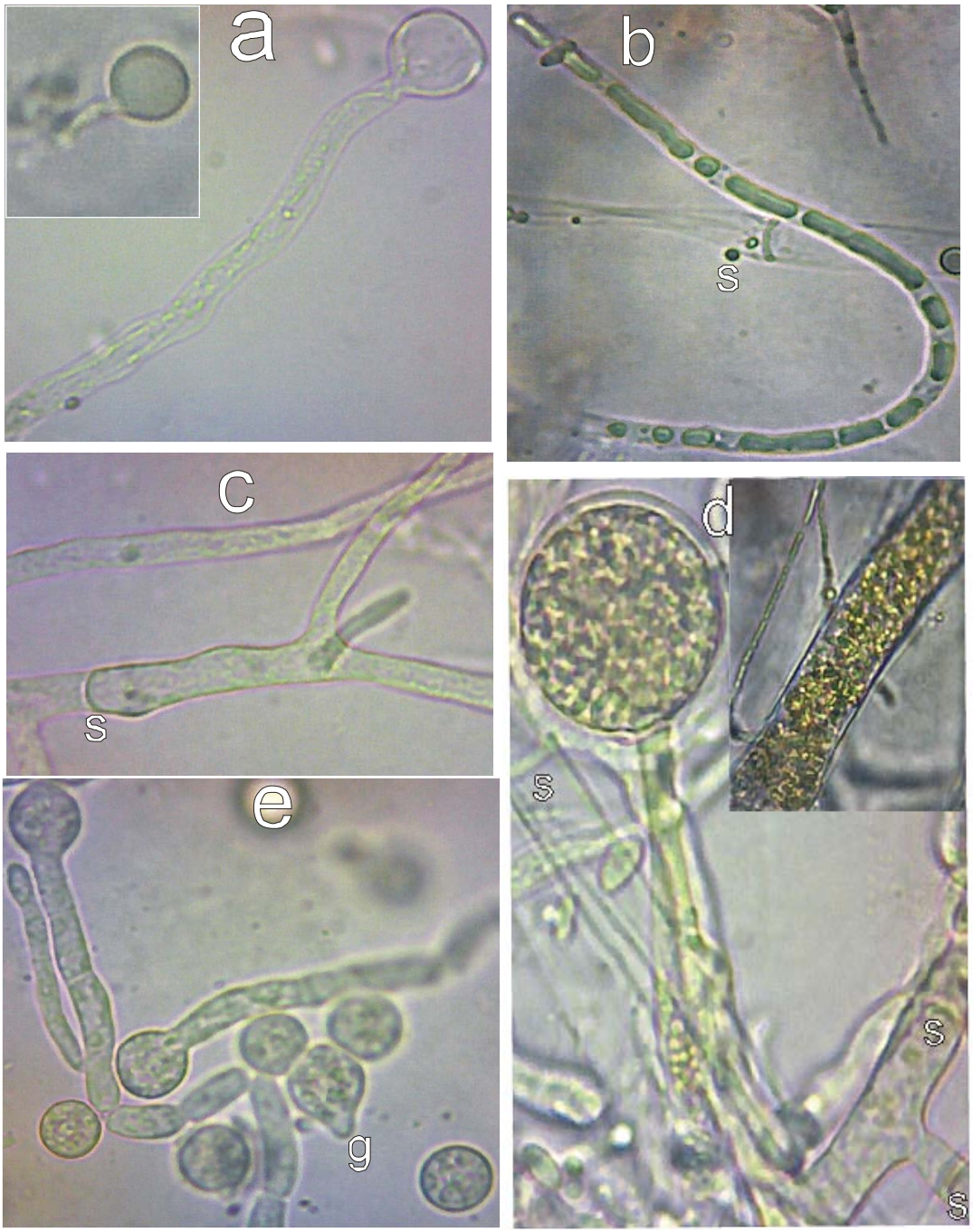

Figure 4 : *Su*bstrate-level mycelium of *Mucor manihotis* after 24h of growth on PDA; **a**, columellum of upright sporophore, inset: laterally borne columellum; **b**, thin filament showing early fragmentation of cytoplasm; **c**, multple branching mucelium; **d**, upright sporophore borne on septate mycelium, inset; mycelium with fragmented cytoplasm; **e**, thallo-arthric growth; g, germ tube, s, septum. Magnification: 2500x.

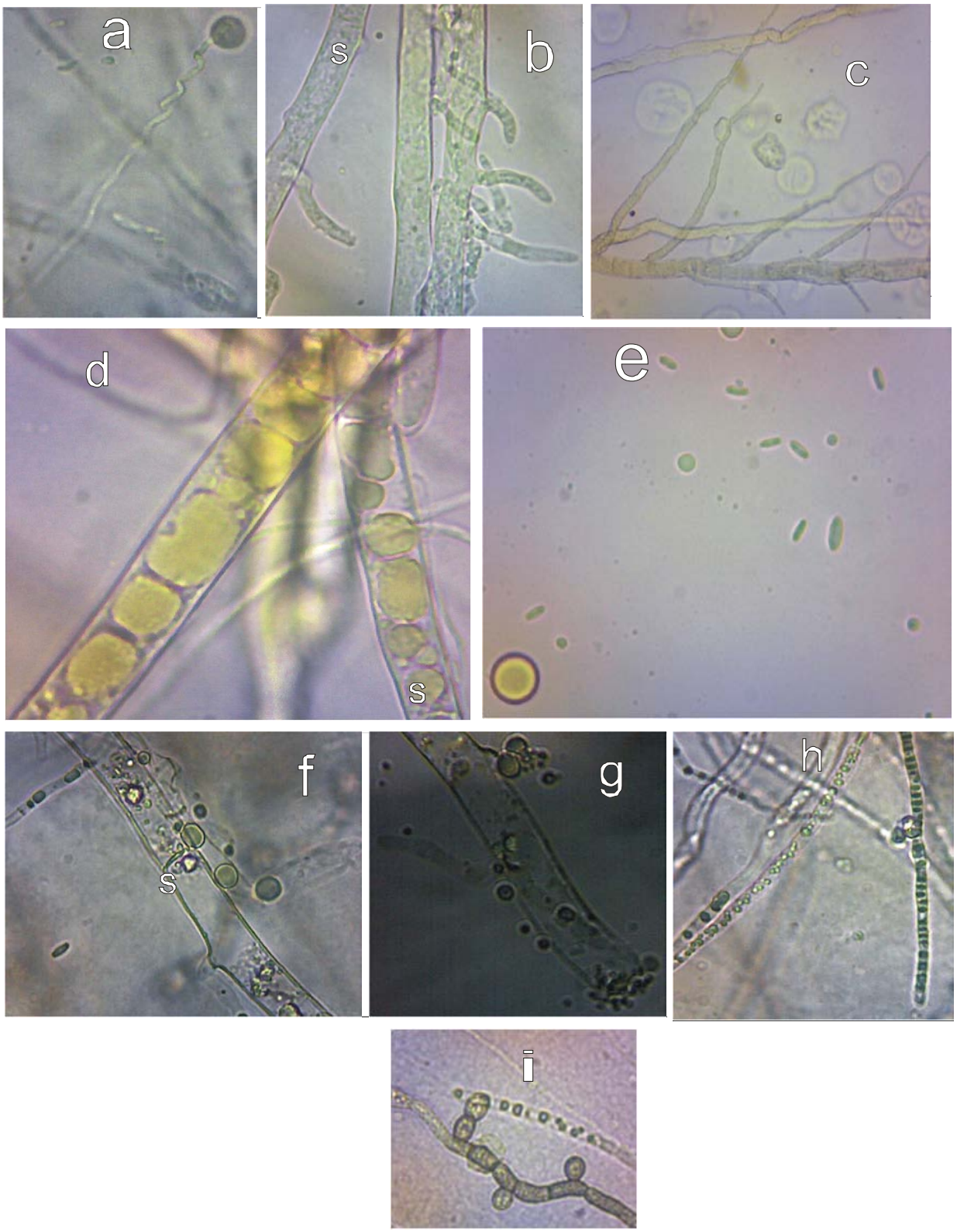

Figure 5 : Mucor manihotis: **a**, curvy sporophore terminating in globose columellum, x800; **b**, multiple germ tubes of septate mycelium, x1000; **c**, elongating hyphal branches forming mycelia, x800; **d**, hyphae with cytoplasmic cleavages, x1000; **e**, sporangiospores, x2500; **f**, septate hypha & protoplasts, x2500; **g**, hypha release protoplasts on rupture, x2500; **h**, protoplast formation within tubular compartments, x2500; **i**, internal & branch conidial formation of thallic growth, x1000; a-c @ 72h, d-g @ 120h, f-i @ 191h of growth

2 a. Cytodifferentiation of Mucor species

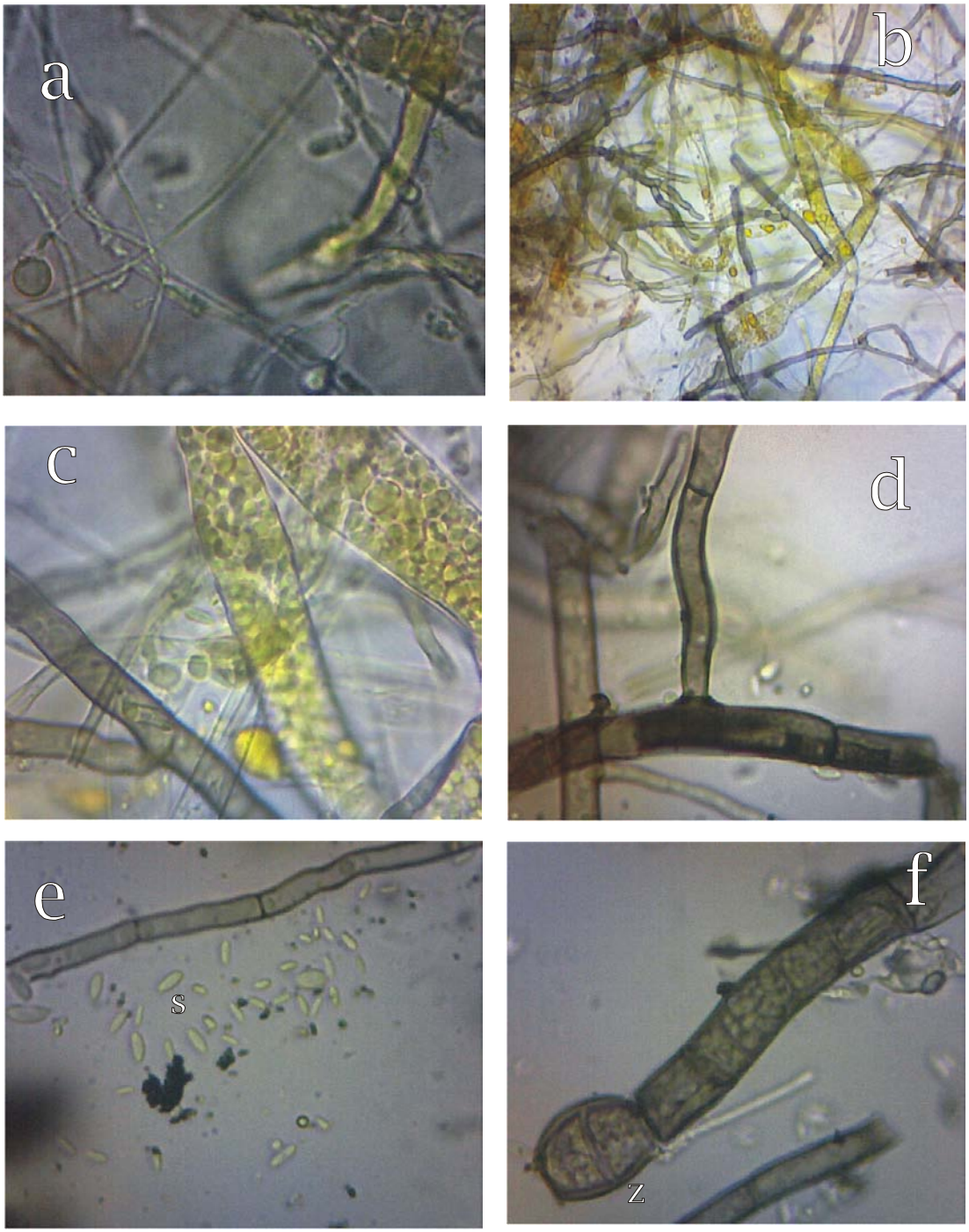

Figure 6 : Mucor manihotis PDA culture after 9days of growth; observe the melanized walls of filaments, a-f, and septa, d-f, s-sporangiospores; z- chlamydospore. Magnification, a, b -800x; c – f, 1000x

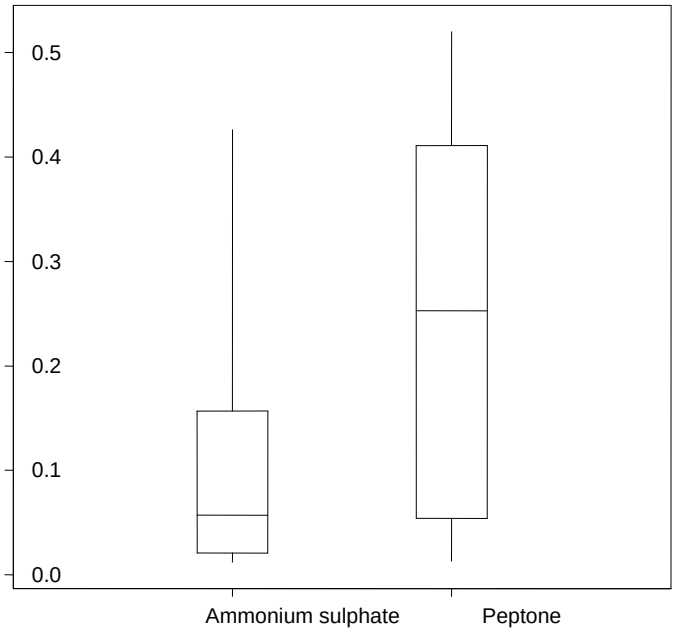

Figure 7a : Box plot of cummulative growth data of *Mucor manihotis* cultivated in minimal medium incorporated with organic or inorganic nitrogen source. Growth in the organic nitrogen source, peptone, was profoundly enhanced

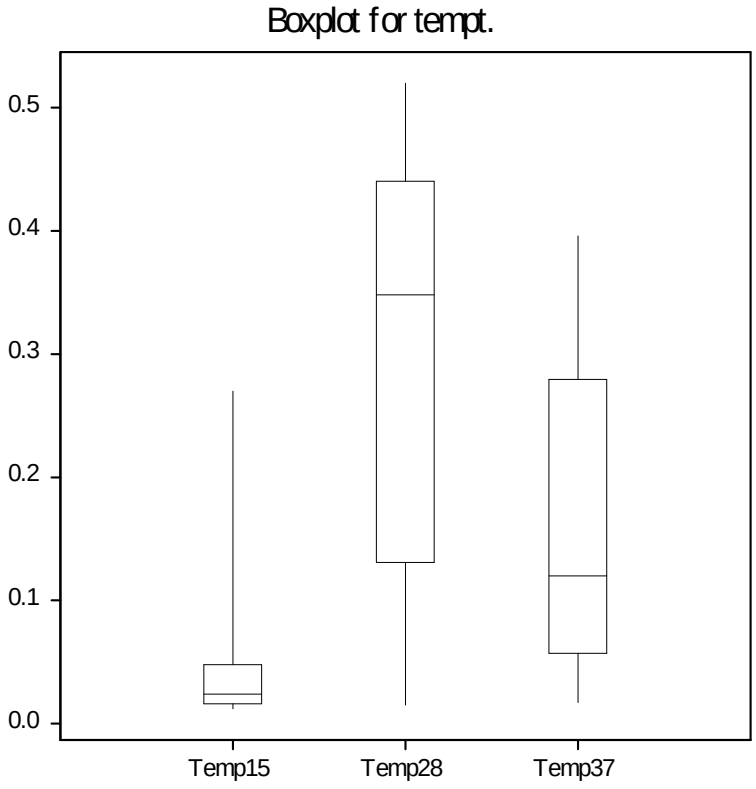

Figure 7b : Box plot of growth data of *Mucor manihotis* cultivated in minimal medium and incubated at the various temperature levels. At 28°C, growth was considerably enhanced and was least at 15oC where variablity was also greatest, represented by the extended whisker. However, it was pertinent to point out that in spite of the different cryptic forms induced, growth followed normal population dynamics

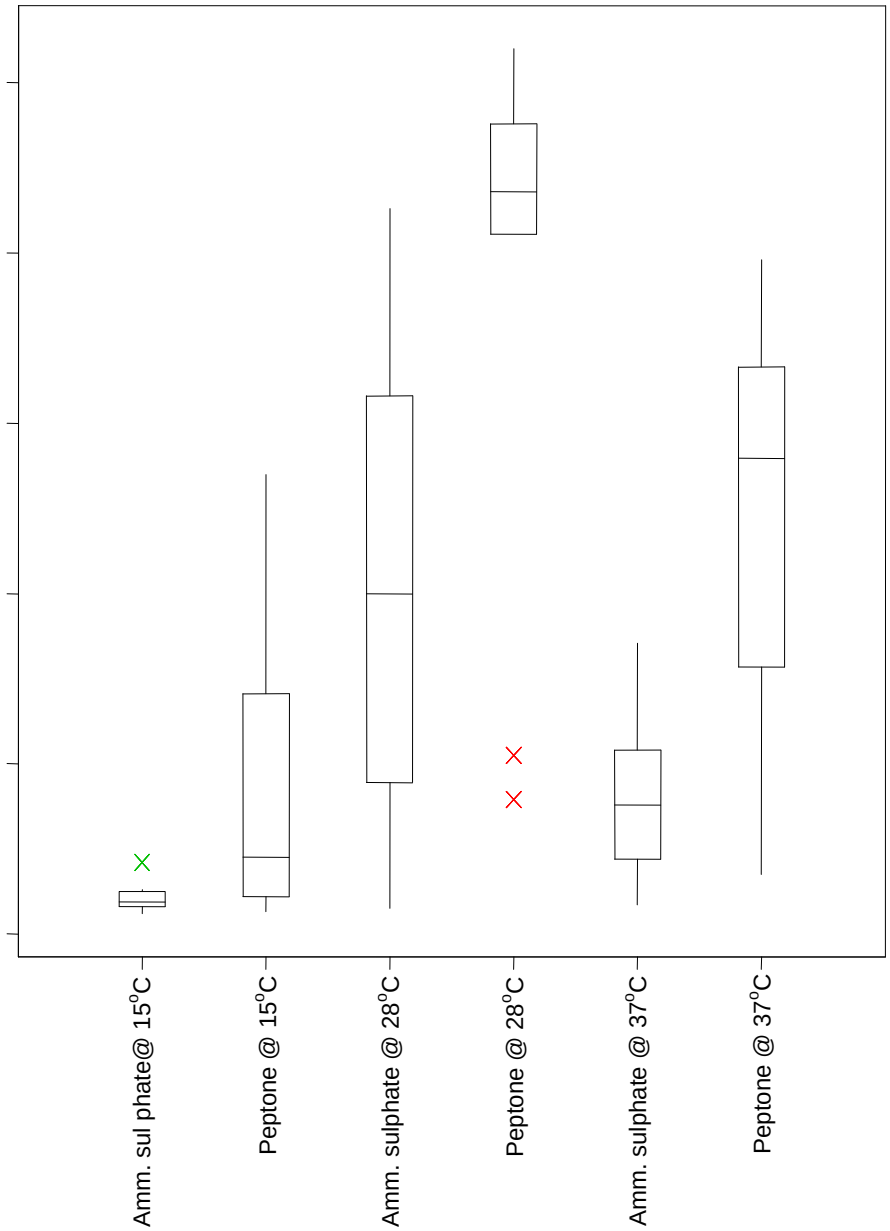

Figure 8 : Box plot of growth data of*Mucor manihotis* cultivated in ammonium sulphate and peptone incorporated minimal medium and incubated at the various temperature levels. At each temperature level growth in peptone incorporated broth was outstanding

3 a. Cytodifferentiation of Mucor species

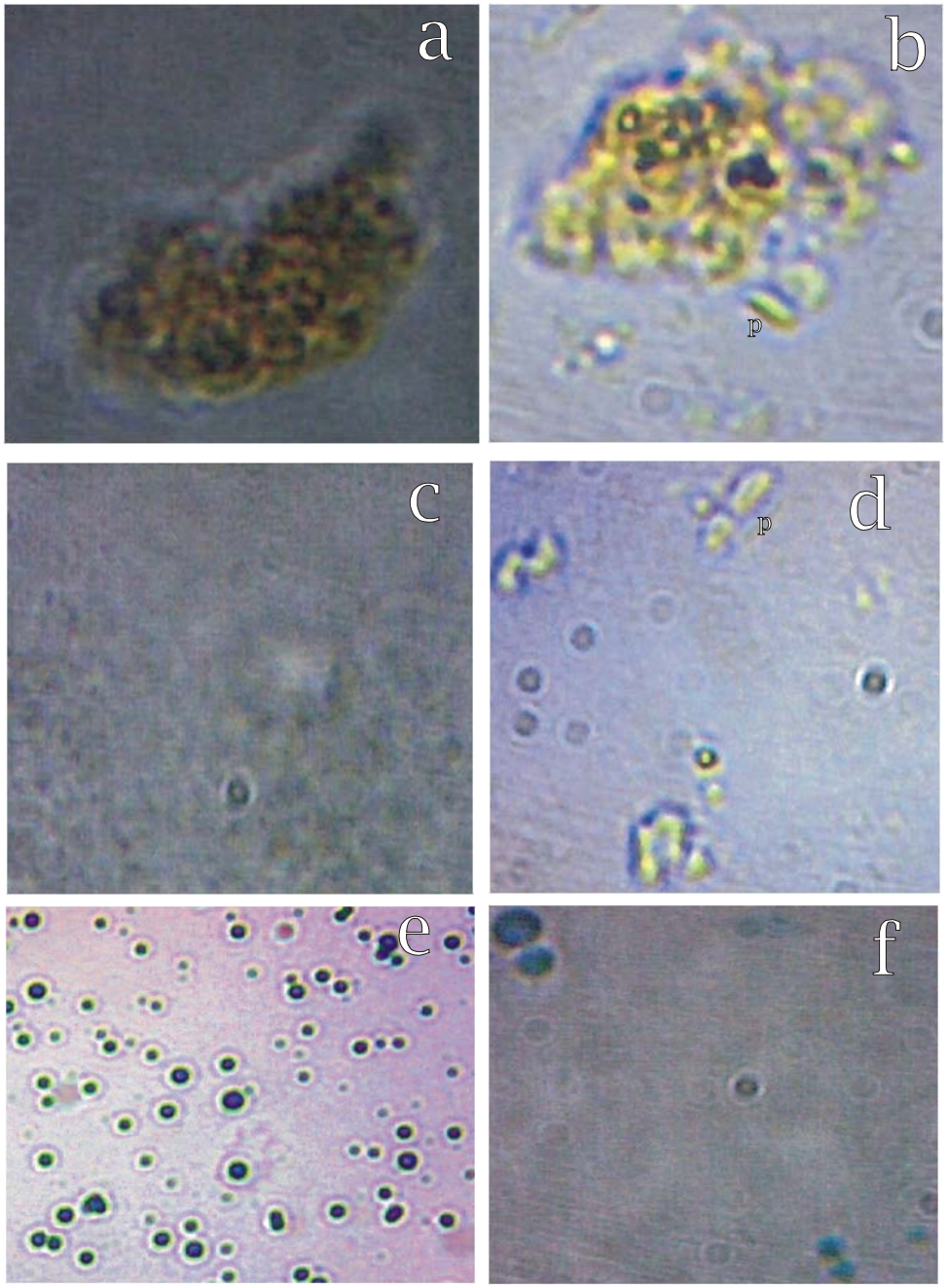

Figure 9 : Growth forms of *Mucor manihotis* induced in $(NH_4)_2SO_4$ incorporated minimal medium after 96h at temp 15°C; a, differentiating, x2500mag; b, individual neoplastic units culminating as protoplastic units (p, rod-shaped in this micrograph), x2500mag; c, dispersing formless neoplastic units; d, binary protoplast (p,), x2500mag; e, polar budding yeast cells, x1000mag; f, yeast cells, a short denticle separate daughter from mother cell. x2500mag

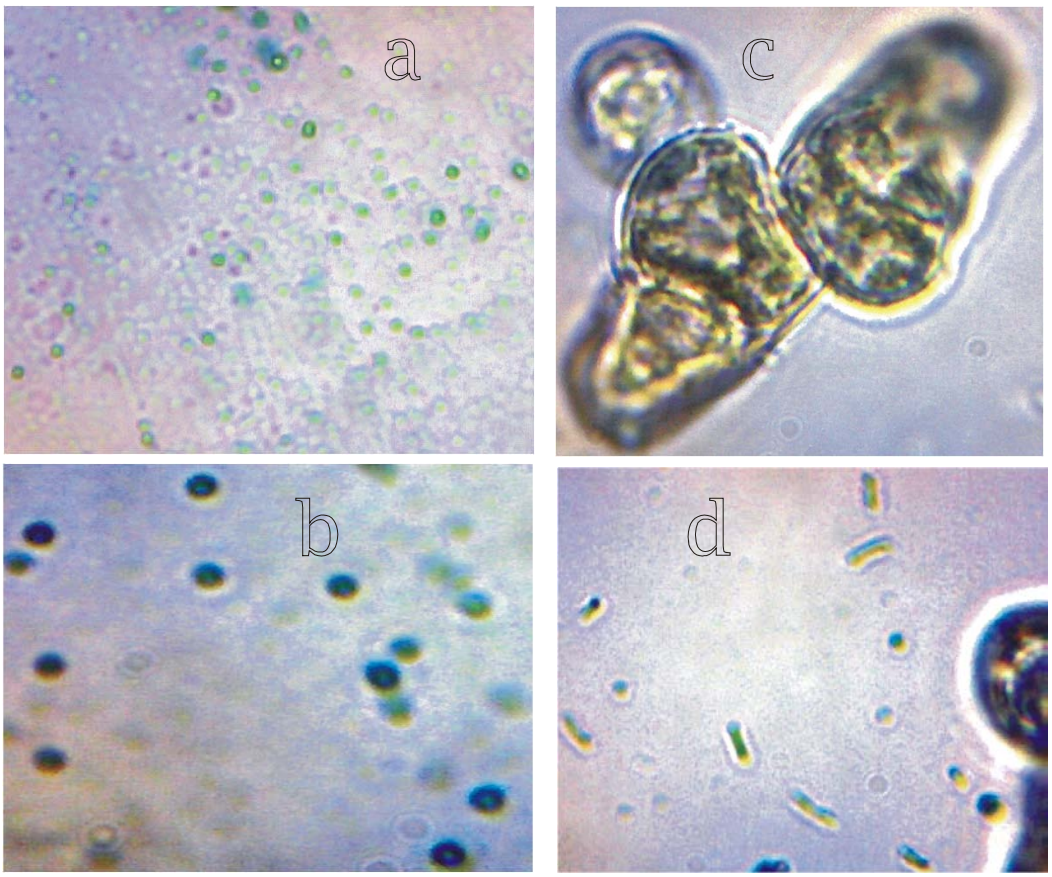

Figure 10 : Growth forms of *Mucor manihotis* induced in $(NH_4)_2SO_4$ incorporated minimal medium after 120h at temp 15°C; a, neoplastic units; b, globose yeast cells; c, enterothallic conidia; d, a lower elevation of (c) showing rod shaped & binary protoplasts. Magnification: x2500mag

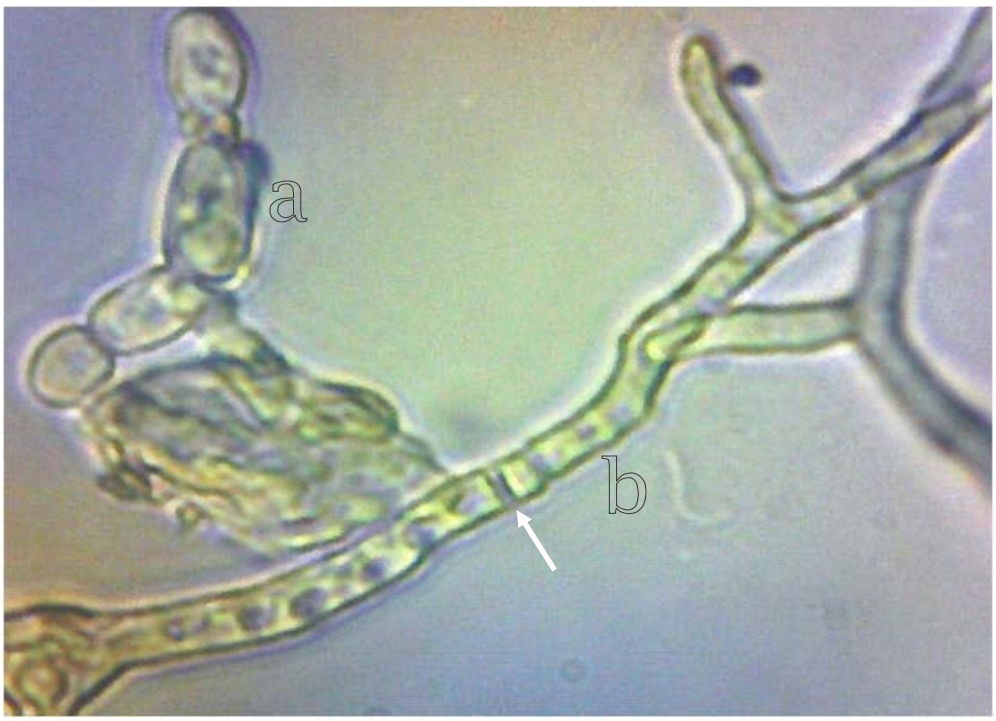

Figure 11 : Growth forms of *Mucor manihotis* induced in $(NH_4)_2SO_4$ incorporated minimal medium after 24h at temp 28°C; a, holoblastic conidia, x1000mag; b, septate fil aments; arrow, septum; x1000mag

3 b. Cytodifferentiation of Mucor species

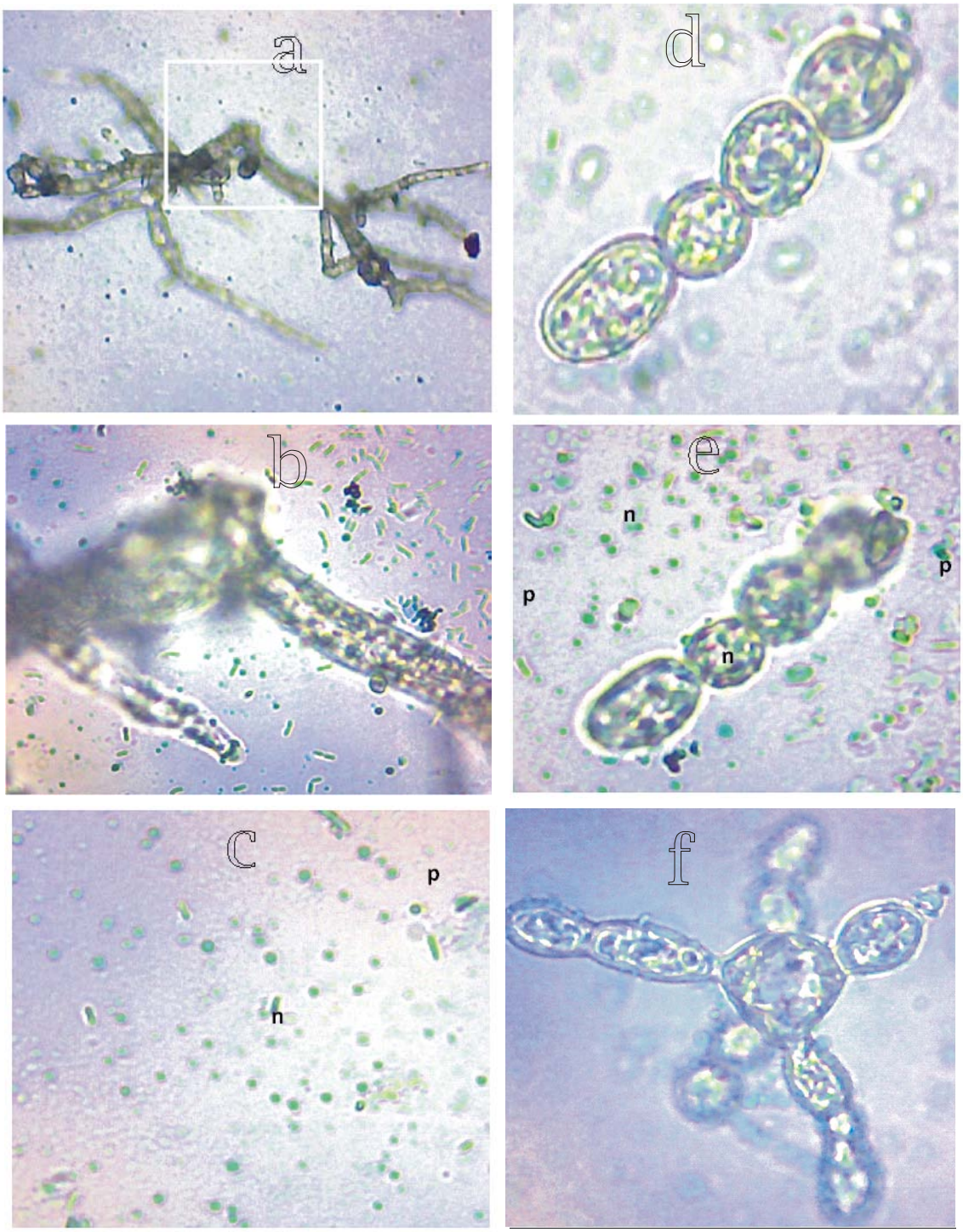

Figure 12 : Growth forms of *Mucor manihotis* induced in $(NH_4)_2SO_4$ incorporated minimal medium after 48h at temp. 28°C; **a**, thallic growth, x800mag; **b**, lower elevation of the section mark 'n' showing rod shaped & binary protoplasts, x2500mag; **c**, neoplastic units 'n' & rod shaped protoplasts, 'p', x2500mag; **d**, holoblastic conidia, x2500mag; **e**, lower elevation of (d) showing neoplastic units & protoplasts x2500mag; **f**, growth cell showing multiple germ tube production; x2500mag

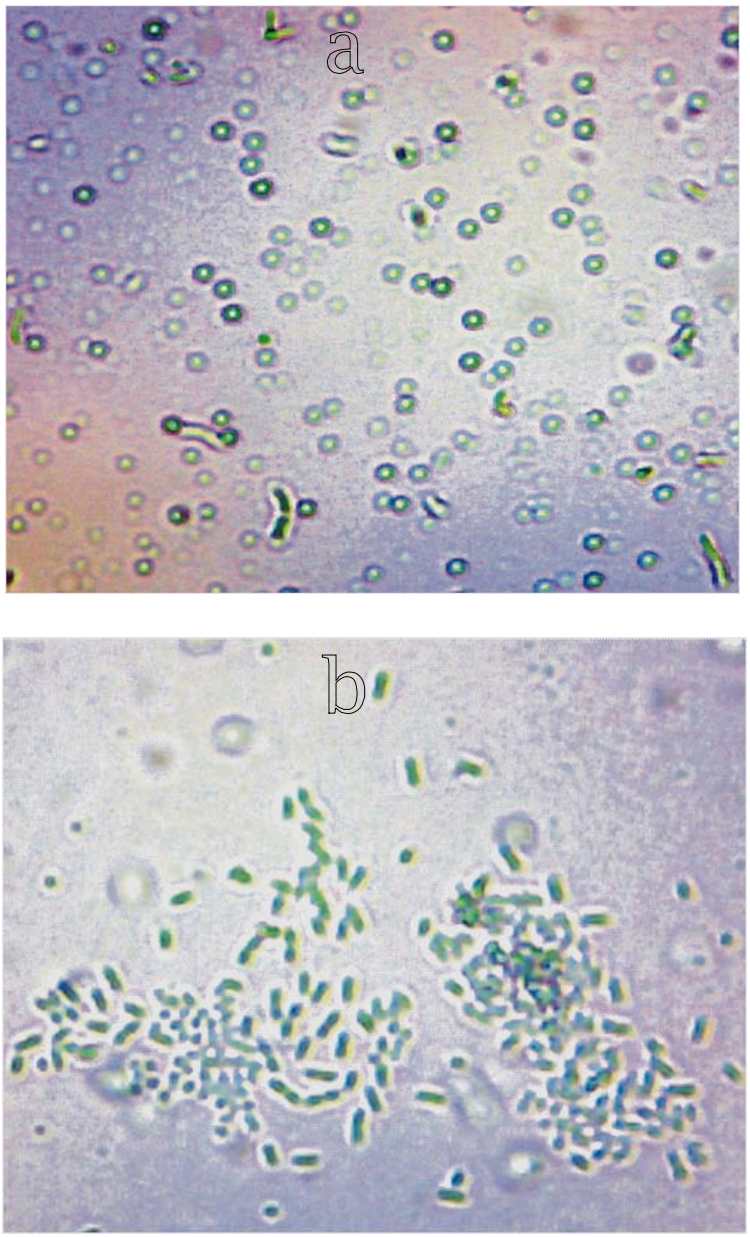

Figure 13 : Growth forms of *Mucor manihotis* induced in $(NH_4)_2SO_4$ incorporated minimal medium after 72h at temp 28°C; a, ultimate neoplastic units & binary protoplasts; b, rod shaped & binary protoplasts, x1000mag

4 a. Cytodifferentiation of Mucor species

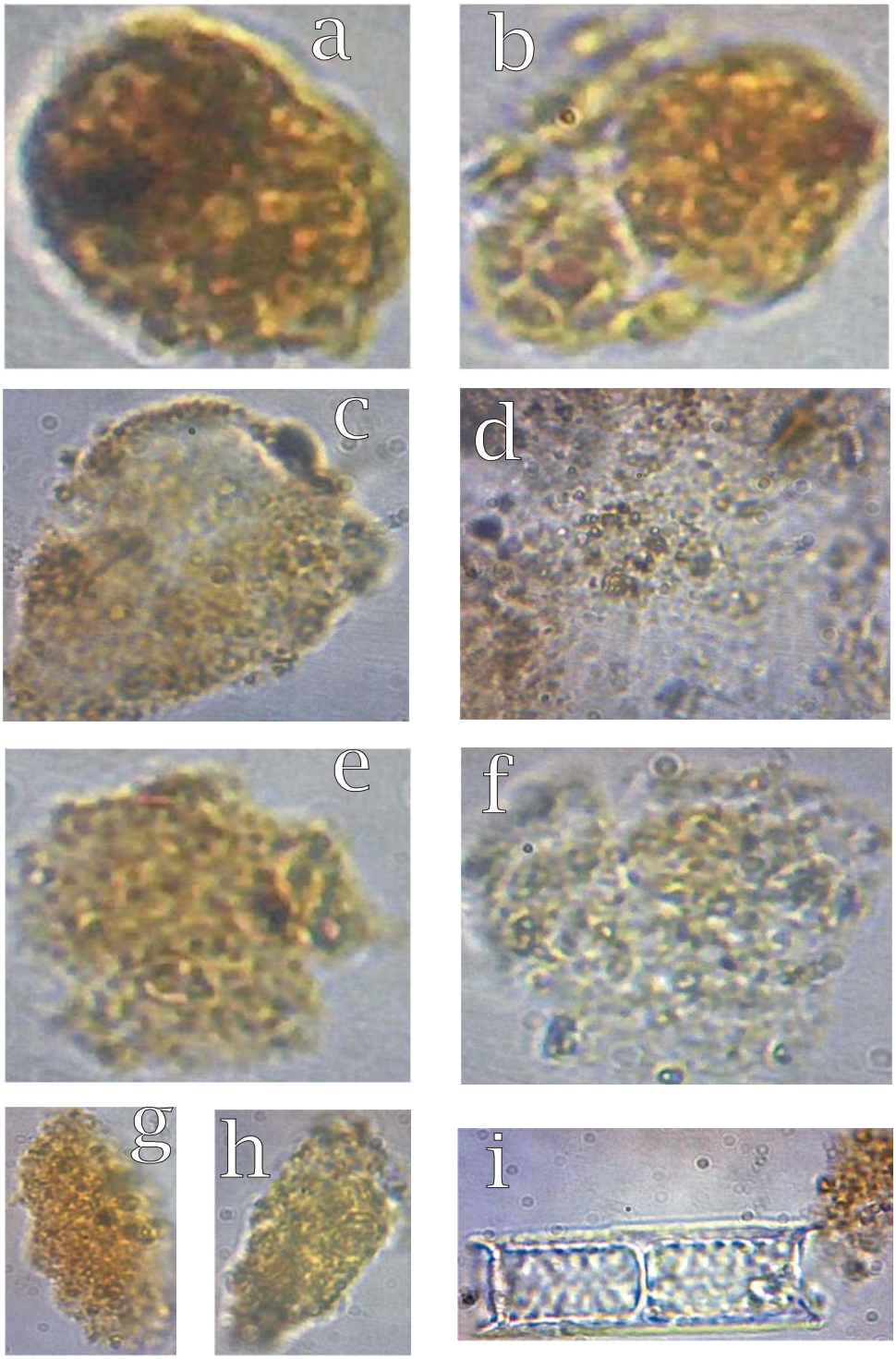

Figure 14 a- i : Growth forms of *Mucor manihotis* induced in $(NH_4)_2SO_4$ incorporated minimal medium after 96h at temp 28° C; a, spheroplast - arising from loss of cell wall; b, cytoplasm, after lysis of cytoplasmic membrane; c-h; generation of provencal entities from neoplasm arising from lysis of germ cell envelop, and i, primeval units from rupture of endoarthrospore. Observe that the entities were at various stages of undefinition. Magnification, 2500x

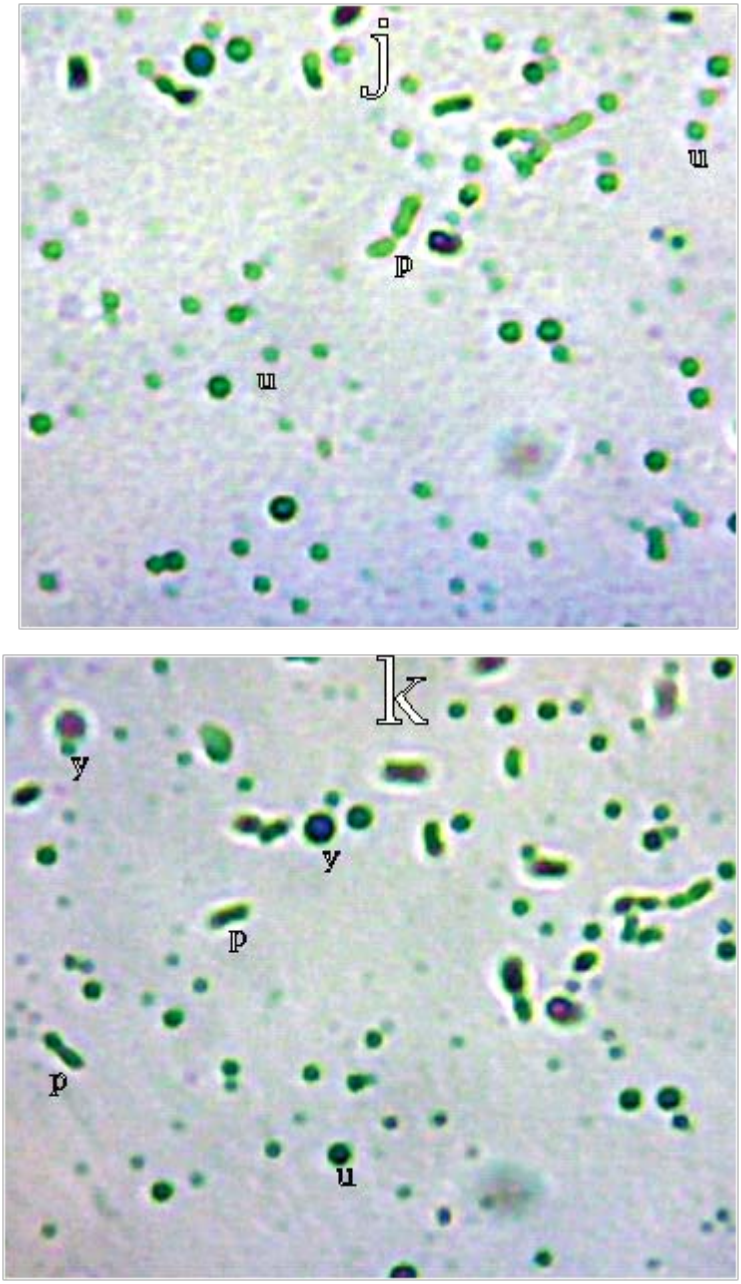

Figure 14 j k : Growth forms of *Mucor manihotis* induced in $(NH_4)_2SO_4$ incorporated minimal medium after 96h at temp 28°C; **j**, ultimate neoplastic units, binary & rod shaped protoplasts; **k**, ultimate neoplastic units (u), single & binary protoplasts (p), and globose unipolar budding yeast cells (y); x1000mag.

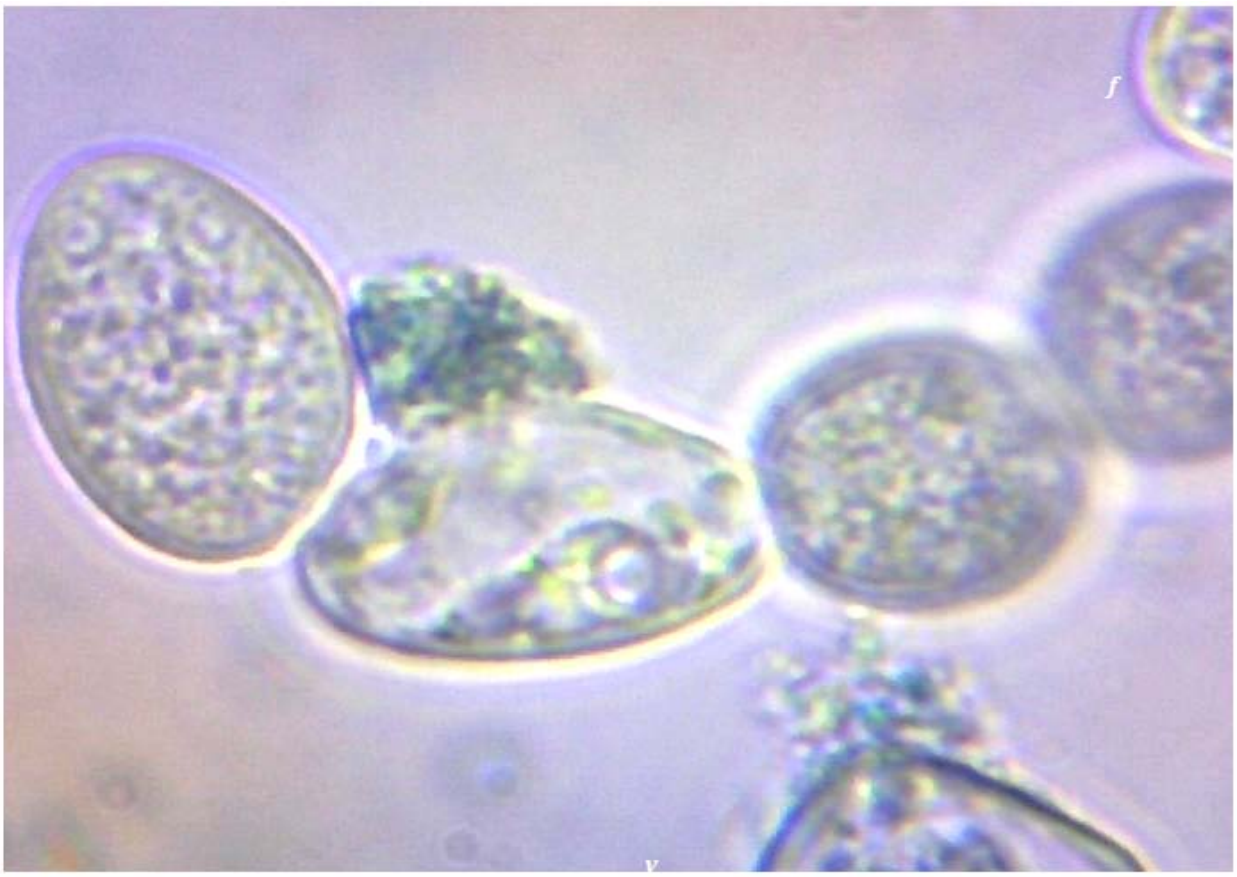

Figure 15 : Growth forms of *Mucor manihotis* induced in $(NH_4)_2SO_4$ incorporated minimal medium after 120h at temp 28°C; holoblastic conidia showing ruptured conidial wall (top & bottom) with the release of neoplastic units; this coexisted with protoplasts, unipolar budding yeast cells; x2500mag

4 b. Cytodifferentiation of Mucor species

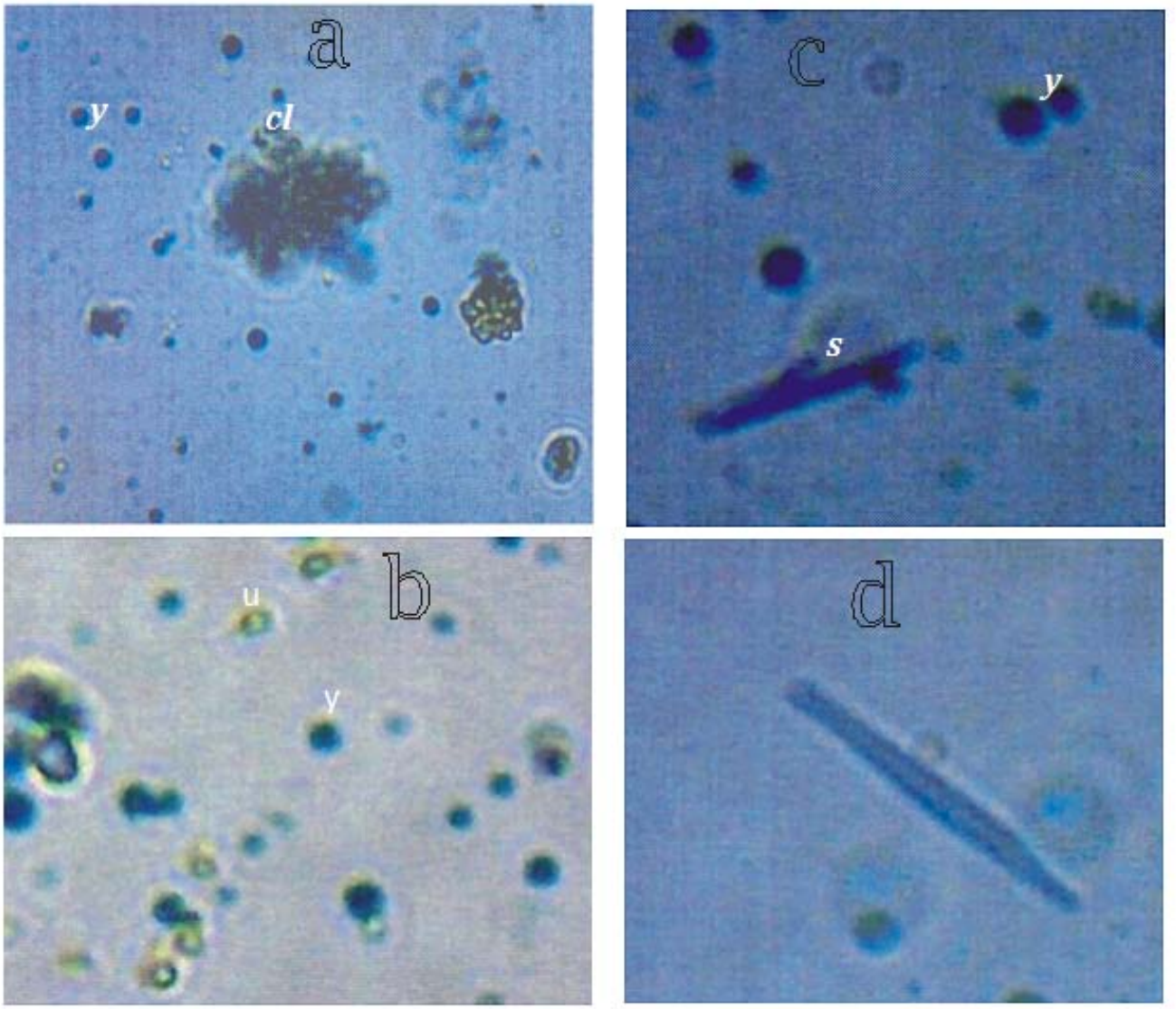

Figure 16 : Growth forms of *Mucor manihotis* induced in $(NH_4)_2SO_4$ incorporated minimal medium after 24h at temp 37°C; **a**, cluster of provencal entities (cl), differentiating units (y) & globose yeast cell; **b**, ultimate neoplastic units (u) & yeast cells (y); **c**, unipolar budding yeast cells (i) & spindle shaped yeast cell (ii); **d**, another elevation of the spindle shaped cell shown in 'c' above; x2500mag.

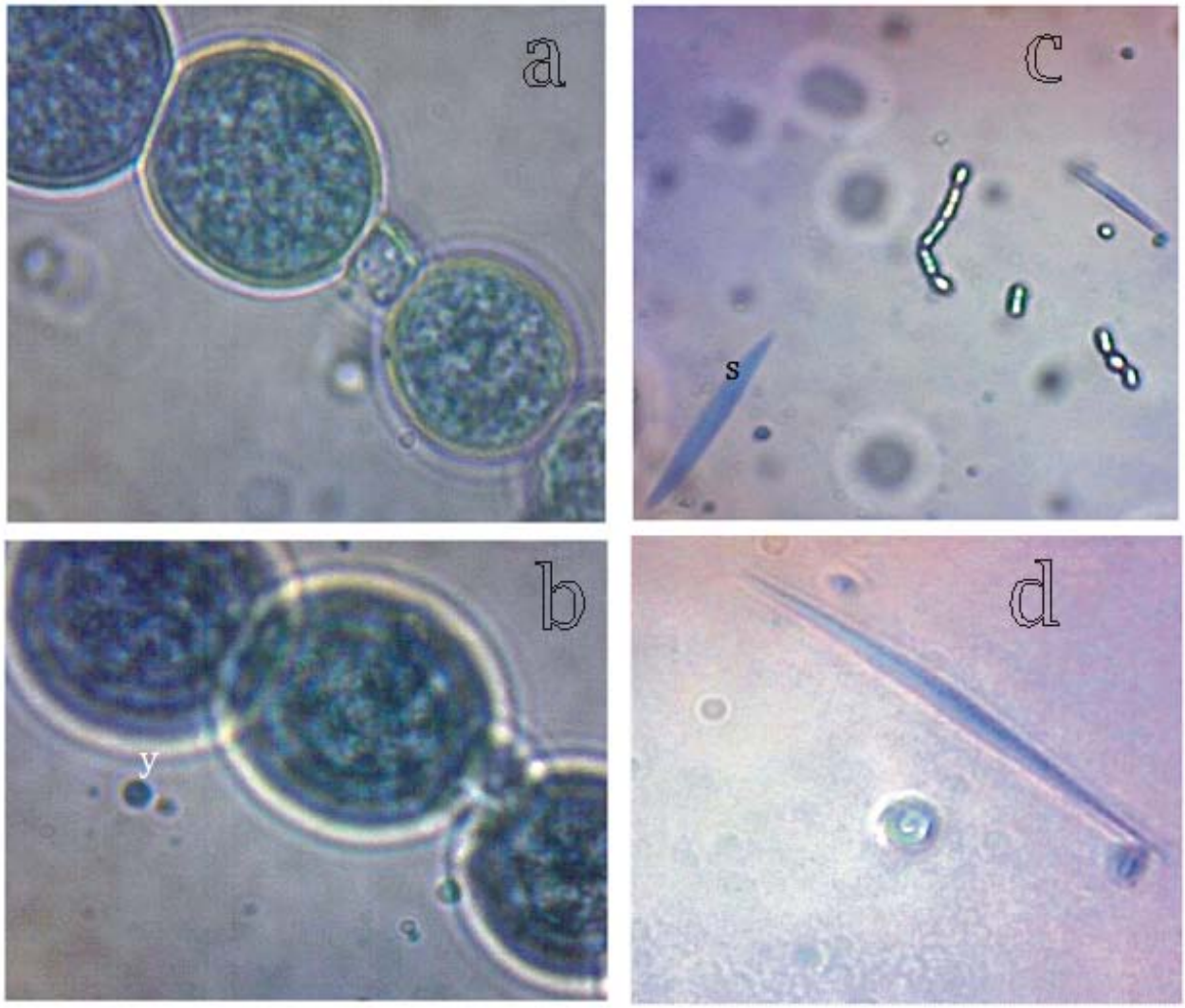

Figure 17 : Growth forms of *Mucor manihotis* induced in $(NH_4)_2SO_4$ incorporated minimal medium after 48h at temp 37° C; a, holoblastic conidia; b, another elevation of the holoblastic conidia revealing unipolar budding yeast cell (y); c, holoblastic conidia & spindle shaped cells (s); d, refocus on 's' above. All magnifications are at 2500x

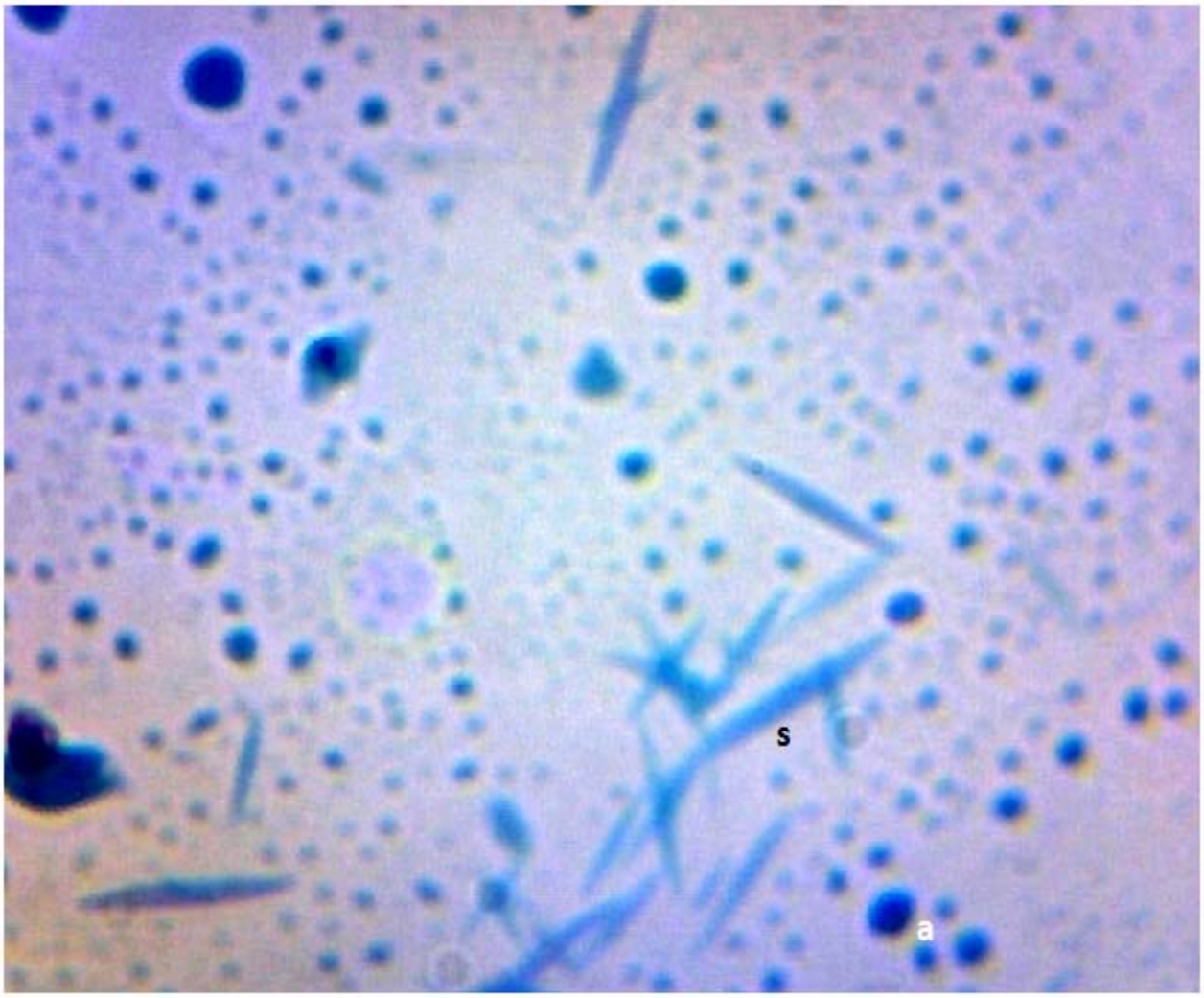

Figure 18a : Growth forms of *Mucor manihotis* induced in $(NH_4)_2SO_4$ incorporated minimal medium after 72h at temp 37° C; a, globose yeast cells; b, spindle shaped yeast cells (s); mag; 2500x

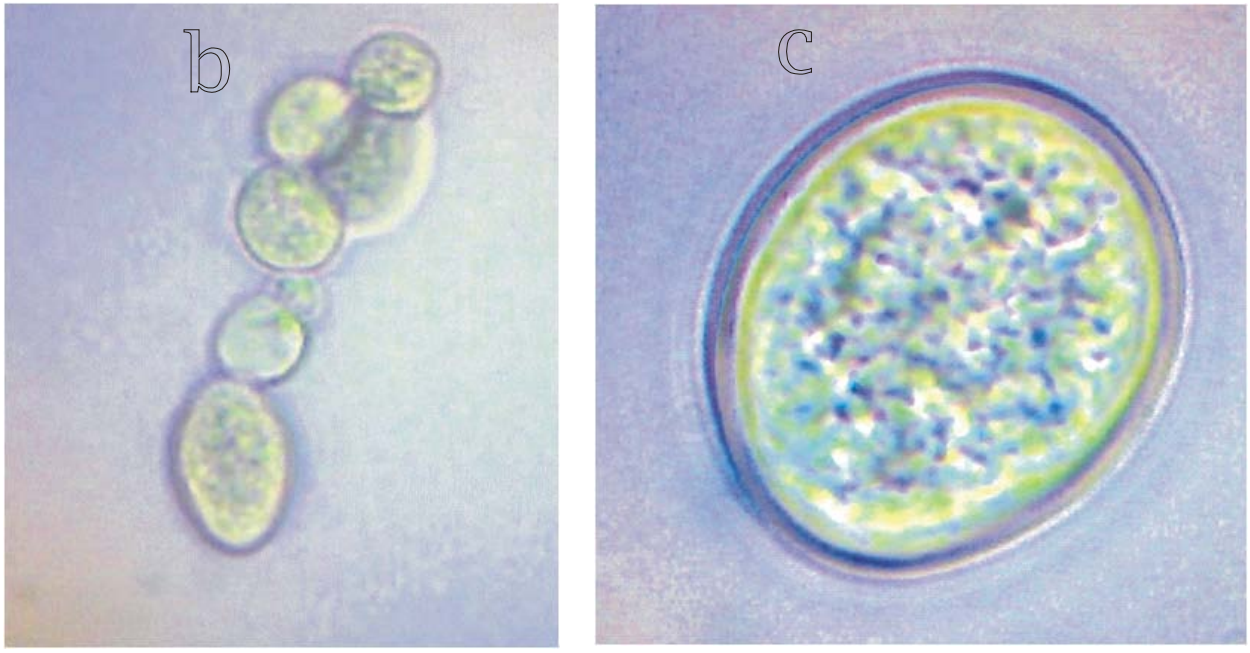

Figure 18 b c : Growth forms of *Mucor manihotis* induced in $(NH_4)_2SO_4$ incorporated minimal medium after 72h at temp 37°C; b, holoblastic conidia, x1000mag; c, globose conidium with differentiated cytoplasm thus appearing a s granular entities, mag; 2500x

5 a. Cytodifferentiation of Mucor species

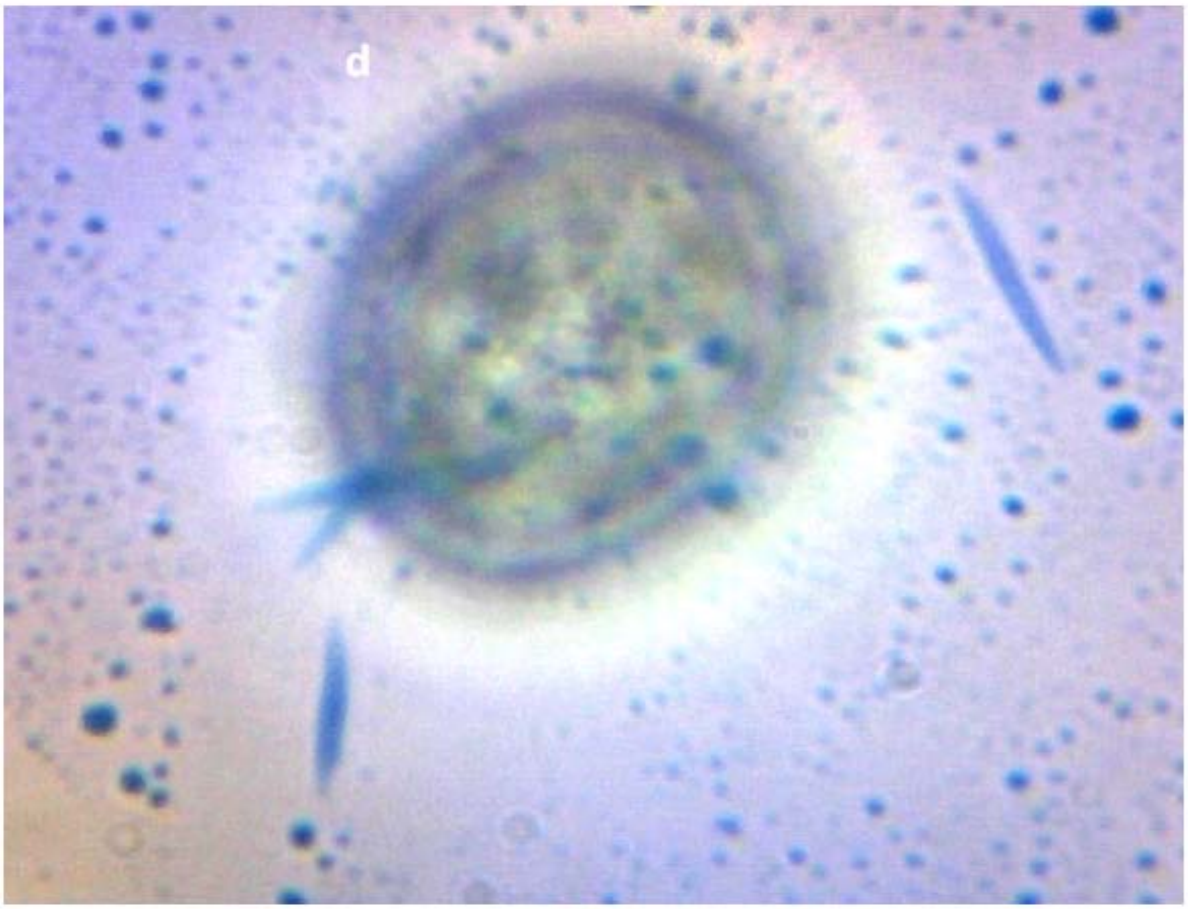

Figure 18d : Growth forms of *Mucor manihotis* induced in $(NH_4)_2SO_4$ incorporated minimal medium after 72h at temp 37°C; another elevation of the conidium in fig 22b, showing globose & spindle shaped yeast cells; mag; 2500x

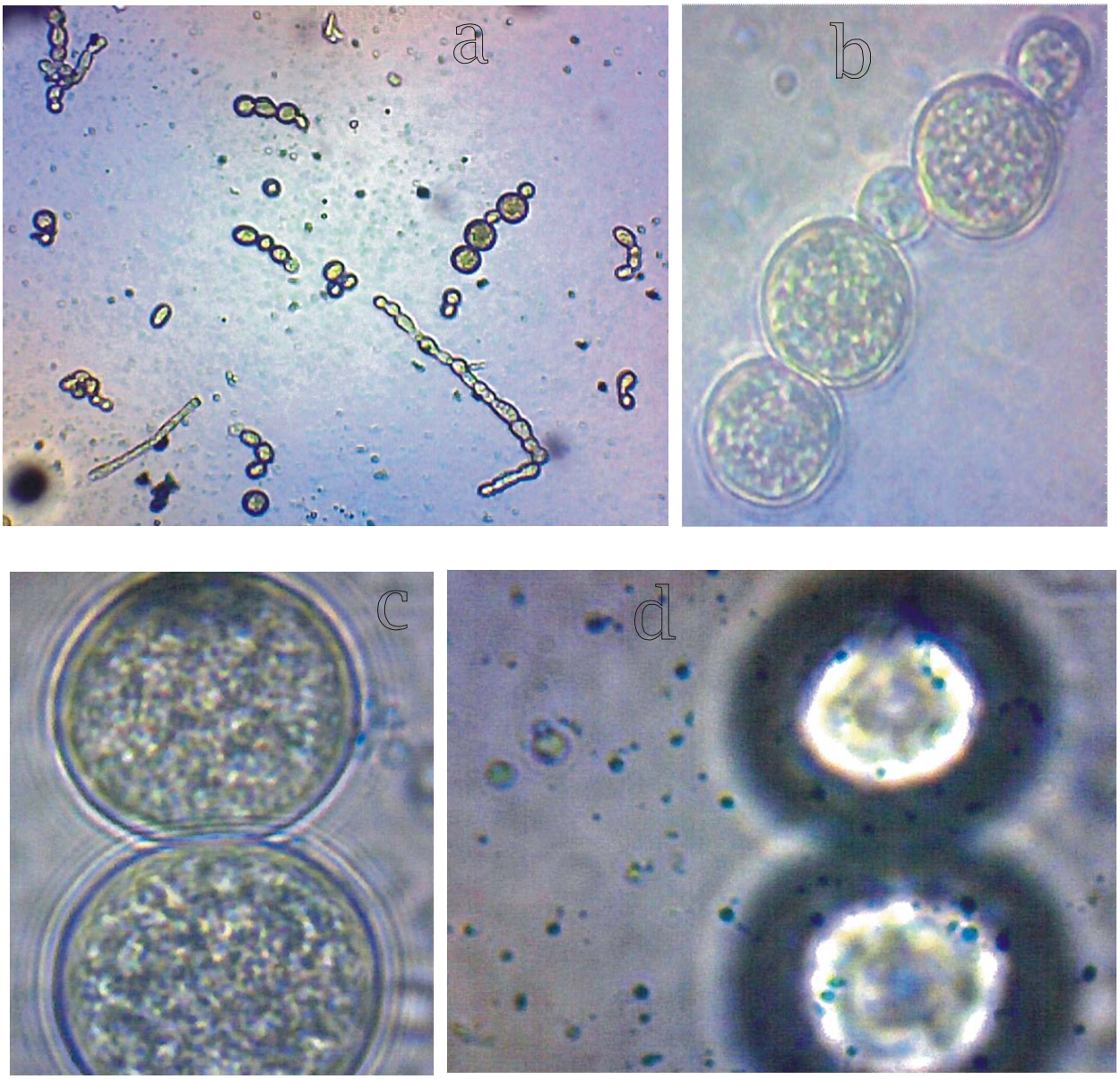

Figure 19 a-d : Growth forms of *Mucor manihotis* induced in $(NH_4)_2SO_4$ incorporated minimal medium after 96h at temp 37°C; **a**, various forms of holoblastic conidia, x800mag; **b**, holoblastic conidia arrowed in 'a', x1000mag; **c**, holoblastic conidia in 'b' at x2500mag showing granular cytoplasm; **d**, another elevation of the conidia in fig 23c, showing coinduced globose & budding yeast cells; mag; 2500x

5 b. Cytodifferentiation of Mucor species

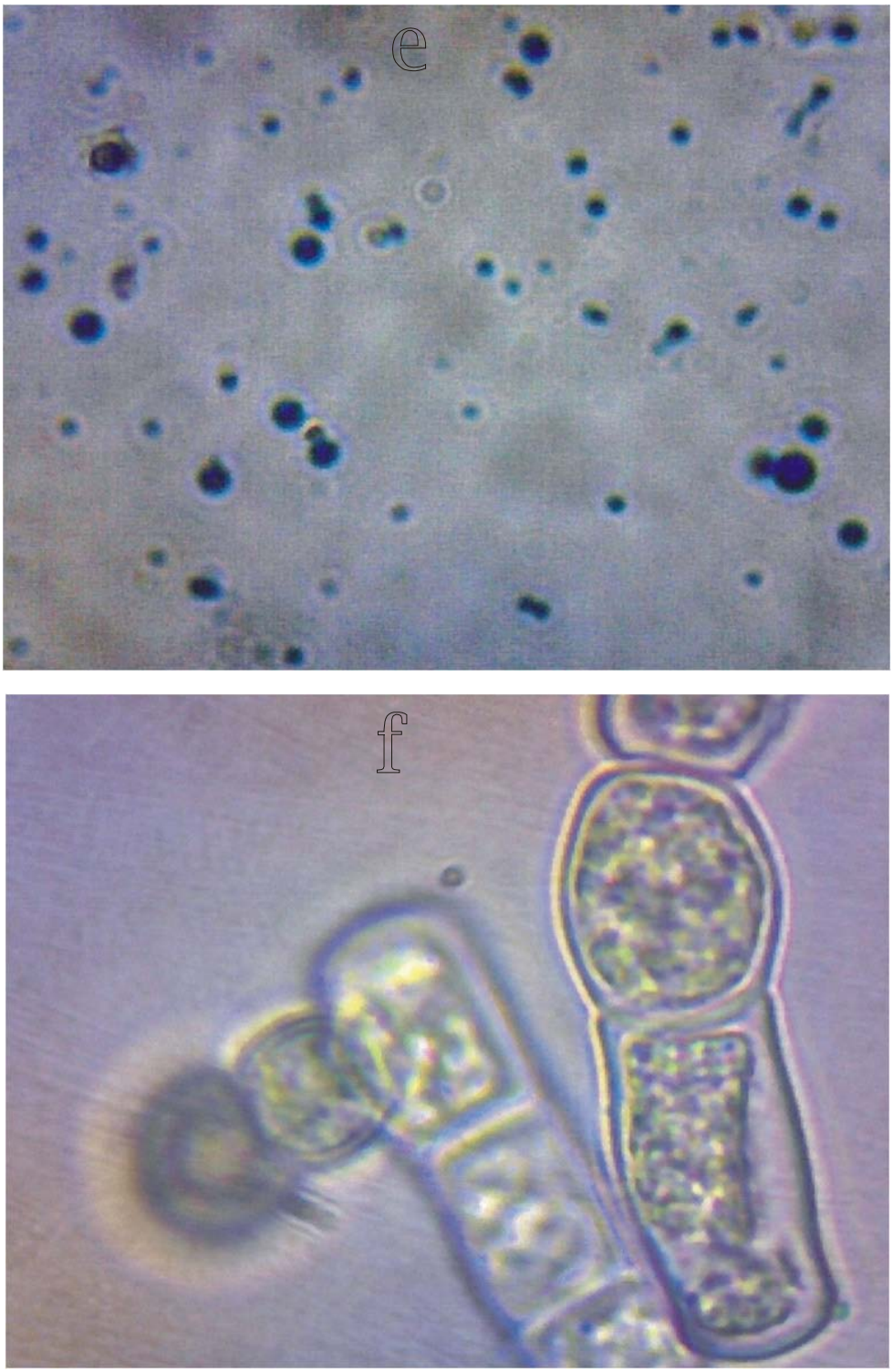

Figure 19 e-f : Growth forms of *Mucor manihotis* induced in $(NH_4)_2SO_4$ incorporated minimal medium after 96h at temp 37°C; e, globose yeast cells – this was the most predominant form & co-existed with spindle shaped yeast cells, x2500mag; f, thallo-arthric conidia, this was however scanty, x2500mag

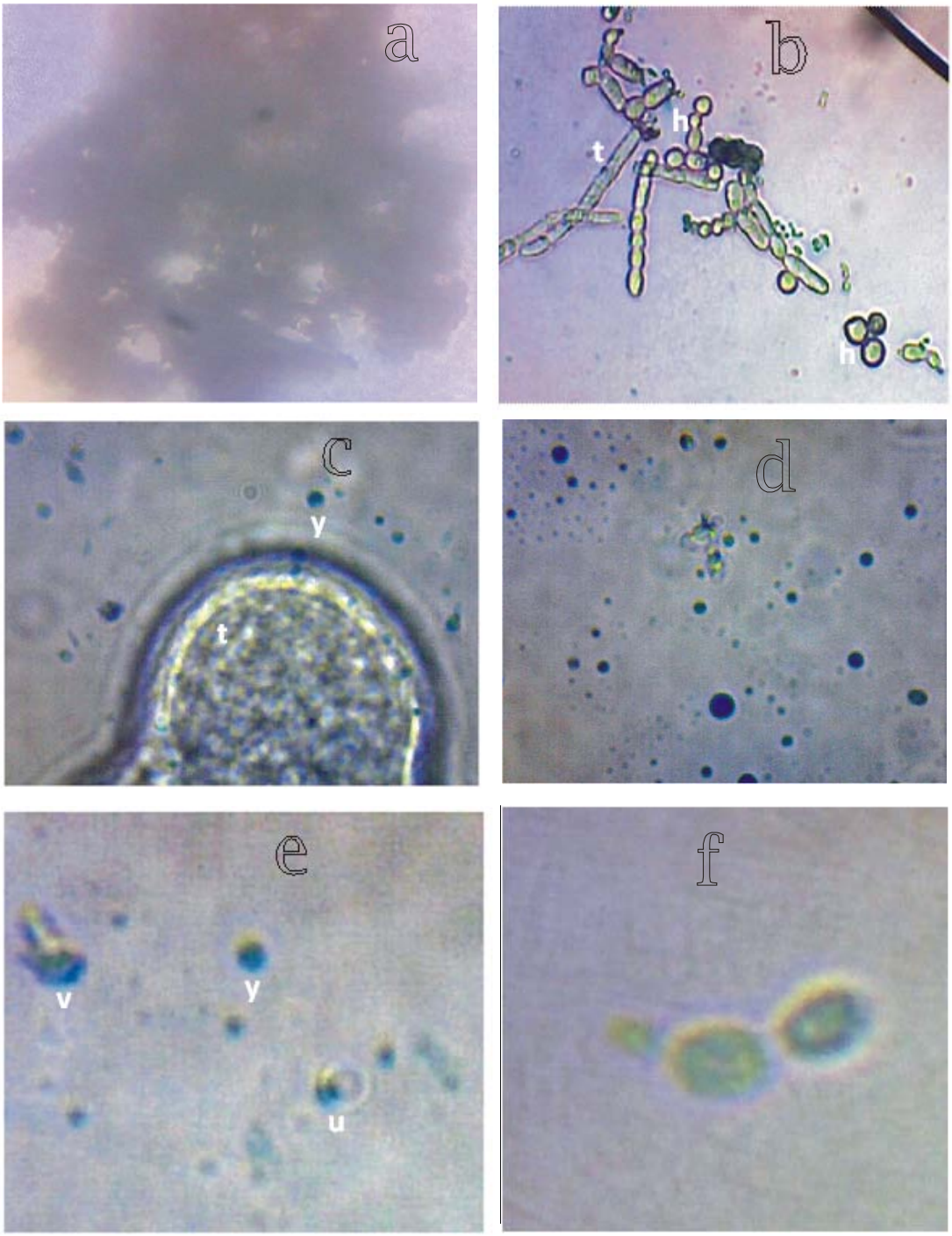

Figure 20 : Growth forms of *Mucor manihotis* induced in $(NH_4)_2SO_4$ incorporated minimal medium after 120h at temp 37°C; **a**, cluster of provencal neoplastic units (appeared finely grainy @ this mag); **b**, various forms of holoblastic, 'h' & thallic, 't' conidia; **c**, globose yeast cells, 'y', adjacent to thallic conidia; **d**, globose yeast cells; **e**, nascent yeast initial 'v' (out of focus); y (globose yeast), u (ultimate neoplastic unit); **f**, ovoidal yeast cells – these along with globose & spindle yeast cells were predominant forms coinduced with conidia in this medium. Magnification; a, c-f, x2500; b, x800.

6 a. Cytodifferentiation of *Mucor* species

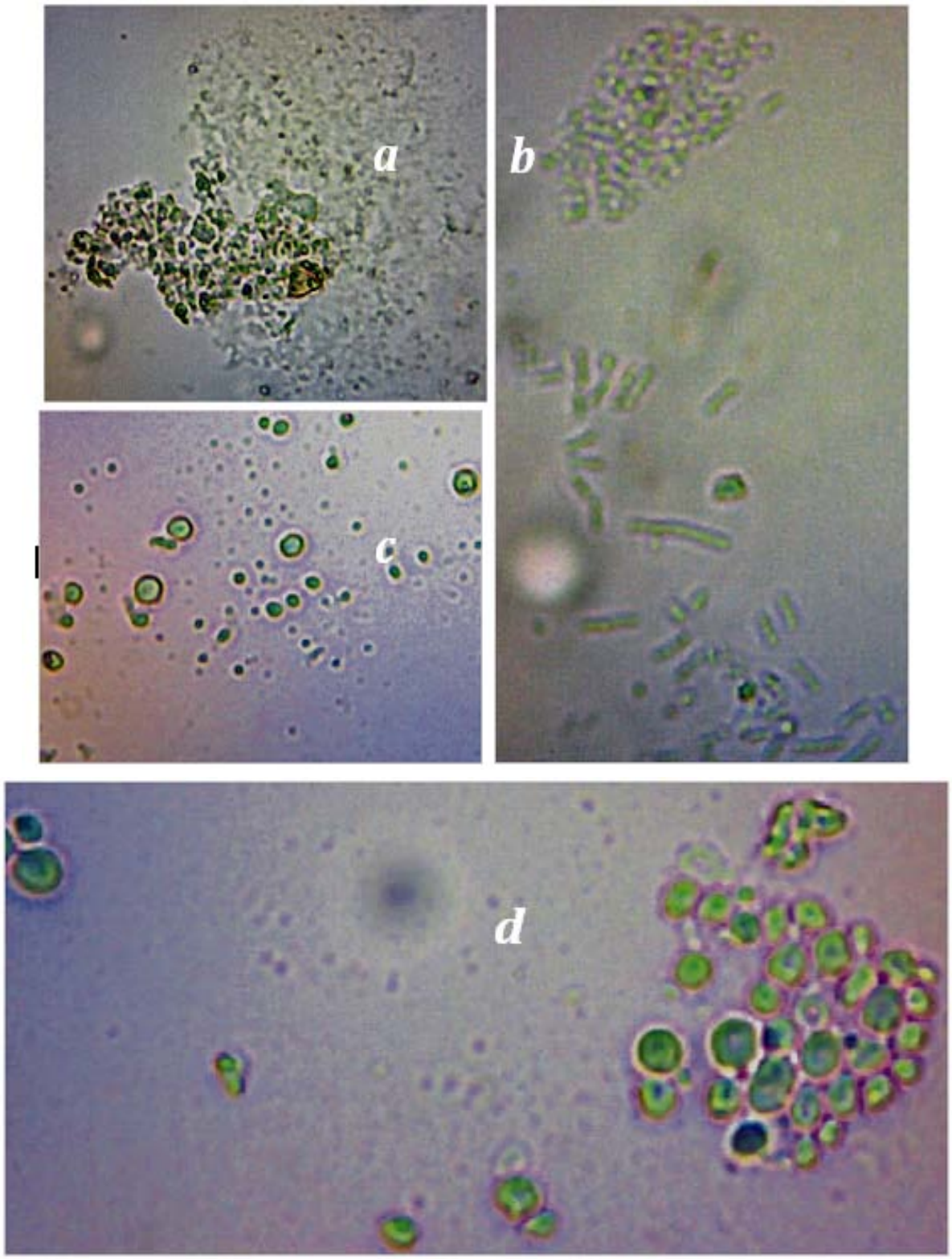

Figure 21 : Growth forms of *Mucor manihotis* induced in peptone incorporated minimal medium after 24h of incubation at temp 15°C; **a**, dispersing nondescript neoplastic entities; **b**, single rod-shaped & binary protoplasts; **c**, globose prevegetative cells; **d**, budding yeast cells. Magnification: 2500x.

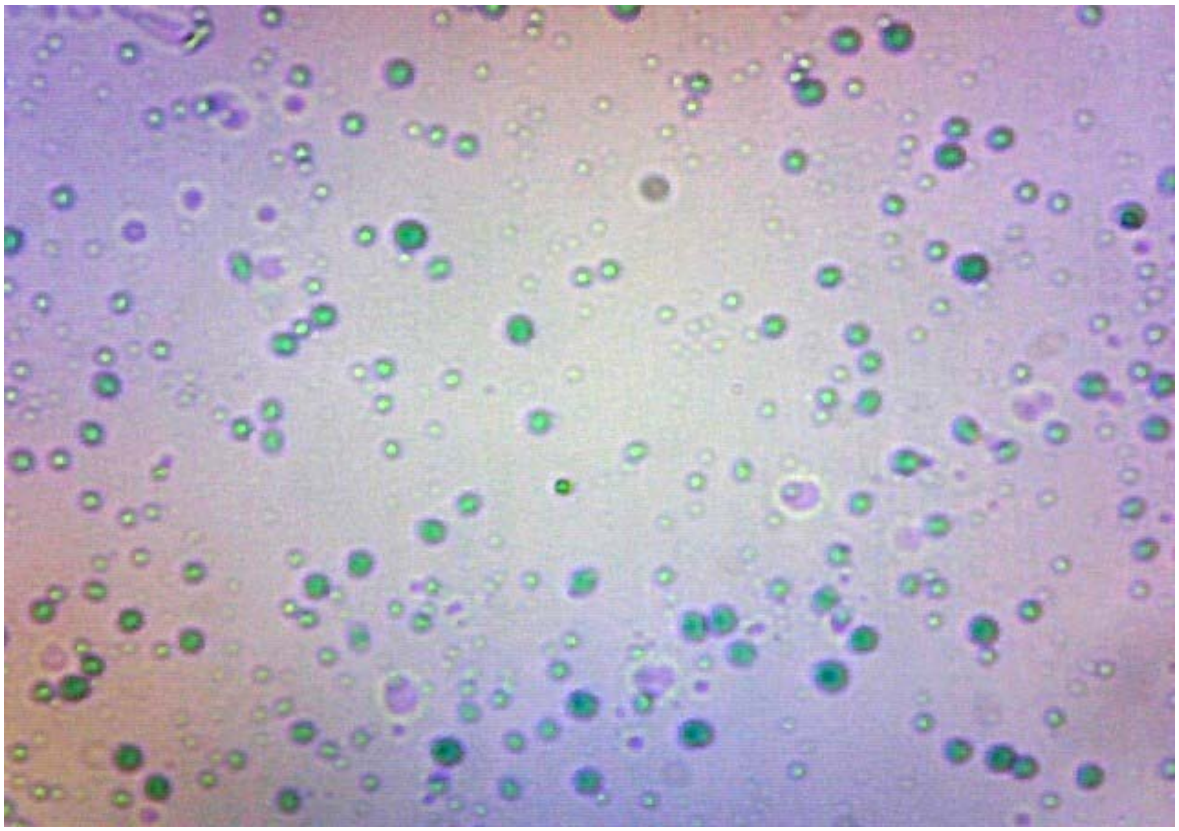

Figure 22 : Growth forms of *Mucor manihotis* induced in peptone incorporated minimal medium after 48h of incubation at temp 15°C showing numerous ultimate neoplastic units. Magnification: 1000x

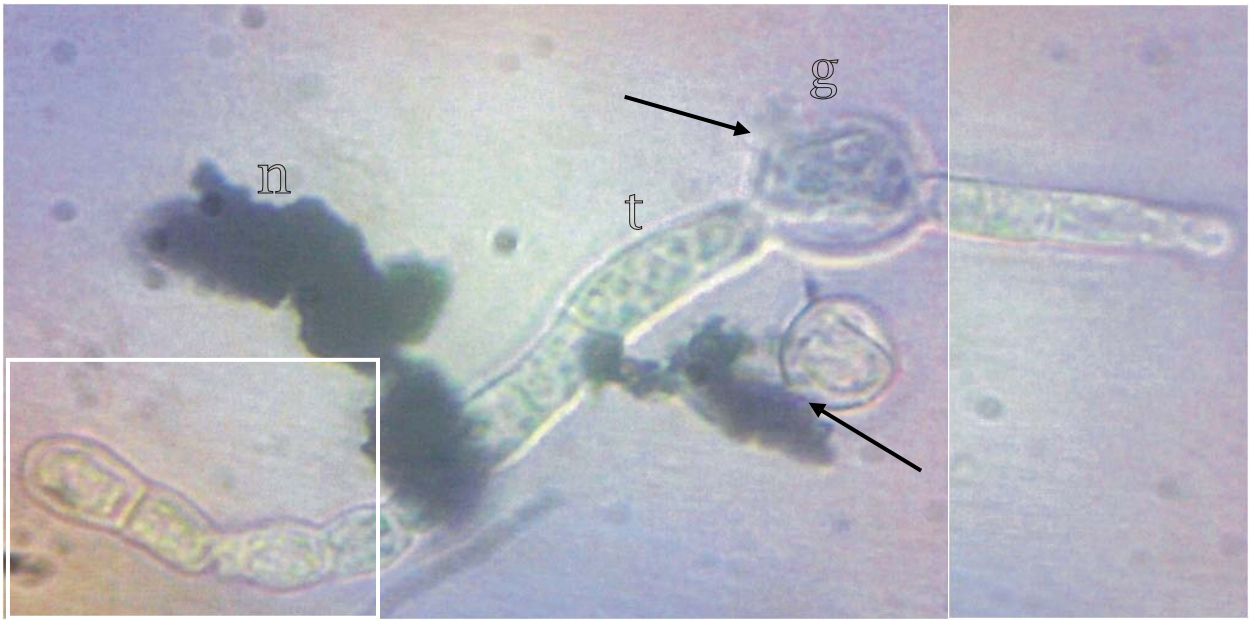

Figure 23 a : Growth forms of *Mucor manihotis* induced in peptone incorporated minimal medium after 72h of incubation at temp 15°C showing thallic growth, 't' and neoplasm, 'n'; g, growth sphere. Note: cell wall of growth sphere ruptured (arrow) releasing clusters of granular units, but subsequently dispersed by broth conventional current. Magnification: 1000x

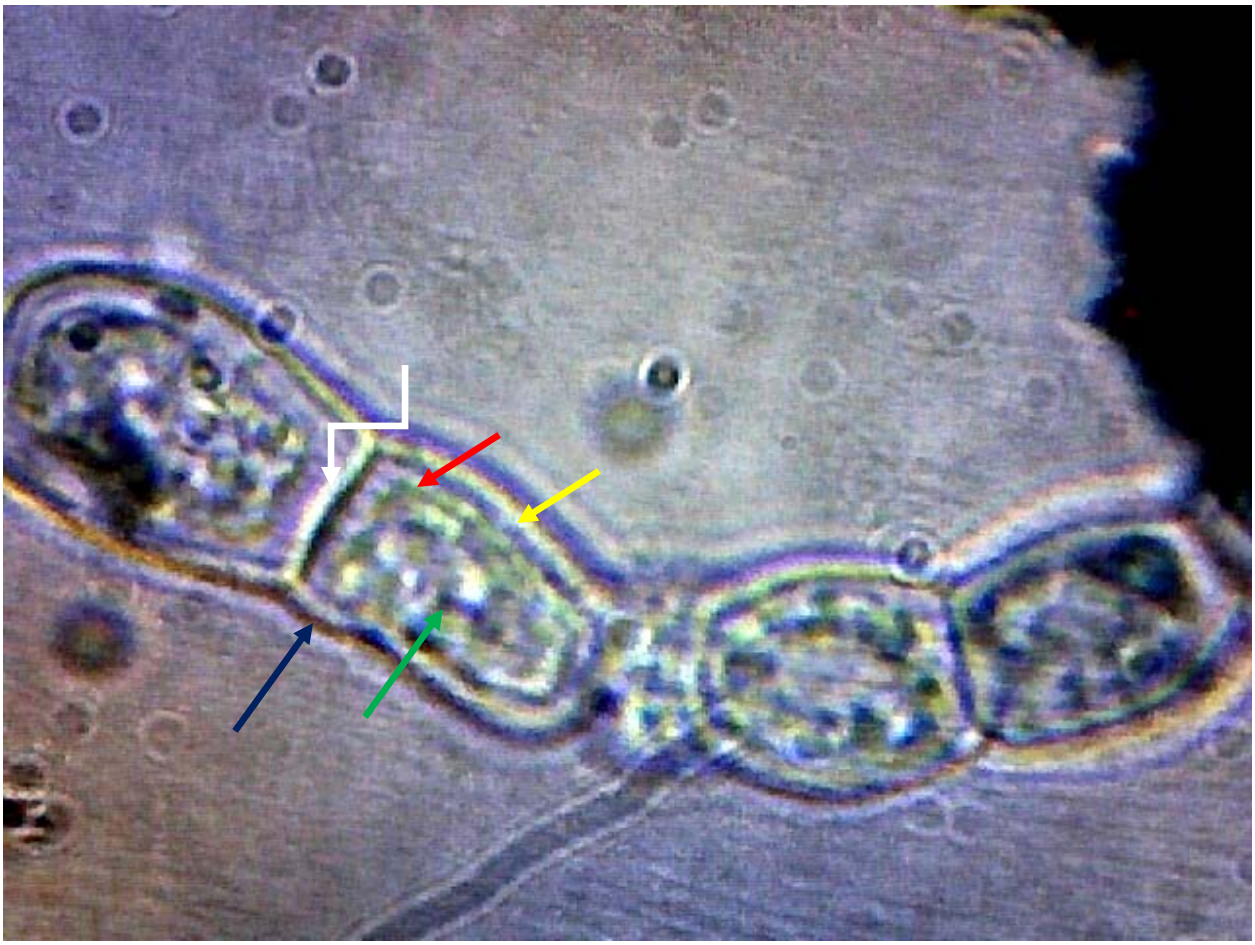

Figure 23 b : Growth forms of *Mucor manihotis* induced in peptone incorporated minimal medium after 72h of incubation at temp 15°C showing part of thallic growth and neoplasm, box in fig. 27a. Arrows indicate characteristics of a true fungus: hyphal wall (blue); internal arthrosporal wall (yellow); septum (white); cytoplasmic membrane (red); cytoplasm (green). Magnification: 2500x

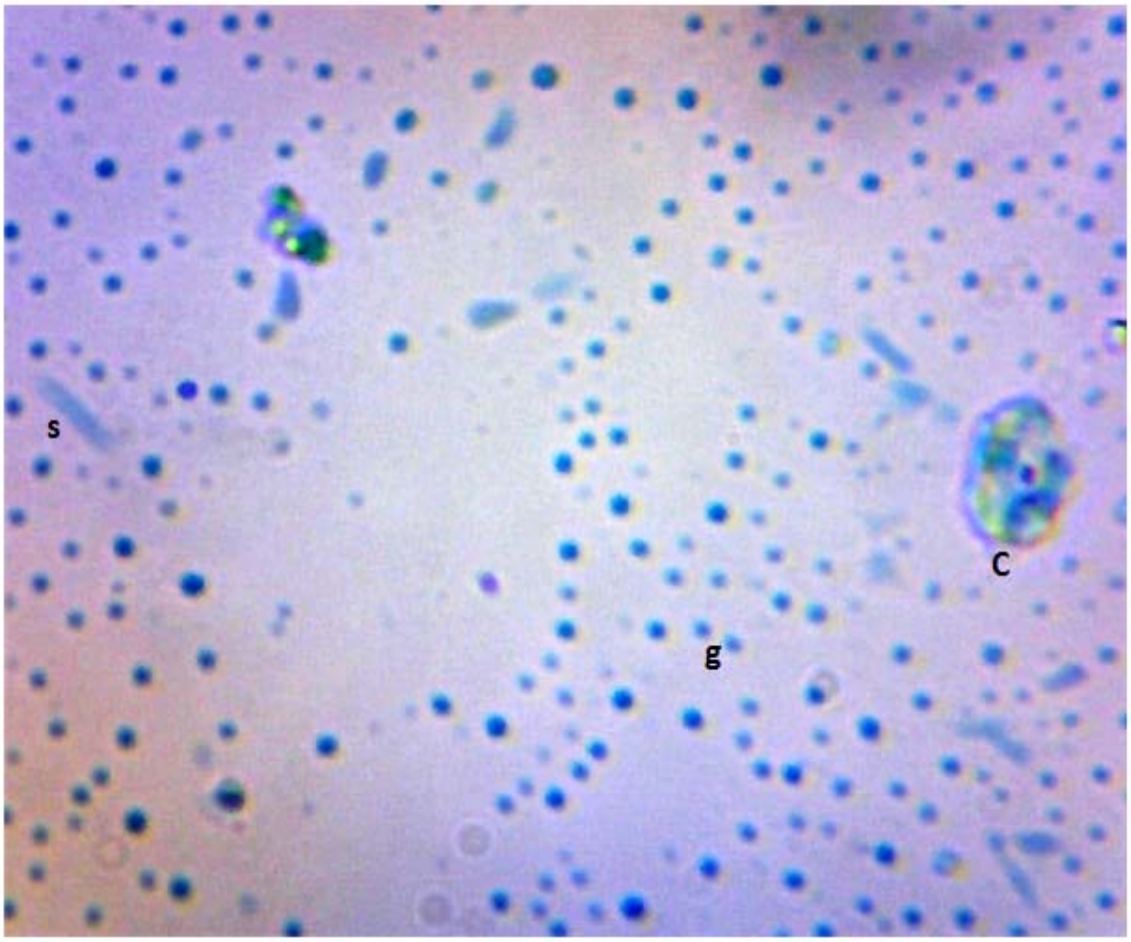

Figure 23 c : Growth forms of *Mucor manihotis* induced in peptone incorporated minimal medium after 72h of incubation at temp 15°C showing cytoplasm (c), globose yeast cells (g) & spindle shaped yeast cell (out of focus). Magnification: 2500x.

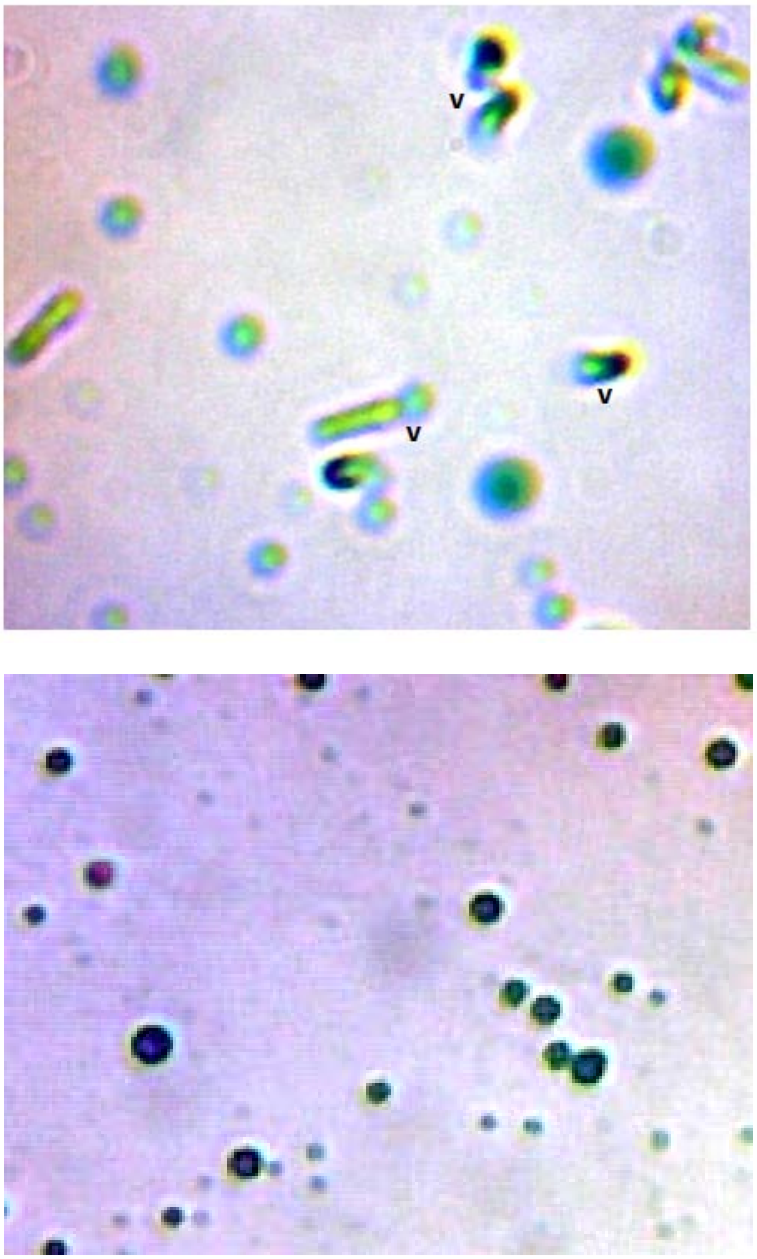

Figure 24 : Growth forms of *Mucor manihotis* induced in peptone incorporated minimal medium after 96h at temp 15° C; a, protoplasts with nascent yeast initial (v); b, budding yeast cells in singles and double. Magnification: 1000x

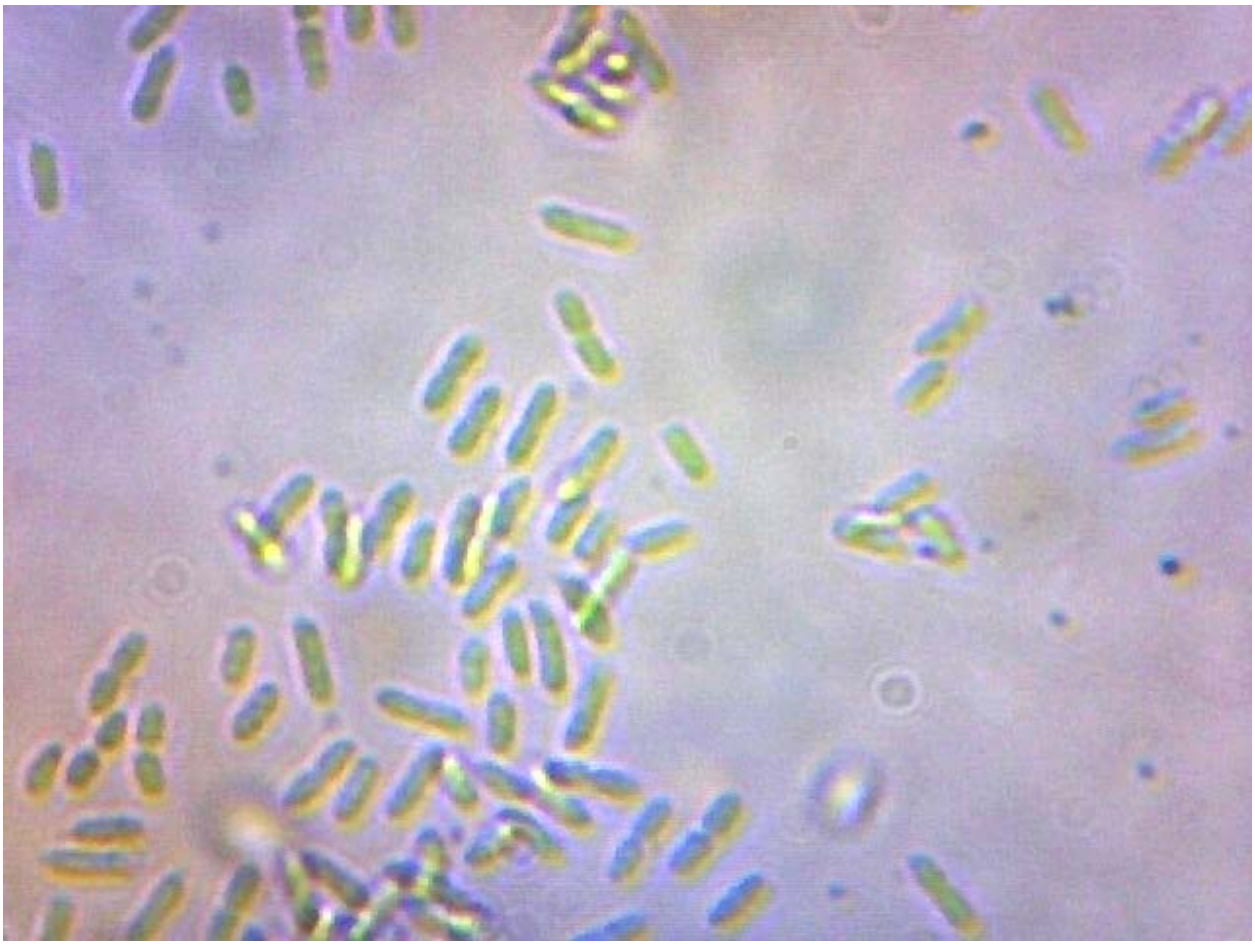

Figure 25 a : Growth forms of *Mucor manihotis* induced in peptone incorporated minimal medium after 120h of incubation at temp 15°C showing rod shaped & binary protoplasts. Magnification: 2500x

6 b. Cytodifferentiation of Mucor species

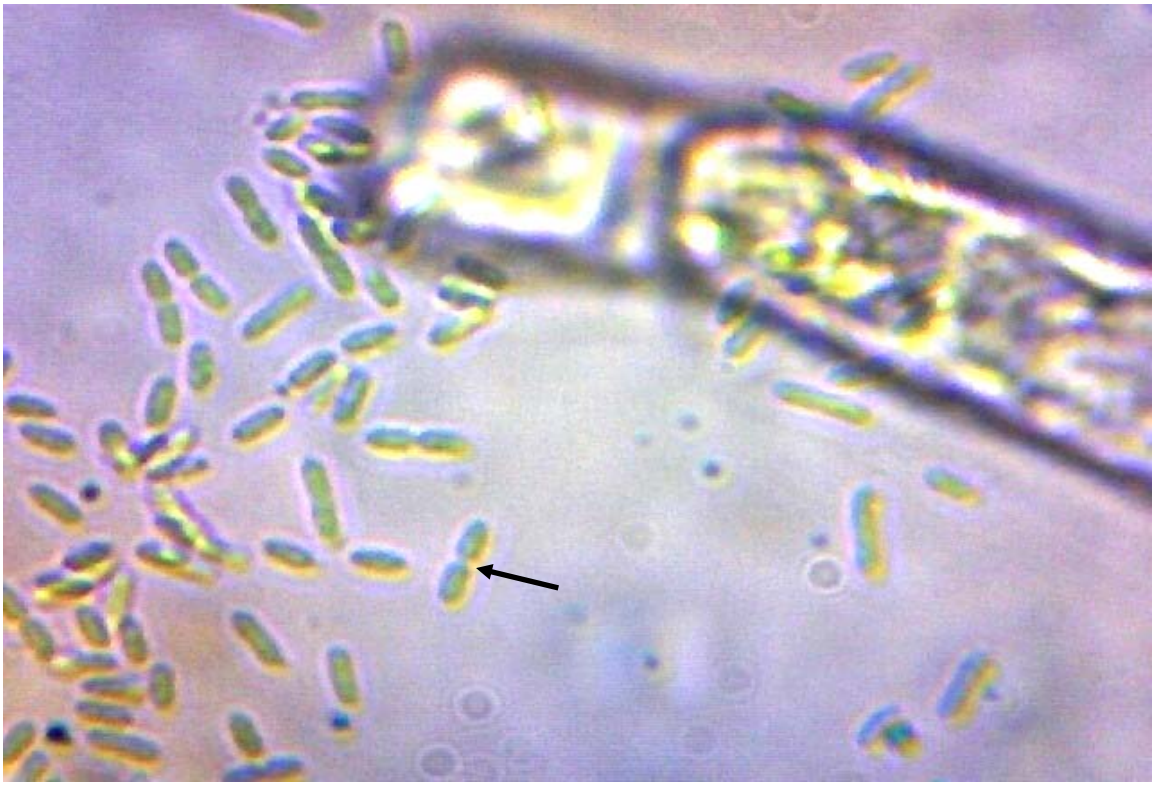

Figure 25 b : Growth forms of *Mucor manihotis* induced in peptone incorporated minimal medium after 120h of incubation at temp 15°C showing protoplasts and thallic growth (out of focus). Observe the short denticle of the binary protoplasts (arrow). Magnification: 2500x

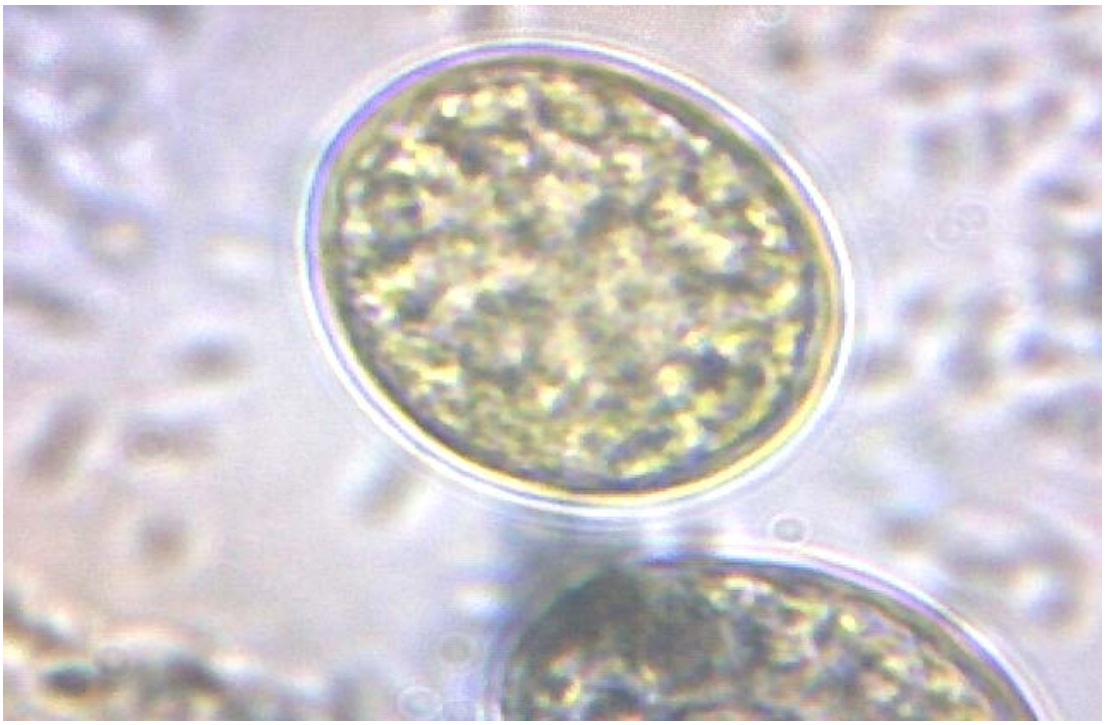

Figure 25 c : Growth forms of *Mucor manihotis* induced in peptone incorporated minimal medium after 120h of incubation at temp 15°C; protoplasm of conidia undergoing differentiation from apparent cytoplasmic consistency. Magnification: 2500x

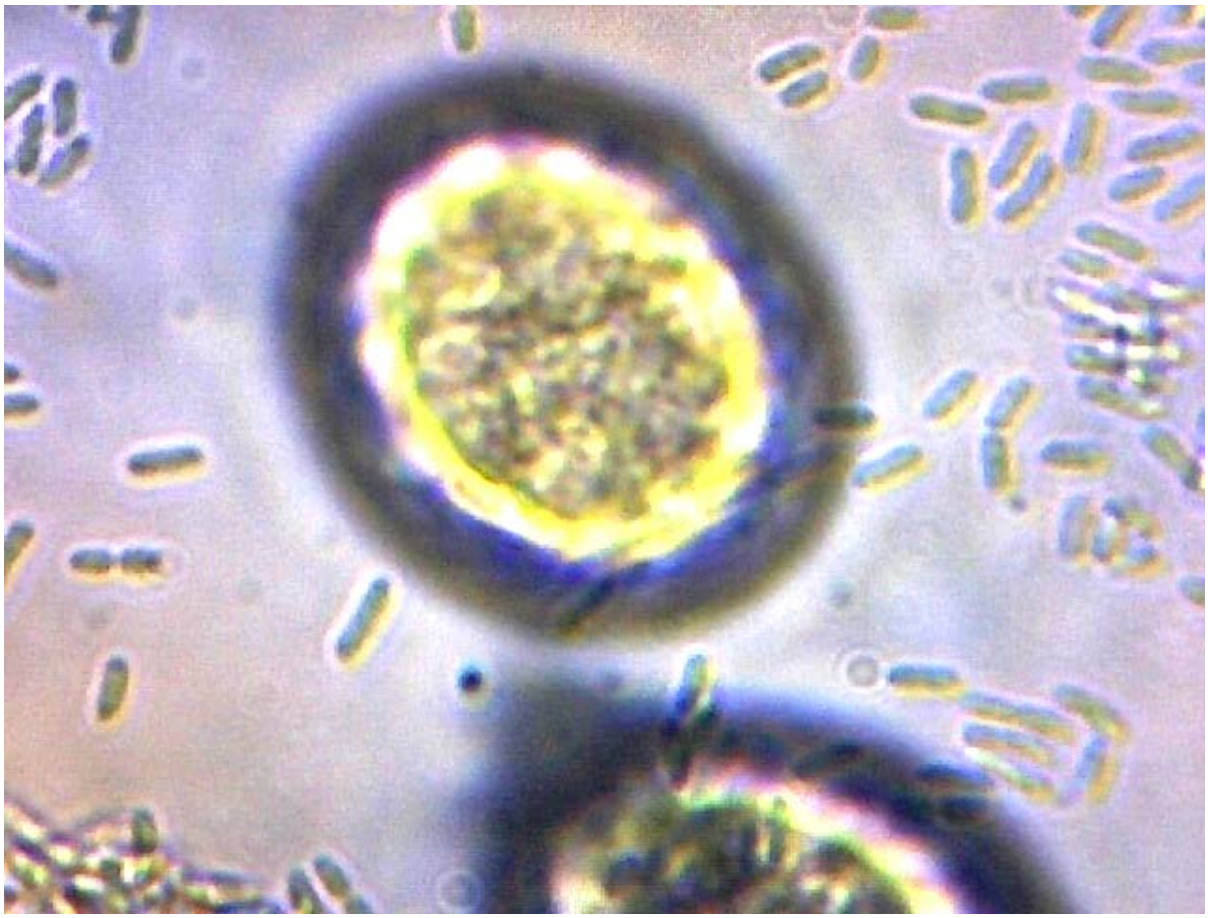

Figure 25 d : Growth forms of *Mucor manihoti*s induced in peptone incorporated minimal medium after 120h of incubation at temp 15°C; another elevation of the conidia in fig. 29c showing numerous rod shaped and denticulated binary protoplasts. Magnification: 2500x

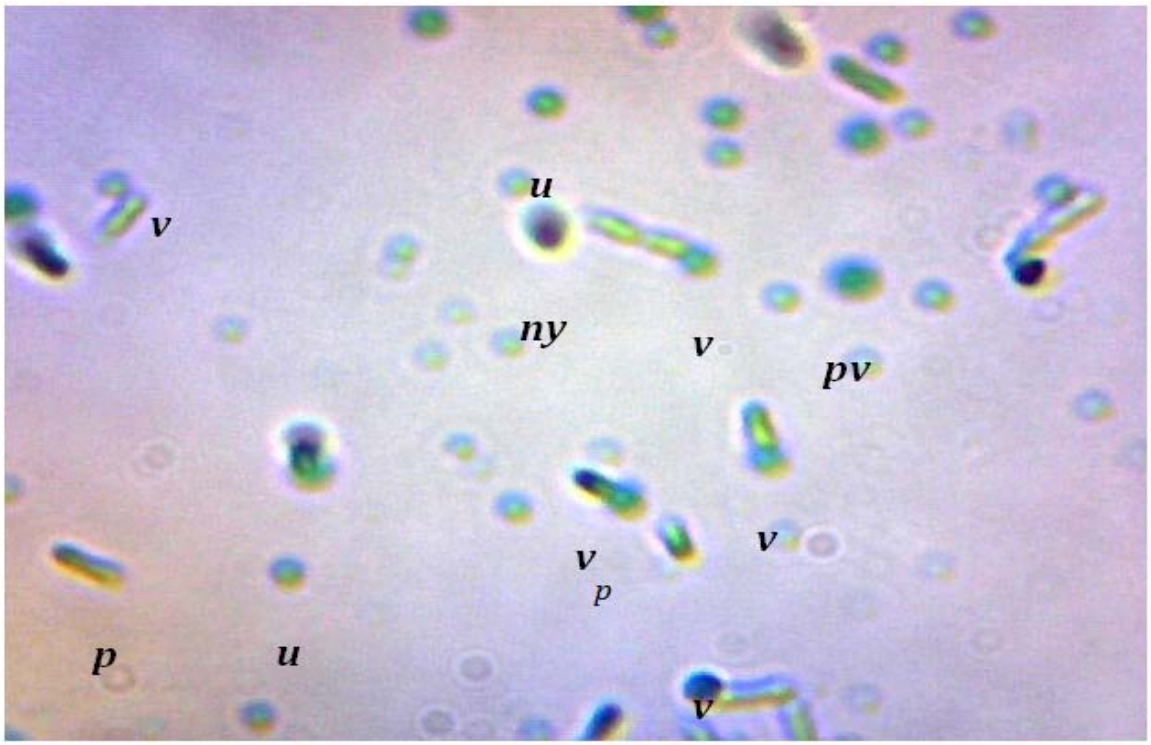

Figure 25 e : Growth forms of *Mucor manihoti*s induced in peptone incorporated minimal medium after 120h of incubation at temp 15°C showing ultimate neoplastic units (u) & protoplasts (p); nascent yeast initial*, v, single or binary, generate prevegetative cell, pv, which* on ceding grow to maturity & subsequently become polar budding. Magnification: 2500x

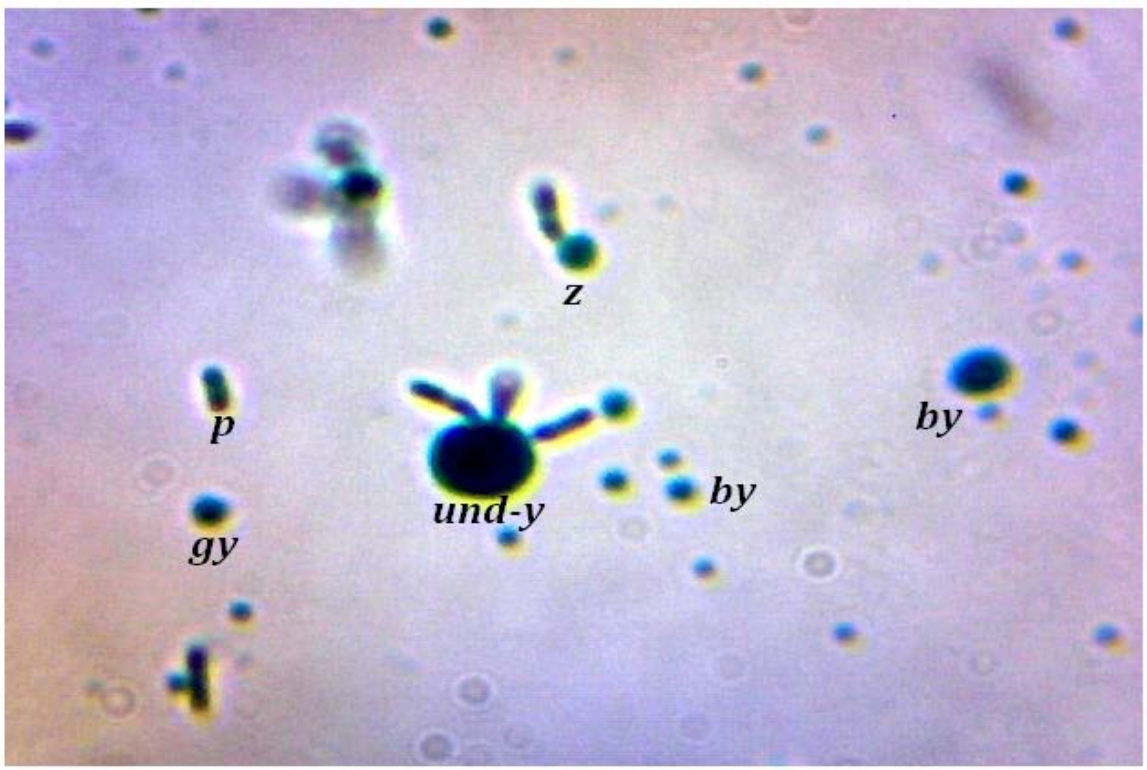

Figure 25 f : Growth forms of *Mucor manihoti*s induced in peptone incorporated minimal medium after 120h of incubation at temp 15°C showing rod-shaped protoplast (p), nascent yeast initial of binary protoplast (z), unipolar budding yeasts (by), globose yeast (gy) and undeclared yeasts (und-y). Magnification: 2500x

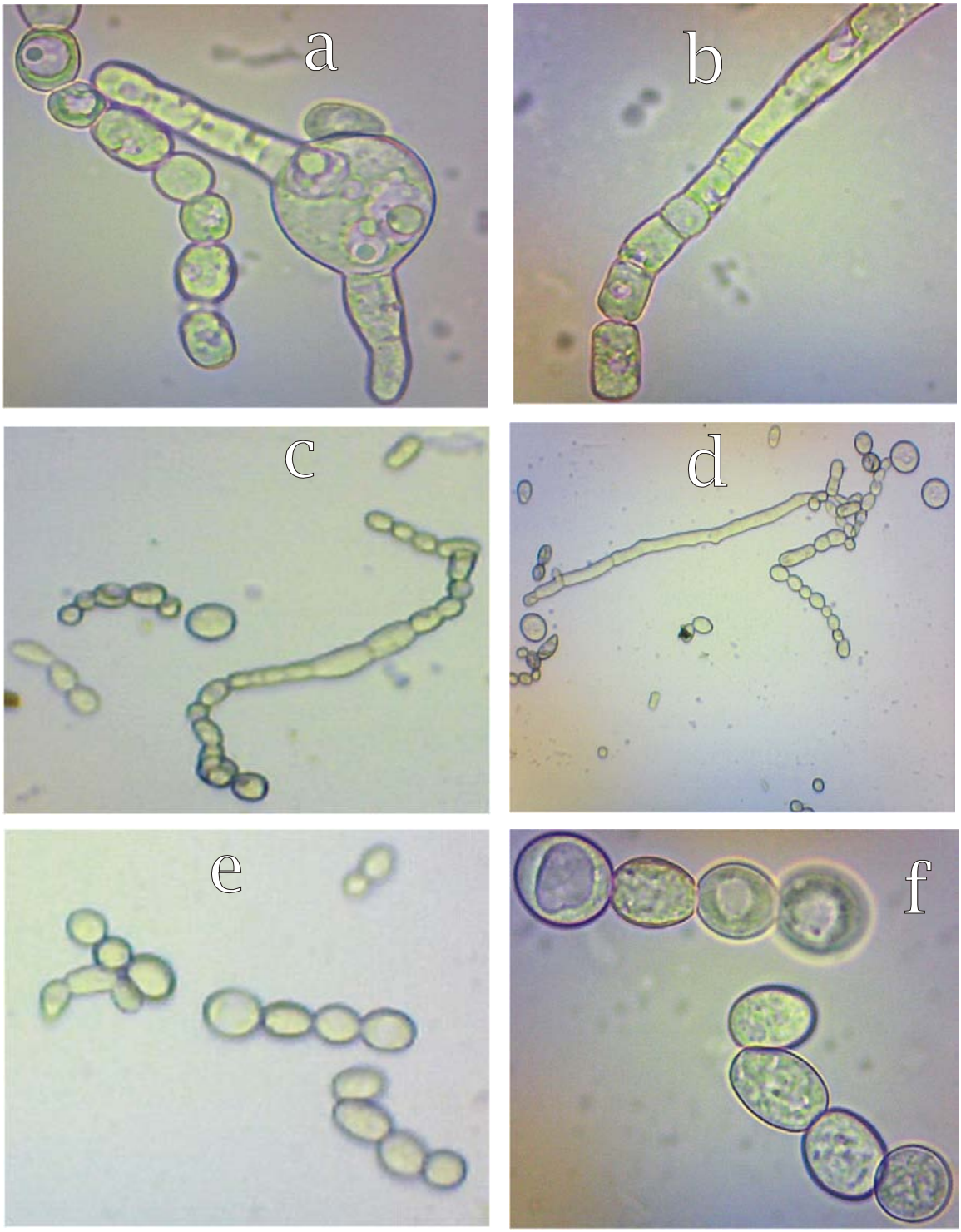

Figure 26 : Growth forms of *Mucor manihotis* induced in peptone incorporated minimal medium after 24h of incubation at temp 28°C showing various types of conidia; **a**, growth sphere with double germ tubes & aligned with holoblastic conidia; **b**, thalloarthric conidia ceding by fragmentation; **c**, types of holoblastic conidia; **d**, arthric conidia formed after determinate thallic growth; **e** forms of holoblastic conidia; **f**, holoblastic conidia 'e' at higher magnification. Magnification: a-b,f: 1000x; c-d: 400x; e, 800x

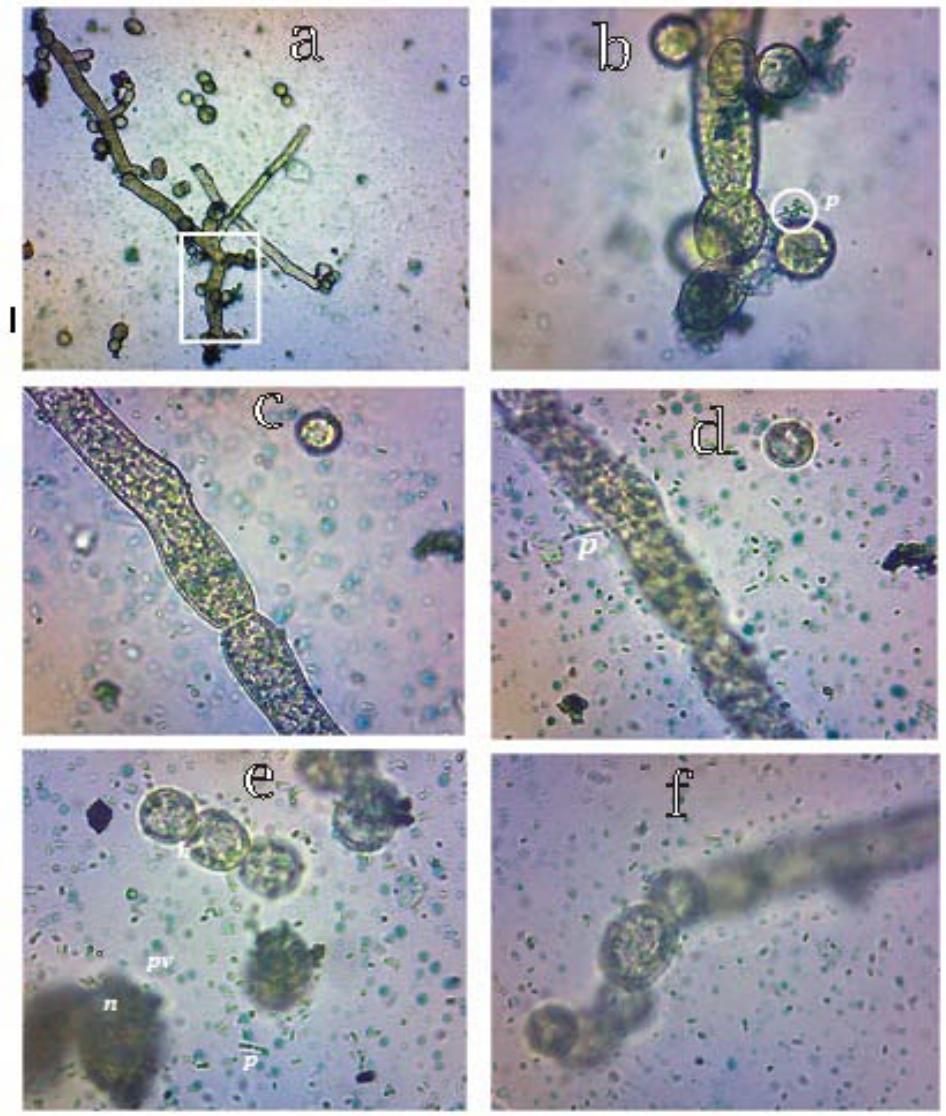

Figure 27 : Growth forms of *Mucor manihoti*s induced in peptone incorporated minimal medium after 48h of incubation at temp 28°C showing various types of conidia; **a**, thallic growth & holoblasstic conidia; **b**, boxed arthrosporal section in 'a'; observe the presence of clinging protoplasts, 'p'; **c**, septate thallic non-ramifying filament; **d**, a lower elevation of 'c' showing neoplastic units, rod shaped & binary protoplasts; **e**, holoblastic conidia 'h', cluster of neoplastic units 'n', protoplasts 'p' & prevegetative cells 'pv'; **f**, thalloarthric conidia formed by apical rounding up amidst neoplastic units & rod shaped protoplasts. Magnification: a, 400x; b-f, 1000x. *Except for neoplastic units, protoplasts & prevegetative cells cytoplasm of cellular structures appear granular*

7 a. Cytodifferentiation of Mucor species

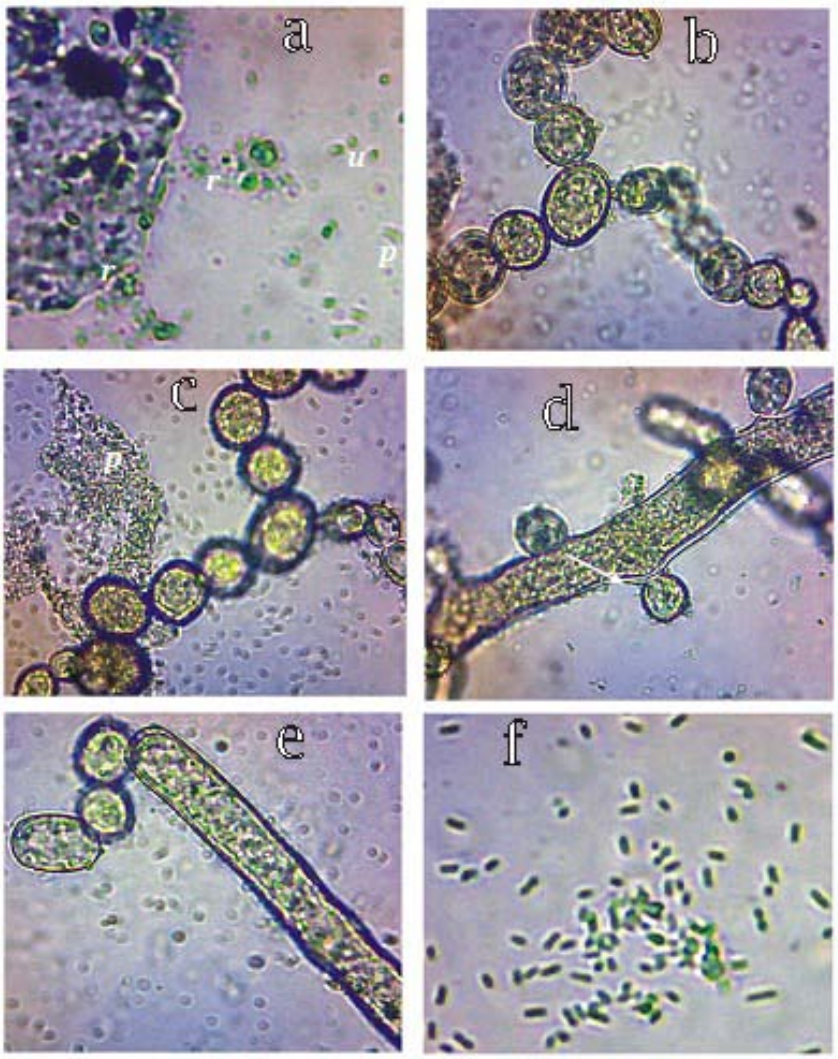

Figure 28 : Growth forms of *Mucor manihoti*s induced in peptone incorporated minimal medium after 72h of incubation at temp 28°C showing various types of conidia; a, clump of provencal neoplastic entities (n), primeval neoplastic units (r), ultimate neoplastic units (u) & protoplasts (p); b, holoblastic conidia with multilateral branching; c, lower elevation of 'b' showing numerous protoplasts (p); d, thallic growth with numerous laterally borne stumpy conidia; arrow indicate extruded protoplasts; e, determinate thallic growth with retrogressive arthrospore formation; f, protoplast (rod and binary). *In these thallic structures protoplasts were observed directly in the cellular compartments*. Magnification: a, 2500x; b-f. 1000x

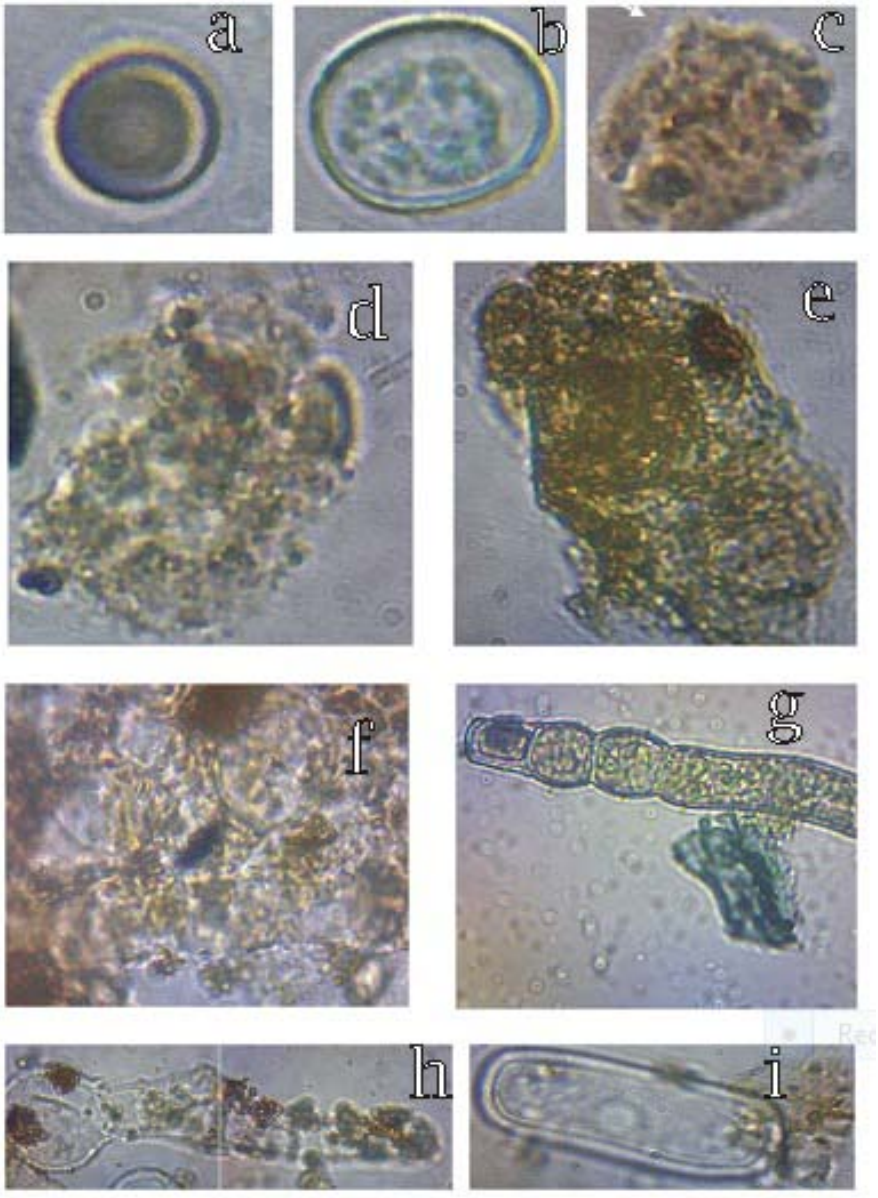

Figure 29 a-i : Growth forms of *Mucor manihotis* induced in peptone incorporated minimal medium after 96h of incubation at temp 28°C; **a**, growth sphere; **b**, growth sphere with differentiating cellular contents; **c**; neoplasm; **d-e,** imploding neoplasm**; f,** dispersing provencal entities; **g**, conidiogenesis after determinate thallic growth, **h,** holothallic conidium & **i**, thalloarthrospore, on rupture spewed thier contents. All magnification except g (1000x) at 2500x

7 b. Cytodifferentiation of Mucor species

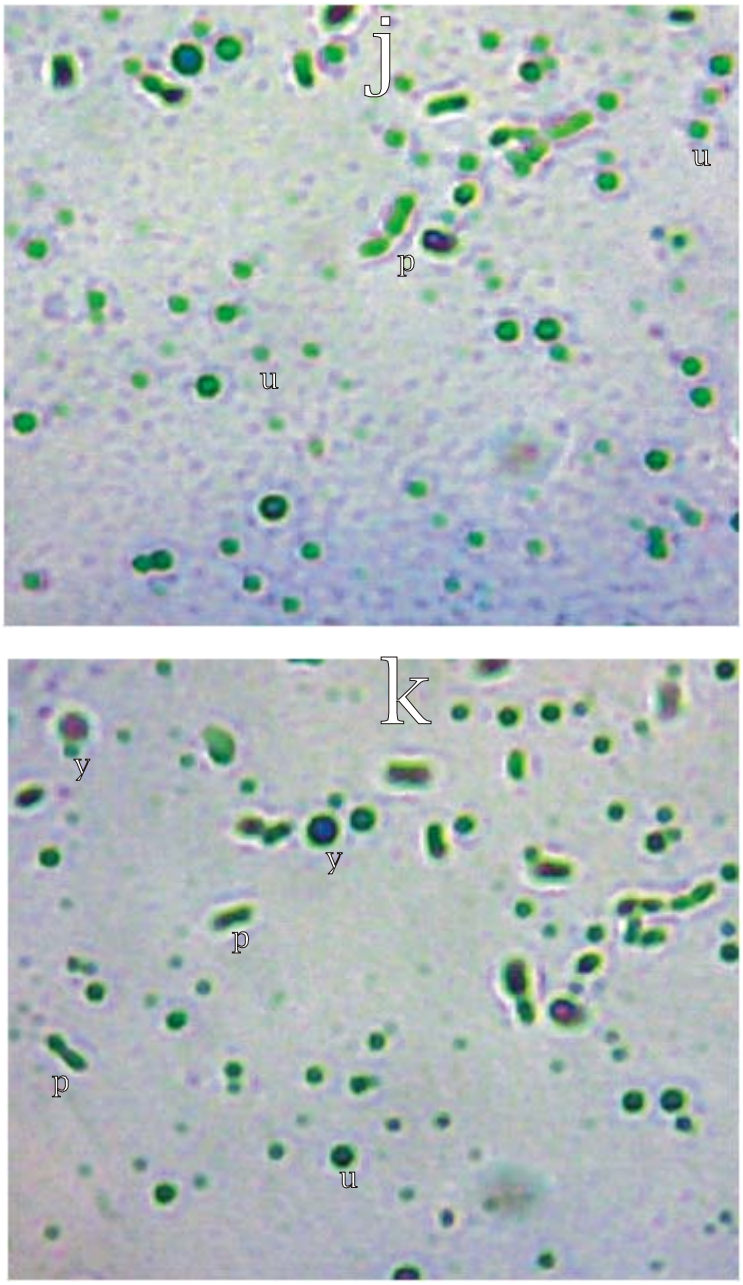

Figure 29 j k : Growth forms of *Mucor manihotis* induced in peptone incorporated minimal medium after 96h of incubation at temp 28°C showing numerous ultimate neoplastic units (u) and protoplasts (p) and yeast cells. Magnification, x1000

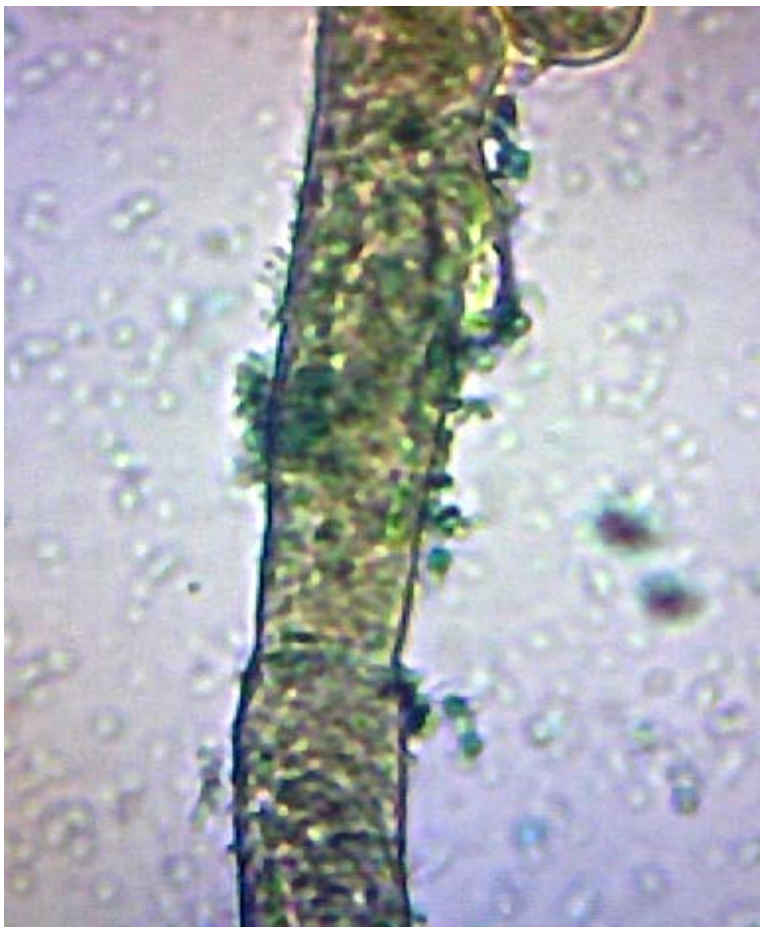

Figure 30 a : Growth forms of *Mucor manihoti*s induced in peptone incorporated minimal medium after 120h of incubation at temp 28°C showing a section of septate thallic growth with protoplasts clinging to the walls; background: unresolved protoplasts. Magnification: 1000x

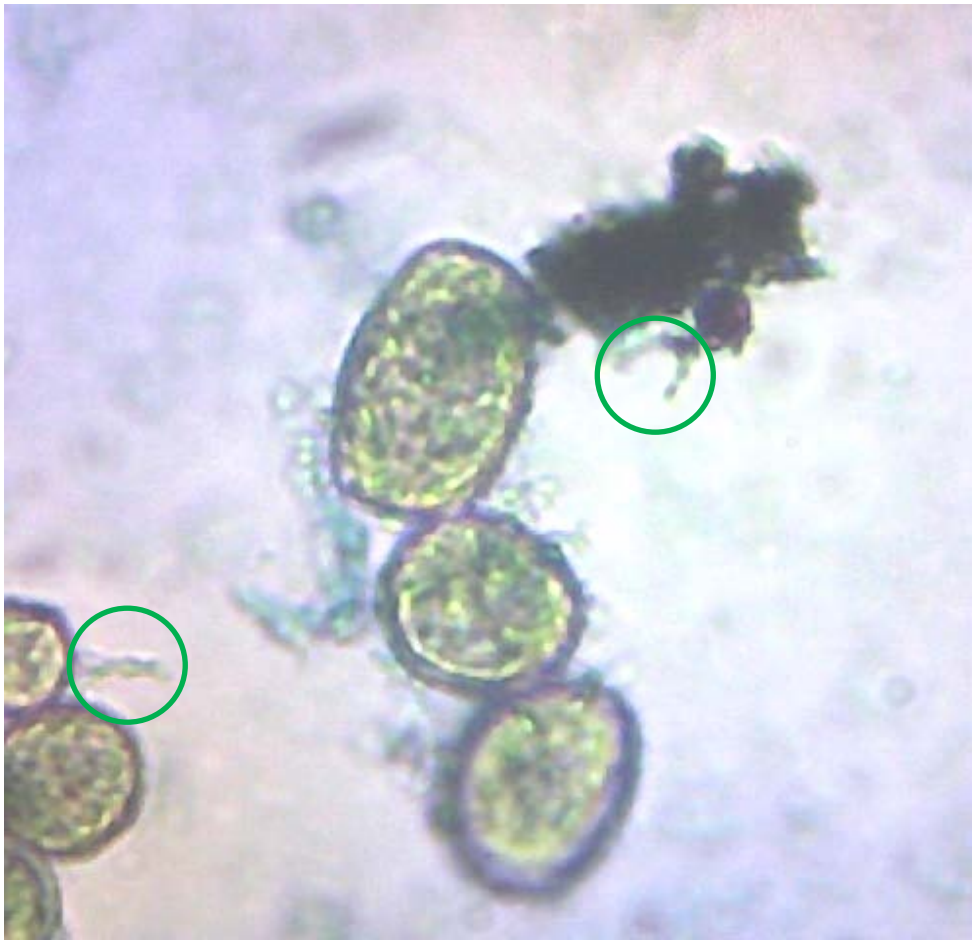

Figure 30 b : Growth forms of *Mucor manihoti*s induced in peptone incorporated minimal medium after 120h of incubation at temp 28°C showing protoplasts emerging form cluster of neoplastic units extruded from holoblastic conidium. Magnification: 1000x

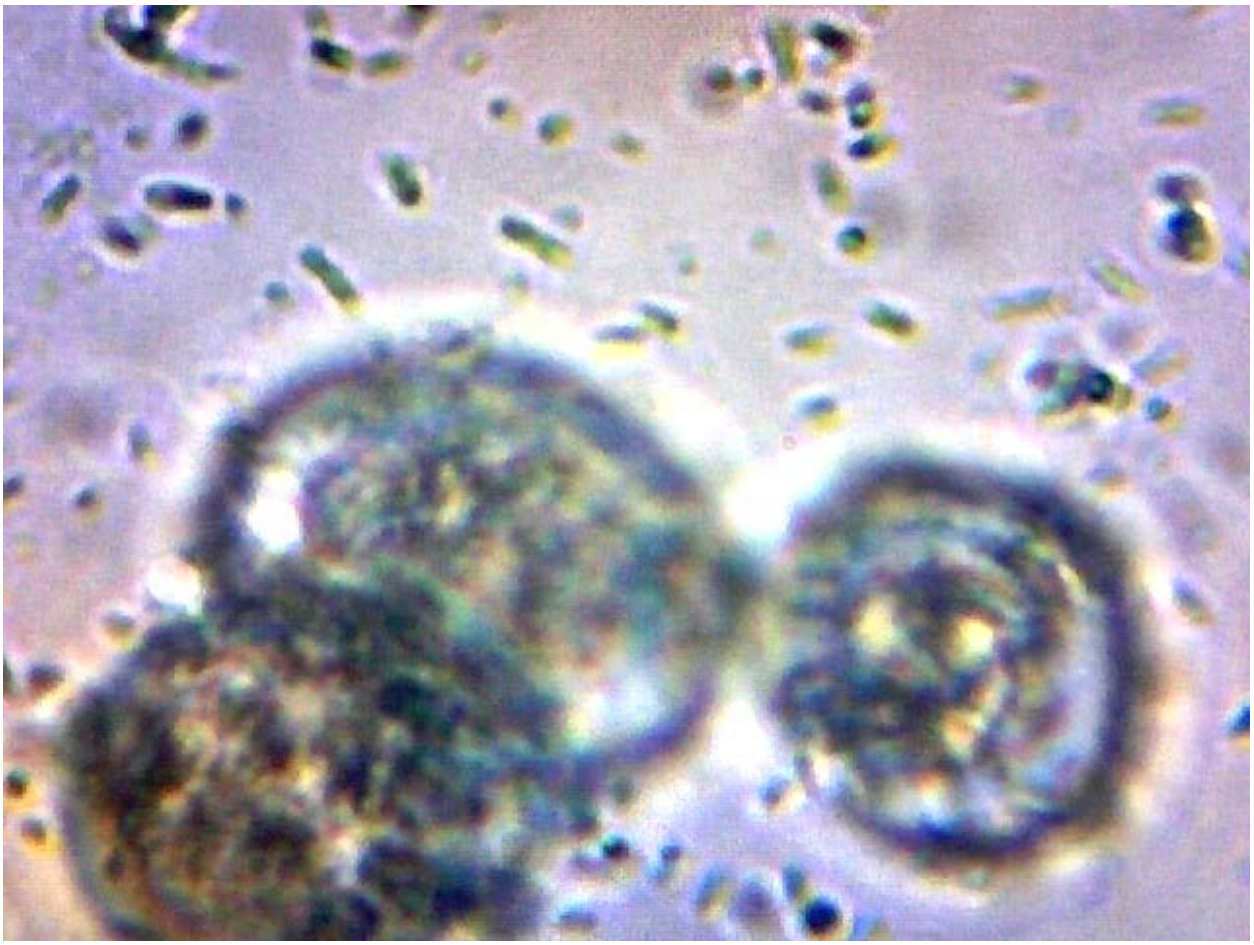

Figure 30 c : Growth forms of *Mucor manihoti*s induced in peptone incorporated minimal medium after 120h of incubation at temp 28°C showing protoplasts & holoblastic conidia (out of focus). Magnification: 2500x

8a.Cytodifferentiation of Mucor species

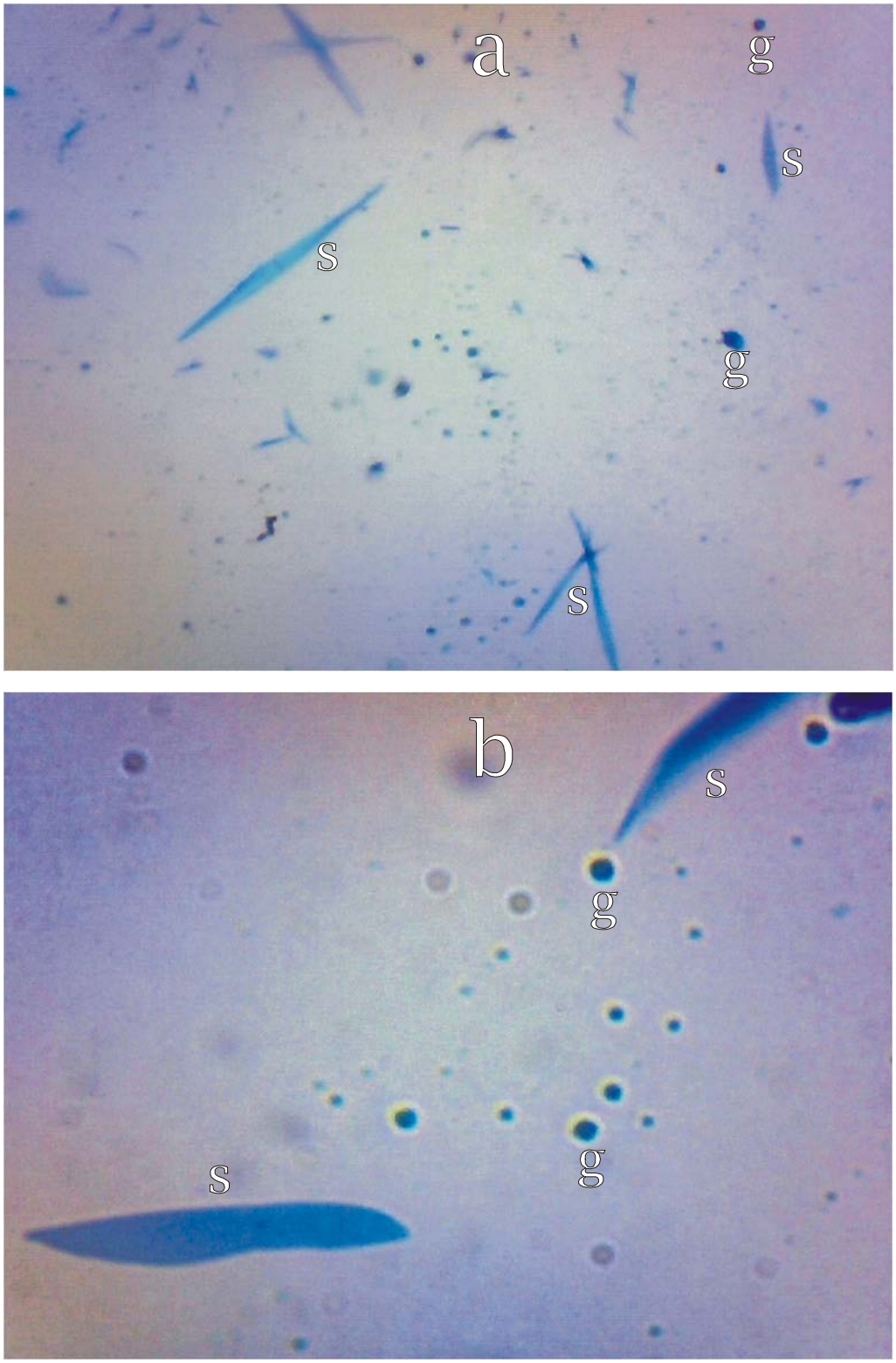

Figure 31 : Growth forms of *Mucor manihotis* induced in peptone incorporated minimal medium after 24h of incubation at temp 37°C showing globose- 'g' & spindle shaped 's' yeast cells. Magnification: a – 1000x; b - 2500x

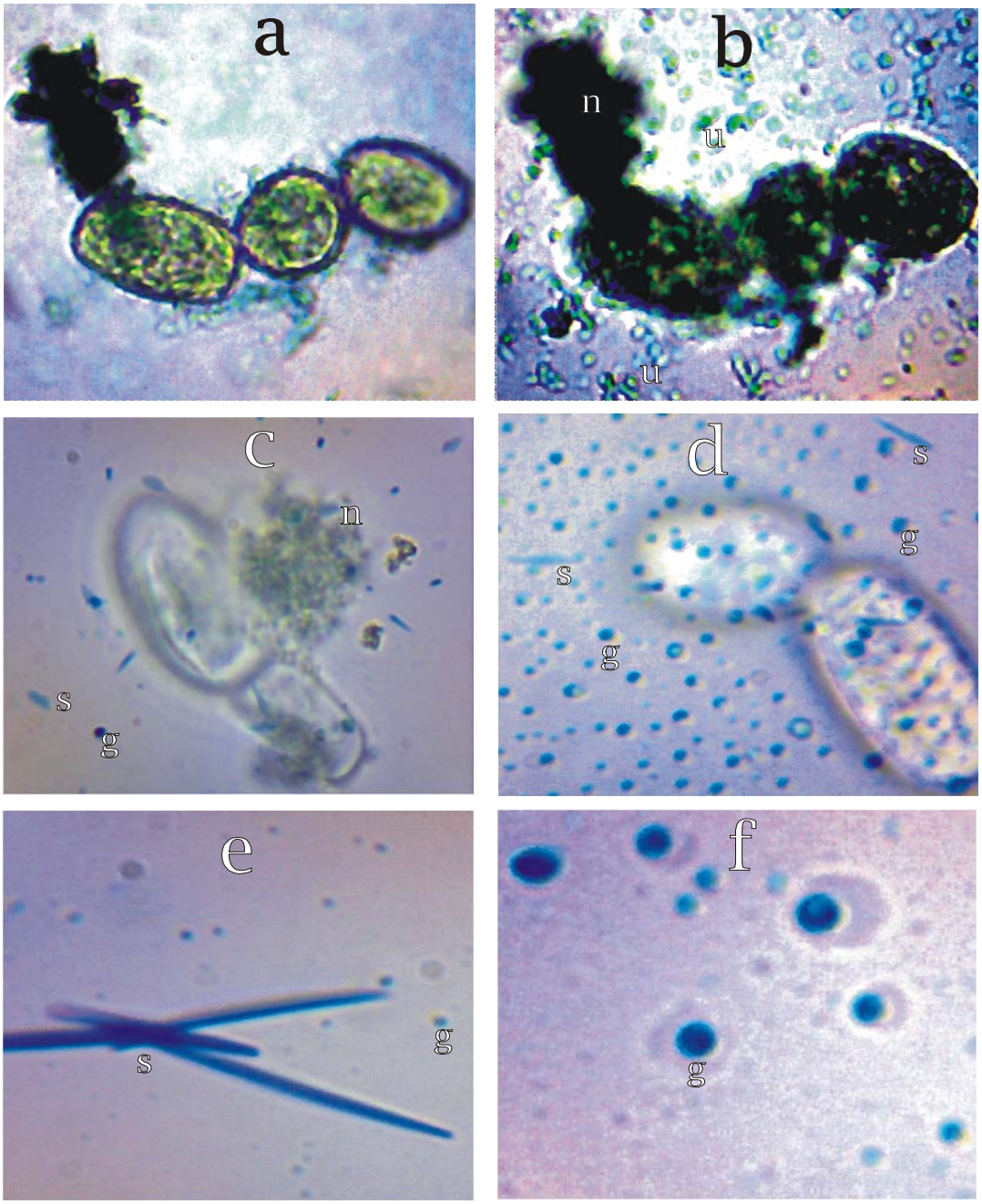

Figure 32 : Growth forms of *Mucor manihotis* induced in peptone incorporated minimal medium after 48h of incubation at temp 37°C; **a**, holoblastic conidia showing conspicuous cytoplasmic differentiation; **b**, another elevation of 'a' showing predominance of ultimate neoplastic units as primeval units 'n' are extruded by one conidium; **c**, this micrograph shows the co-occurrence of neoplastic units (n) conidia (h), globose (g) - and spindle (s) - shaped yeast cells on the same field; **d**, thalloarthric conidia are here out of focus, in the same field range with globose- & spindle yeasts; **e**, another field of the same slide showing elongated spindle shaped yeast cells, sizes of these cells varied greatly; **f**, globose yeast cells. Magnification: 2500x

8b.Cytodifferentiation of Mucor species

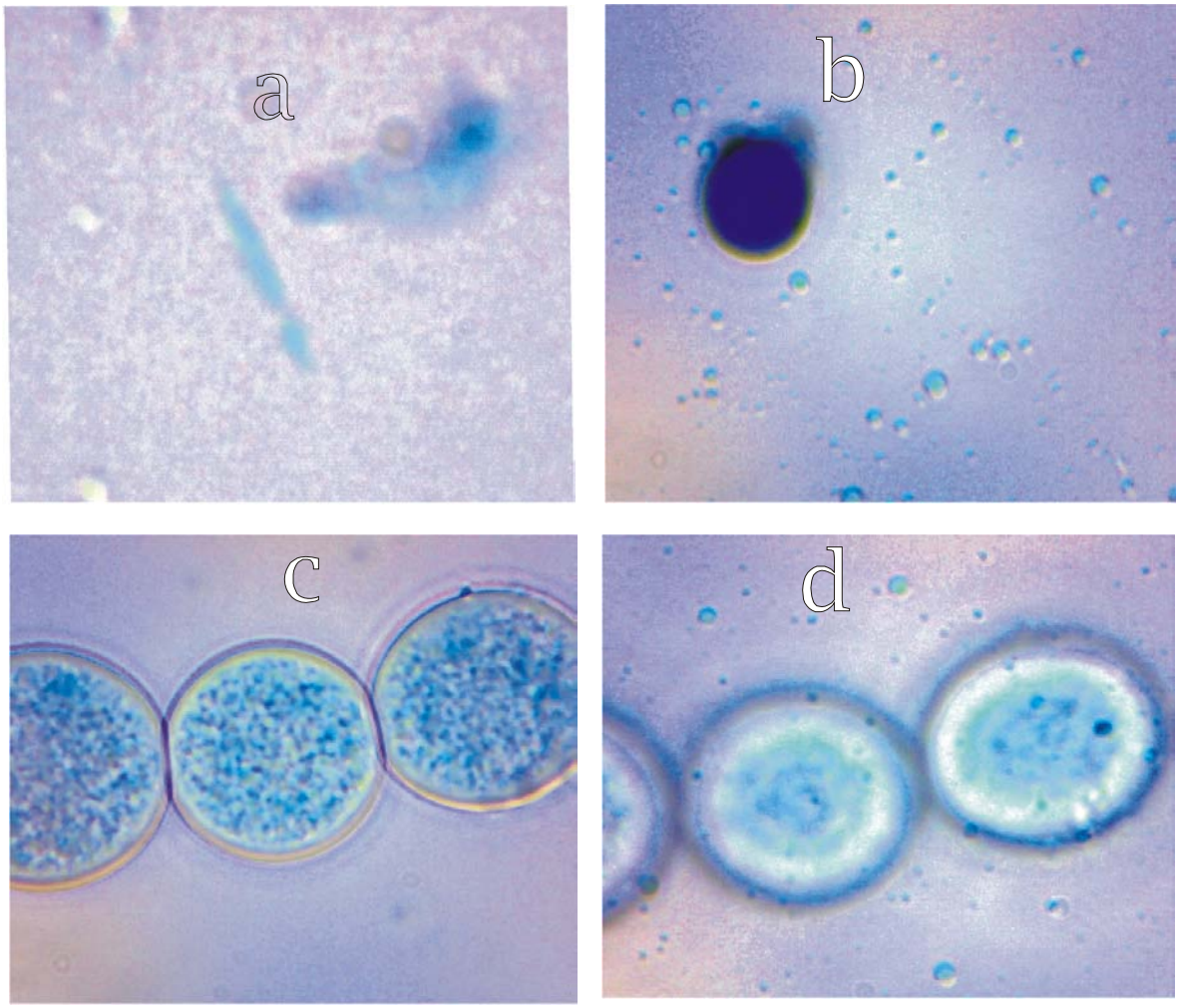

Figure 33 : Growth forms of *Mucor manihotis* induced in peptone incorporated minimal medium after 72h of incubation at temp 37°C showing **a**, spindle shaped yeast cell, **b**, globose yeast cell, **c**, holoblastic conidia with differentiated cytoplasmic content & **d**, another elevation of 'c' revealing globose neoplastic units. Magnification: 2500x

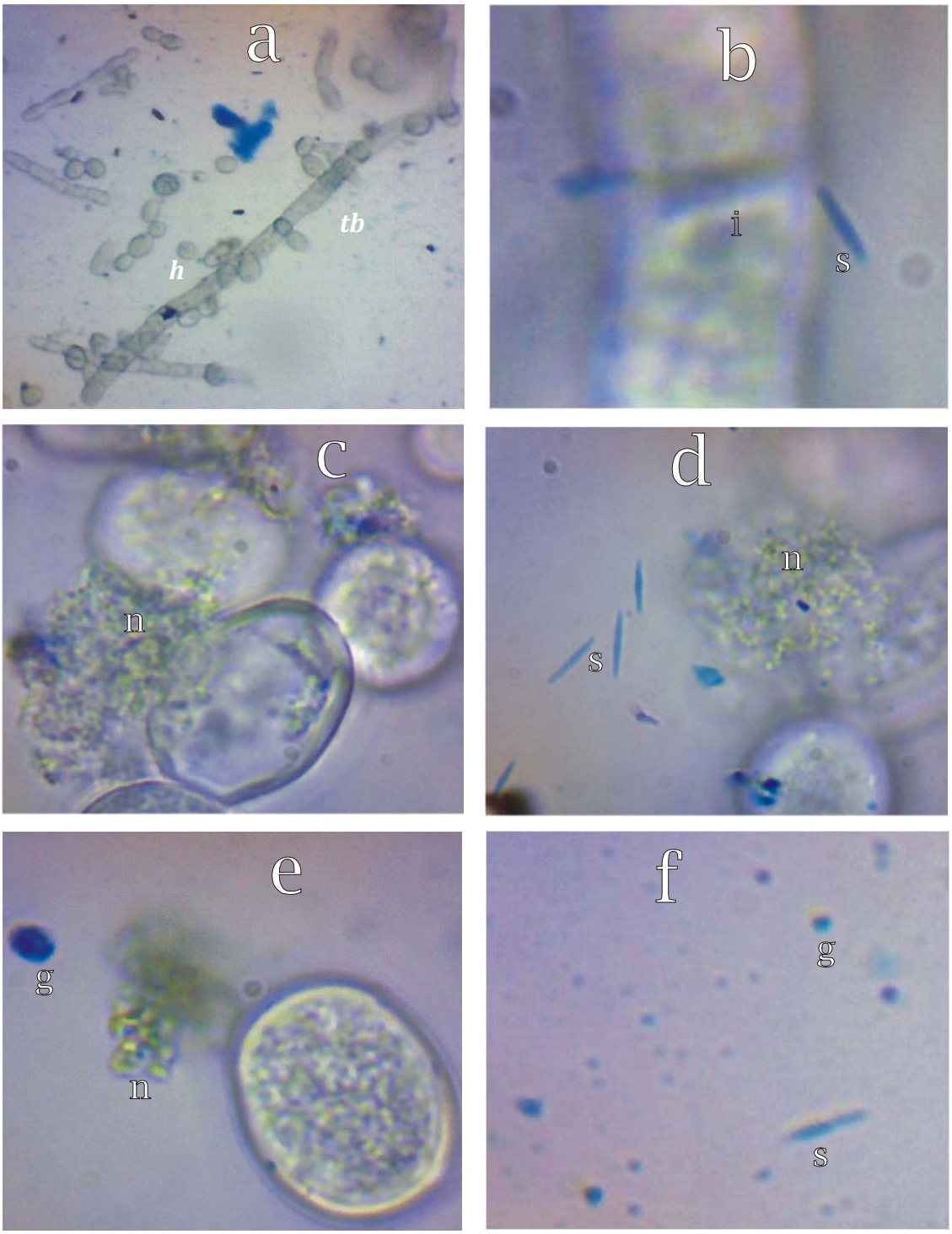

Figure 34 : Growth forms of *Mucor manihotis* induced in peptone incorporated minimal medium after 96h of incubation at temp 37°C showing **a**, thallic growth with blastospores 'tb' & holoblastic conidia 'h'; **b**, septate filament & spindle shaped yeast cell, 's'; **c**, conidial burst & release of neoplastic units 'n'; **d**, lower elevation of 'c' revealing spindle shaped cells; **e**, conidium, neoplastic units & globose yeast cell 'g'; **f**, globose & spindle shaped yeast cells; i=septum. Magnification: a - 400; b-f - 2500x

9a.Cytodifferentiation of Mucor species

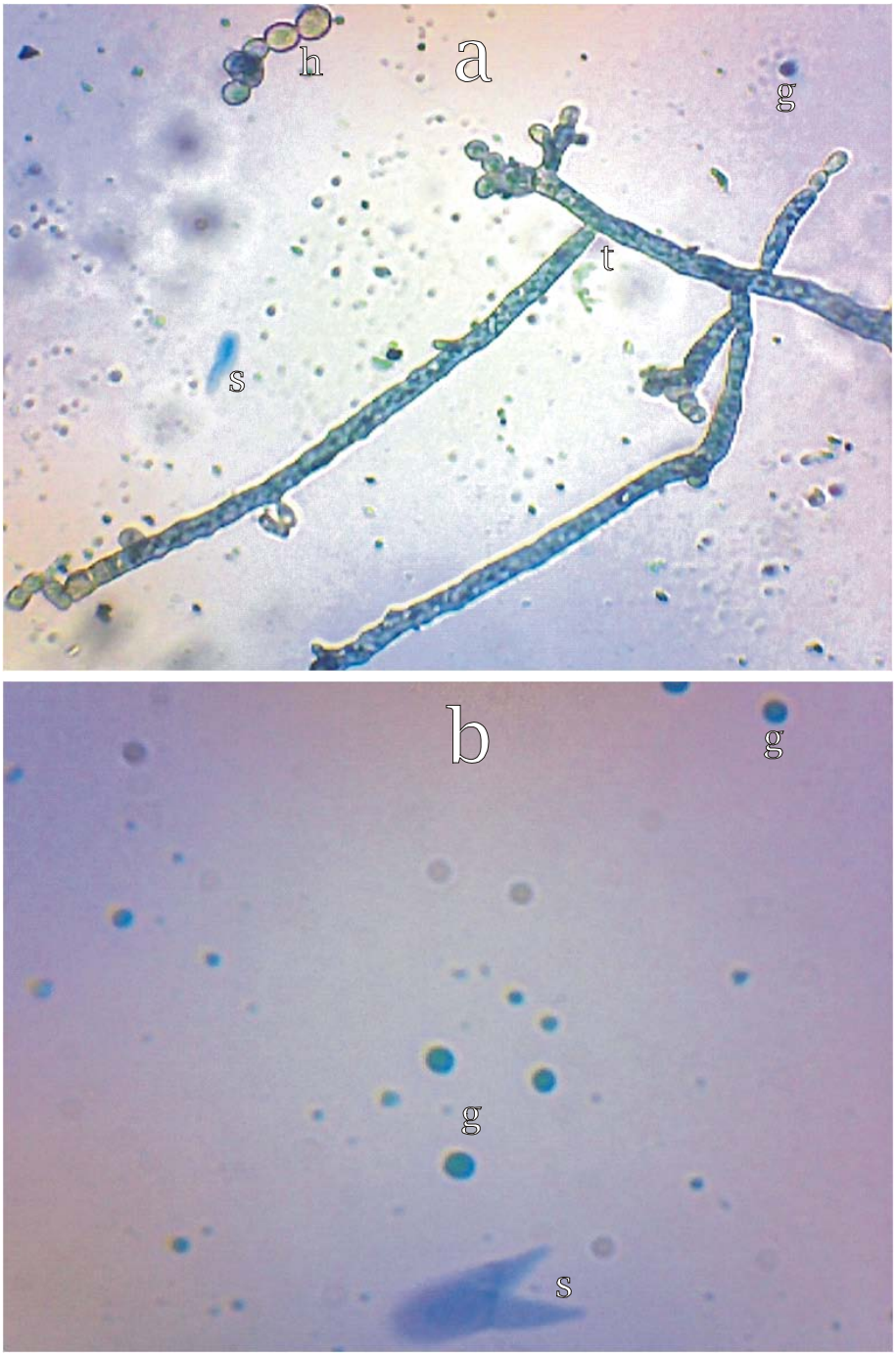

Figure 35 a b : Growth forms of *Mucor manihotis* induced in peptone incorporated minimal medium after 120h of incubation at temp 37°C showing in **a**, thallic growth 't', thalloarthrospores 'ta' formed after determinate thallic growth, in co-occurrence with holoblastic conidia 'h', globose yeast cells 'g' & spindle yeasts cells 's' (out of focus) and in **b**, globose yeast cells & spindle yeast cells (out of focus). Magnification: a - 400; b - 2500x

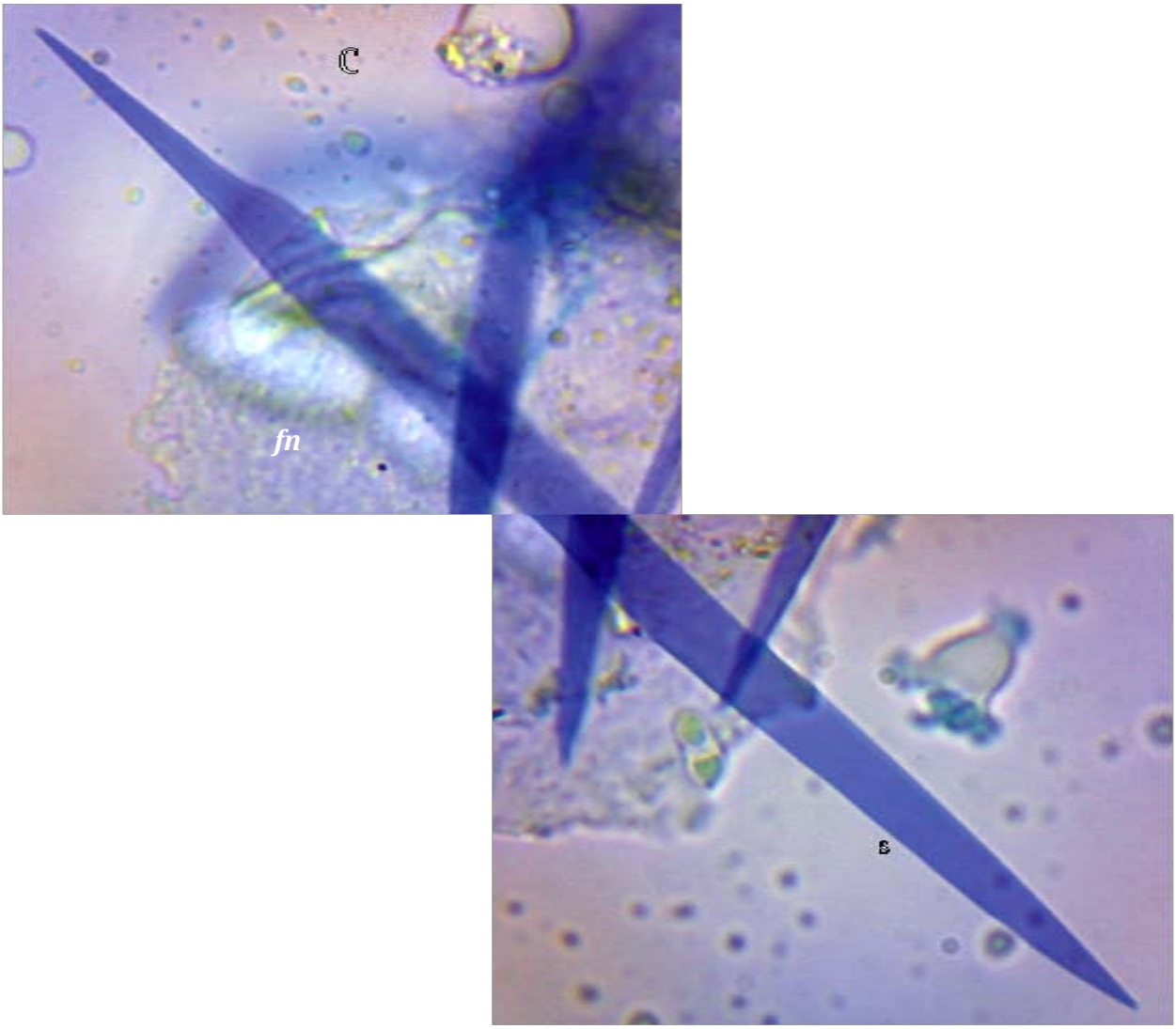

Figure 35 c : Growth forms of *Mucor manihotis* induced in peptone incorporated minimal medium after 120h of incubation at temp 37°C showing in c, spindle yeast cells. Observe fluid neoplasm 'fn' at the background. Magnification, 2500x

9b.Cytodifferentiation of Mucor species

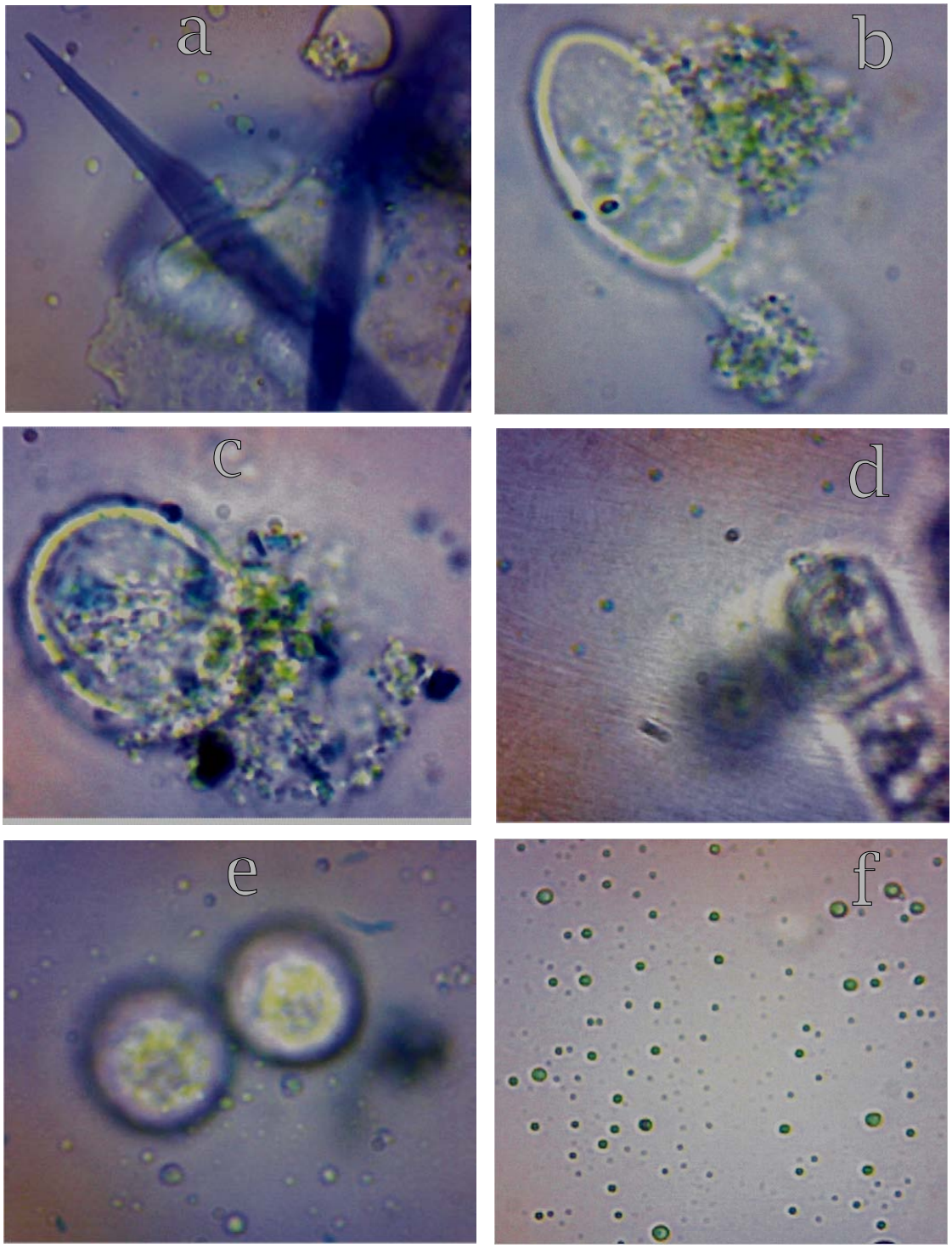

Figure 36 : Growth forms of *Mucor manihotis* induced in peptone incorporated minimal medium after 120h of incubation at temp 37°C & pH5.0; **a**, ultimate neoplastic units perhaps directly pinches off from the fluid neoplasm 'fn' at the background; **b,** numerous primeval entities released after arthrospore (out of focus) rupture; **c,** primeval entities released after conidium bursting; **d,** thalloarthric conidia (out of focus) & ultimate neosplastic units; **e,** ultimate neoplastic units & holoblastic conididia (out of focus); **f,** numerous ultimate neoplastic units. Magnification, 2500x

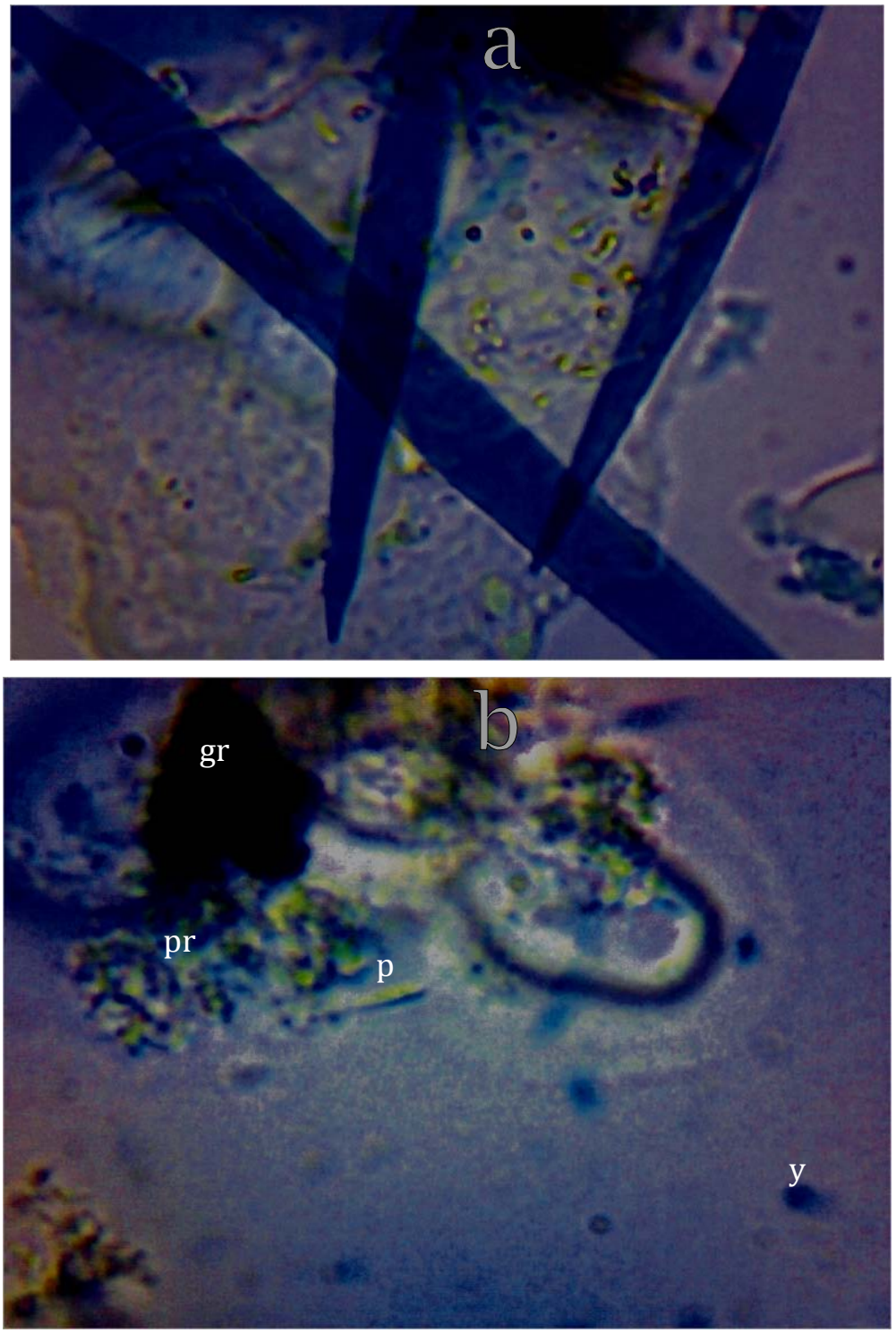

Figure 37 : Growth forms of *Mucor manihotis* induced in peptone incorporated minimal medium after 120h of incubation at temp 37°C & pH5.0 showing in **a,** apices of spindle shaped yeast cell against the background of plastic fluid neoplasm; **b,** cluster of granular units (gr), primeval entities (pr), protoplast (p), out-of-focus bursted arthrospore, & prevegetative yeast cell (bottom, dark blue). Magnification, 2500x

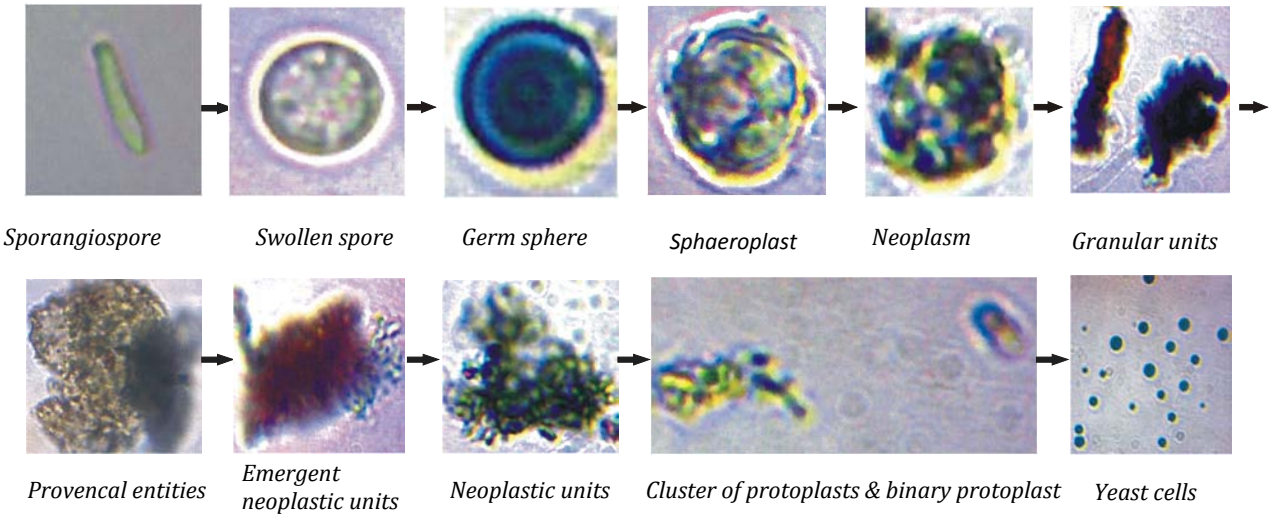

Figure 38 : Sequential induction of unicellular budding globose yeast cells of *Mucor manihotis* in Ammonium sulphate incorporated minimal medium after 3h of incubation at temp 28°C & pH5.0. Magnification, 2500x

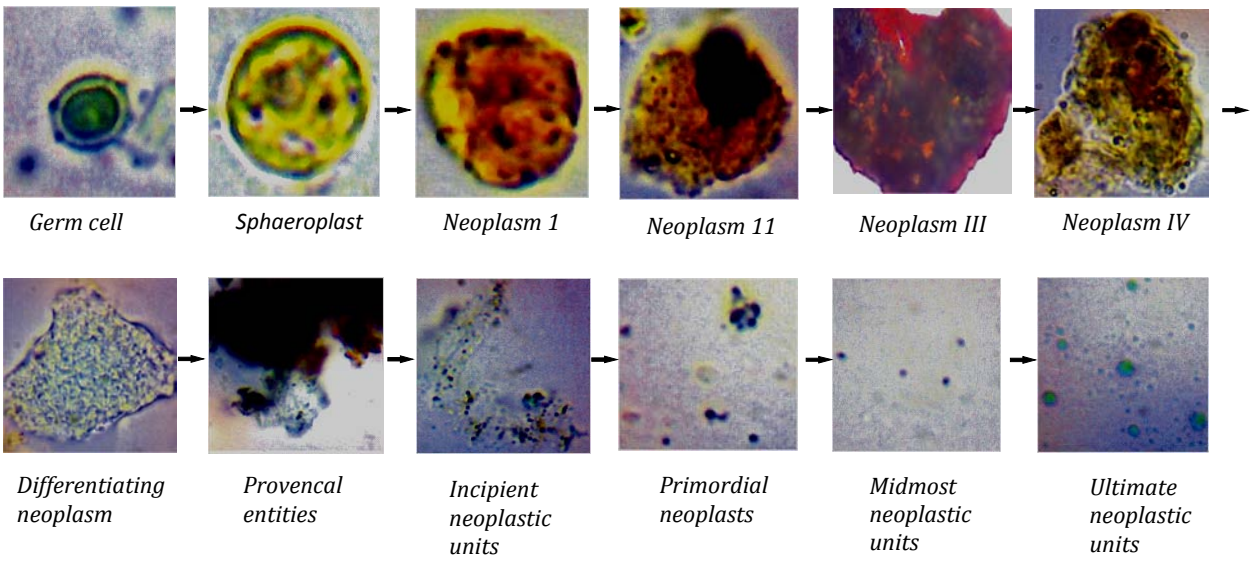

Figure 39 : Sequential induction of ultimate neoplastic units of Mucor manihotis in Ammonium sulphate incorporated minimal medium after 6h of incubation at temp 28°C & pH5.0. Magnification, 2500x

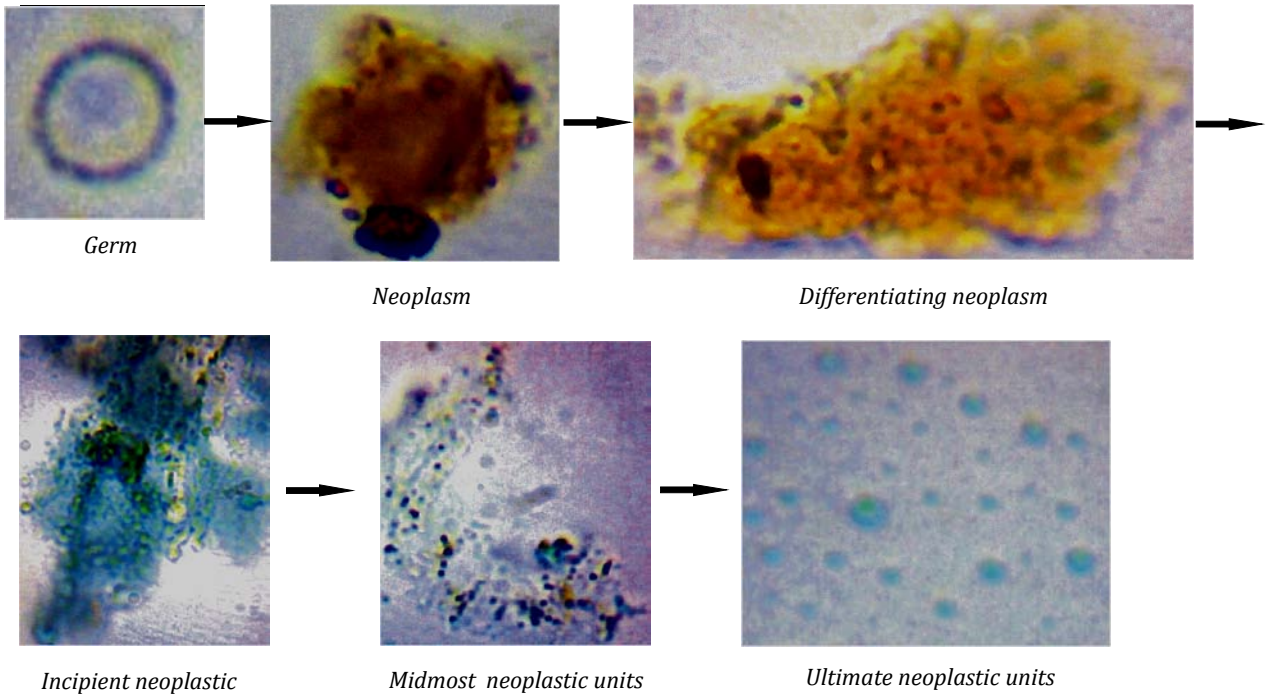

Figure 40 : Sequential induction of ultimate neoplastic units of Mucor manihotis in Ammonium sulphate incorporated minimal medium after 9h of incubation at temp 28°C & pH5.0. Magnification, 2500x

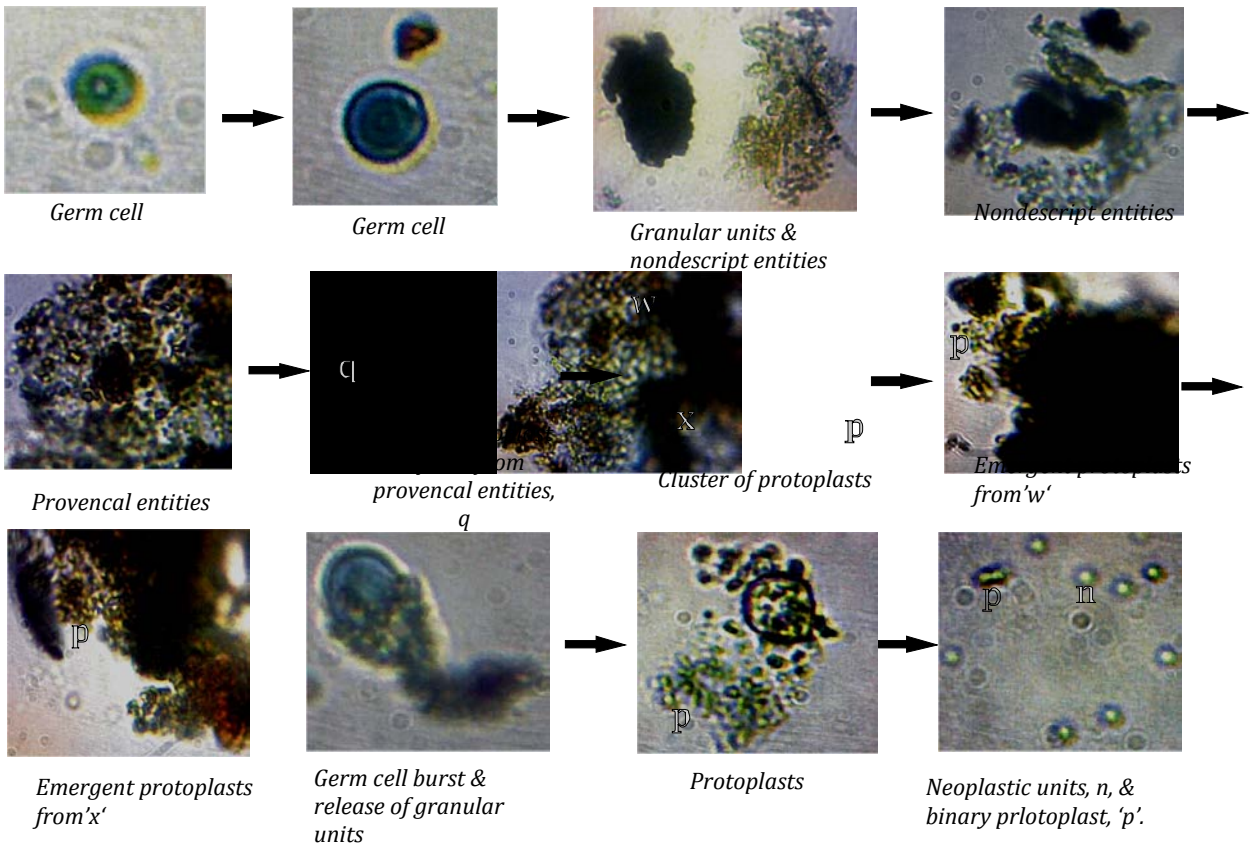

Figure 41 : Sequential induction of protoplasts of Mucor manihotis in Peptone incorporated minimal medium after 3h of incubation at temp 28°C & pH5.0. Magnification, 2500x. (Peptone enhancement of the generation of protoplasts: abridged transition from provencal entities to protoplasts)

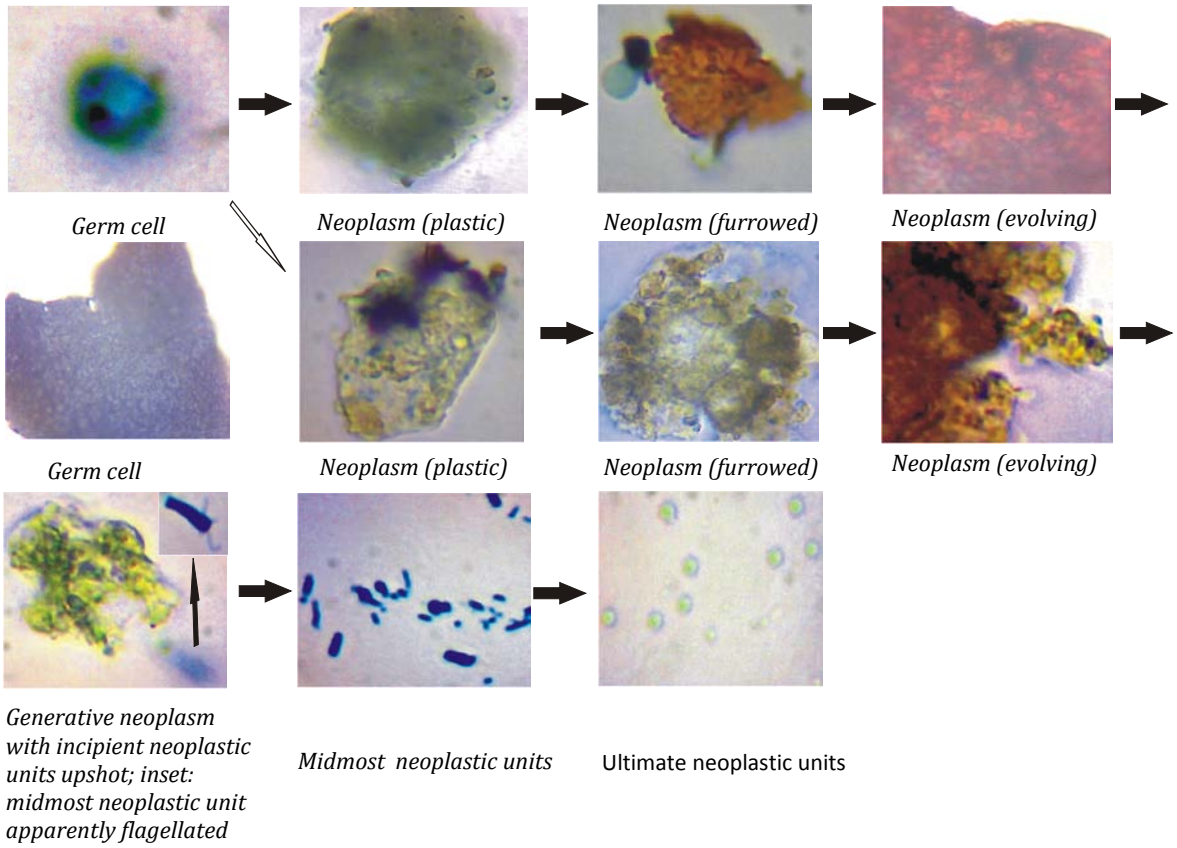

Figure 42 : Induction of neoplasm, nondescript & neoplastic units of *Mucor manihotis* in Peptone incorporated minimal medium after 6h of incubation at temp 28°C & pH5.0. Magnification, 2500x

11a.Cytodifferentiation of Mucor species

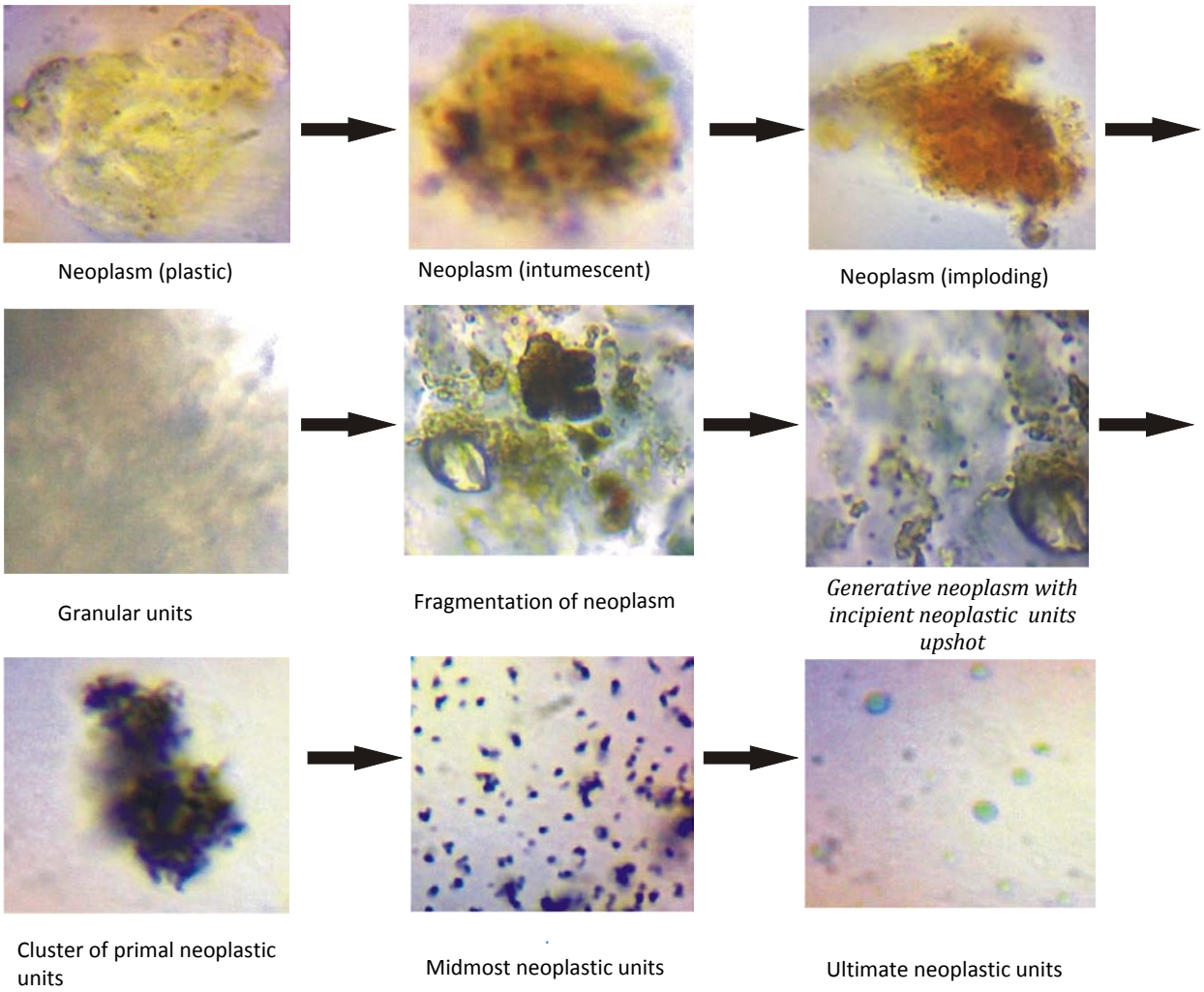

Figure 43 : Induction of neoplasm, nondescript & neoplastic units of *Mucor manihotis* in Peptone incorporated minimal medium after 9h of incubation at temp 28°C & pH5.0. Magnification, 2500x

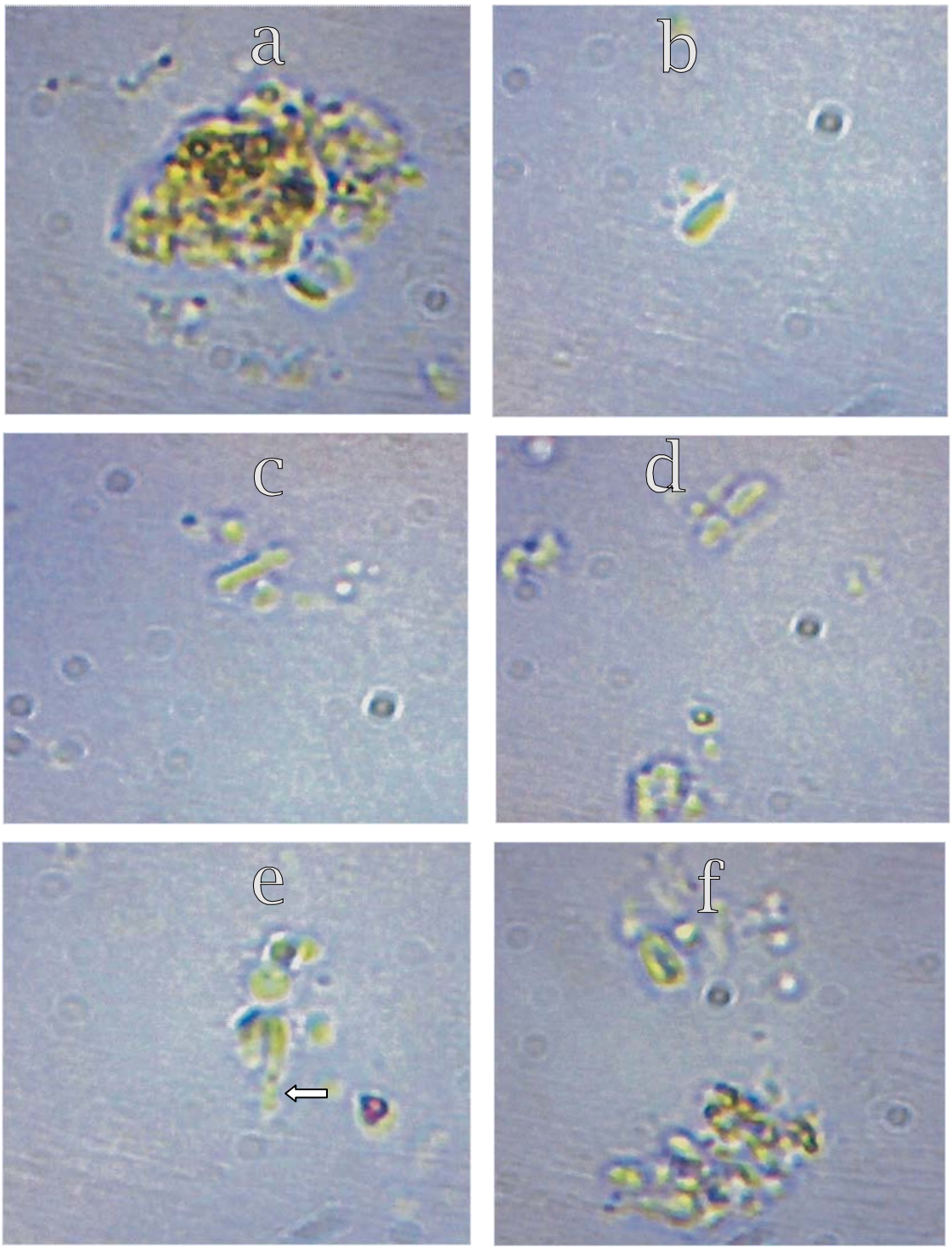

Figure 44 : Growth form of *Mucor manihotis* induced in Ammonium sulphate incorporated minimal medium after 96h of incubation at temp 37°C & pH5.0; **a**, cluster of neoplastic units & emergent protoplast; **b**, isolated protoplast; **c**, a doubling protoplast; **d**, binary protoplast; **e**, a protoplast (horizontal arrow) & a globose yeast cell with daughter bud (vertical arrow); **f**, cluster of protoplasts. Magnification: 2500x

11b.Cytodifferentiation of Mucor species

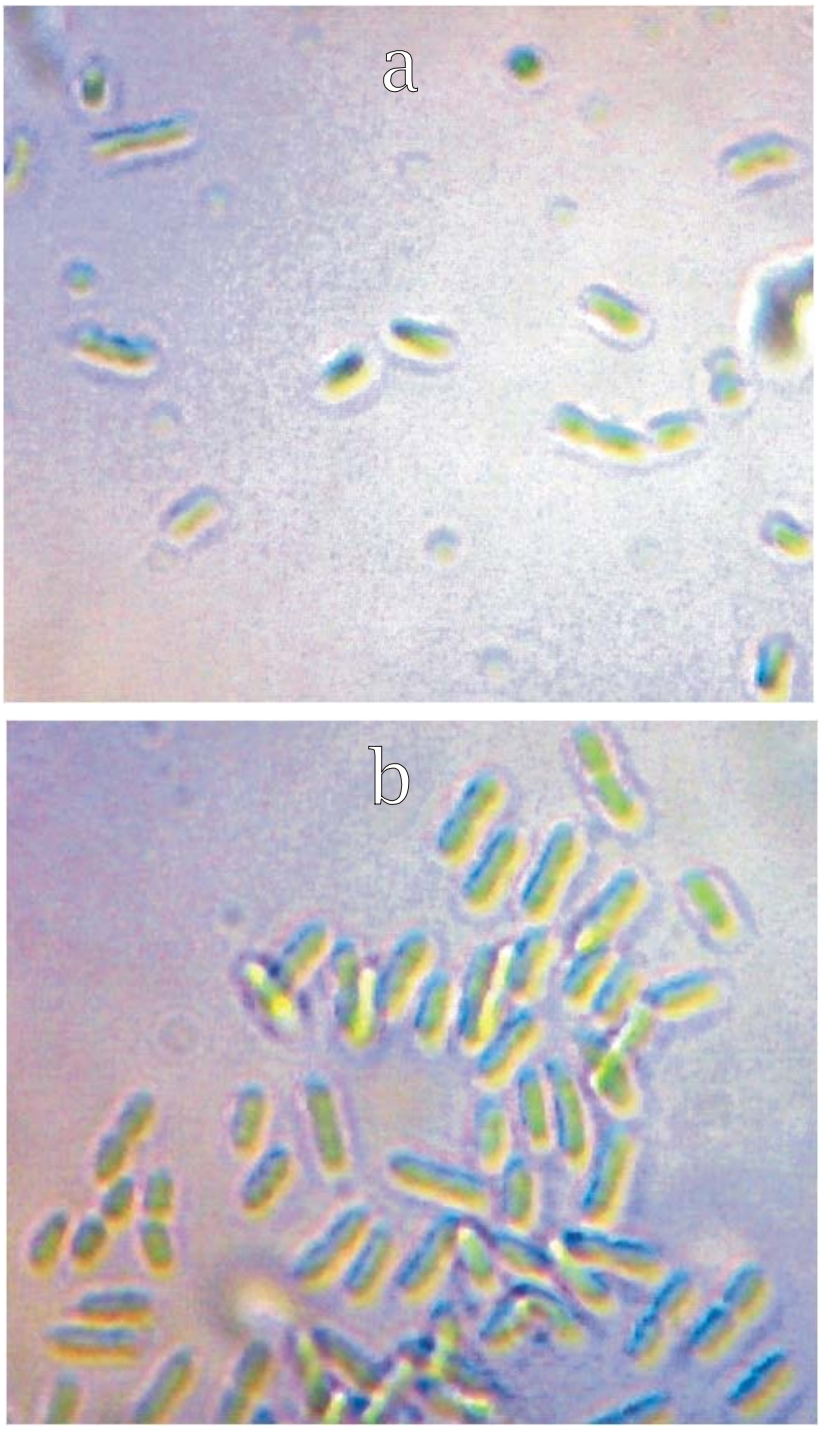

Figure 45 : Growth form of *Mucor manihotis* induced in Ammonium sulphate (a) - & peptone (b) - incorporated minimal media after 120h of incubation at temp 15°C & pH5.0; observe that the denticulate protoplasts in 'a' were less robust in comparison with those of 'b'. Magnification: 2500x

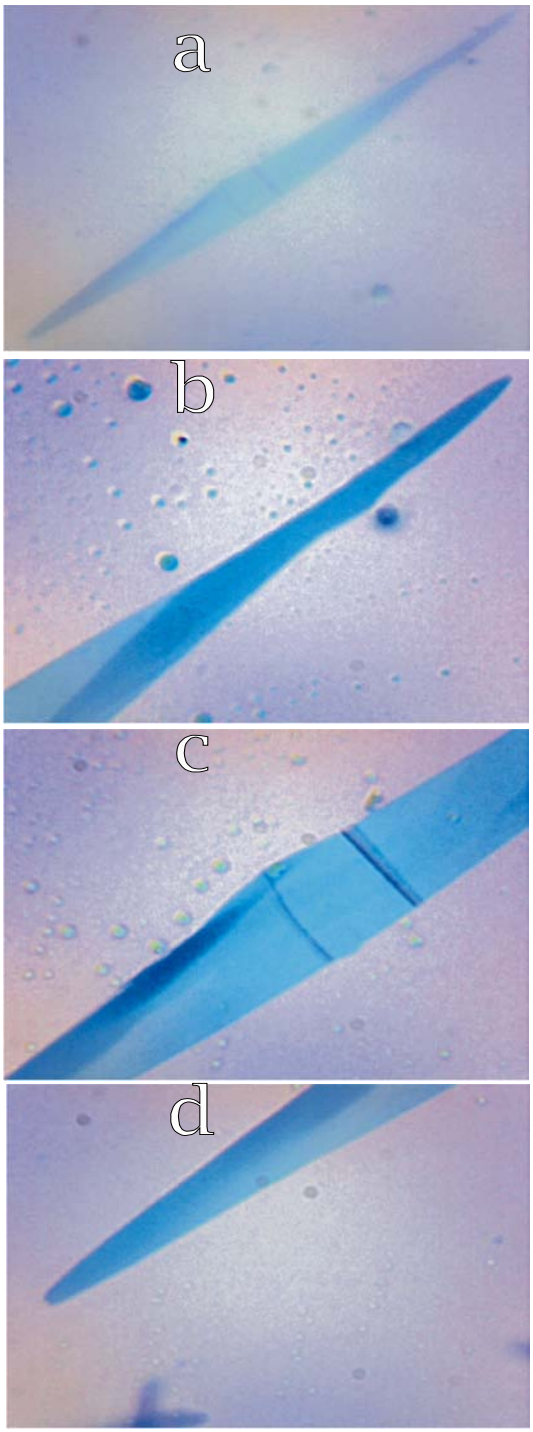

Figure 46 : Spindle shaped yeast form of *Mucor manihotis* induced in peptone incorporated minimal medium after 24h of incubation at temp 37°C & pH5.0; **a**, whole cell; **b**, upper segment; **c**, central segment with two cross walls; **d**, lower segment, observe the truncate tip. Note: the sorrounding cells are globose yeast cells. Magnification, 2500x

12a.Cytodifferentiation of Mucor species

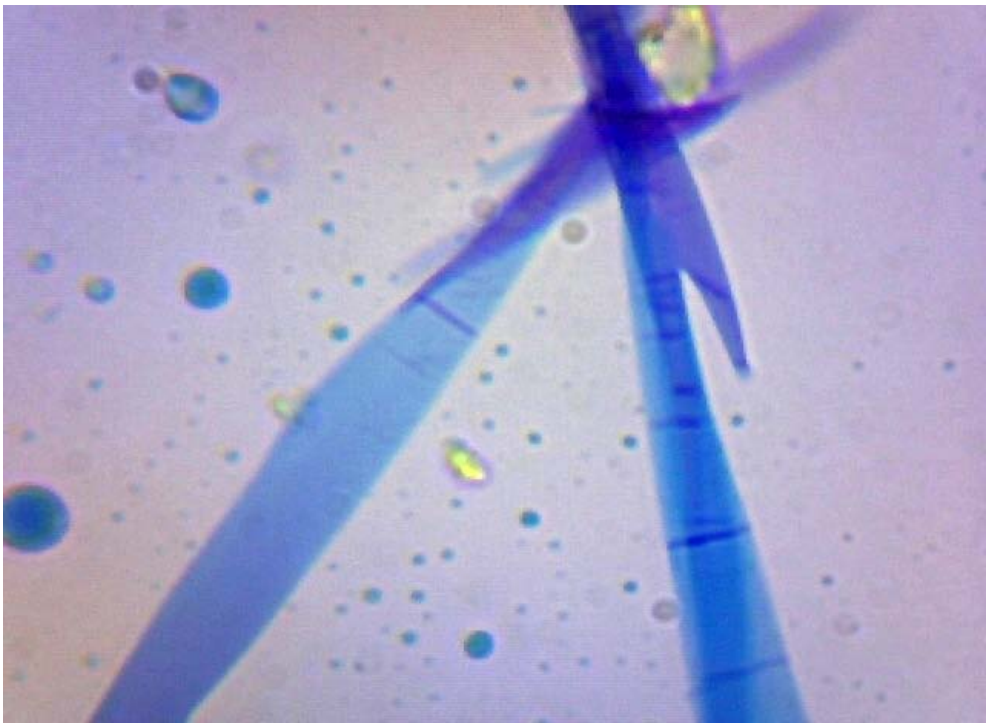

Figure 47 : Sections of Spindle shaped yeast & globose yeast form of *Mucor manihotis* induced in peptone incorporated minimal medium after 24h of incubation at temp 37°C & pH5.0; multiple cross walls are shown on the spindle yeasts; also observe the numerous prevegetative cells with various sizes, at the background. Magnification, 2500x

Figure 48 : Flask cultures of induced yeast cells of *Mucor manihotis* after two weeks of growth; *left*, Ammonium sulphate-incorporated culture; *right*, Peptone-incorporated culture. At termination of experiments conducted at pH 5.0 & temp. 15°, 28°, or 37°C, the flasks were left on the laboratory side bench at 28±1°C, ambient. The reversion to aerial mat that was re-induced in each of the flasks was observed following the *after-experiment* unperturbed period of incubation

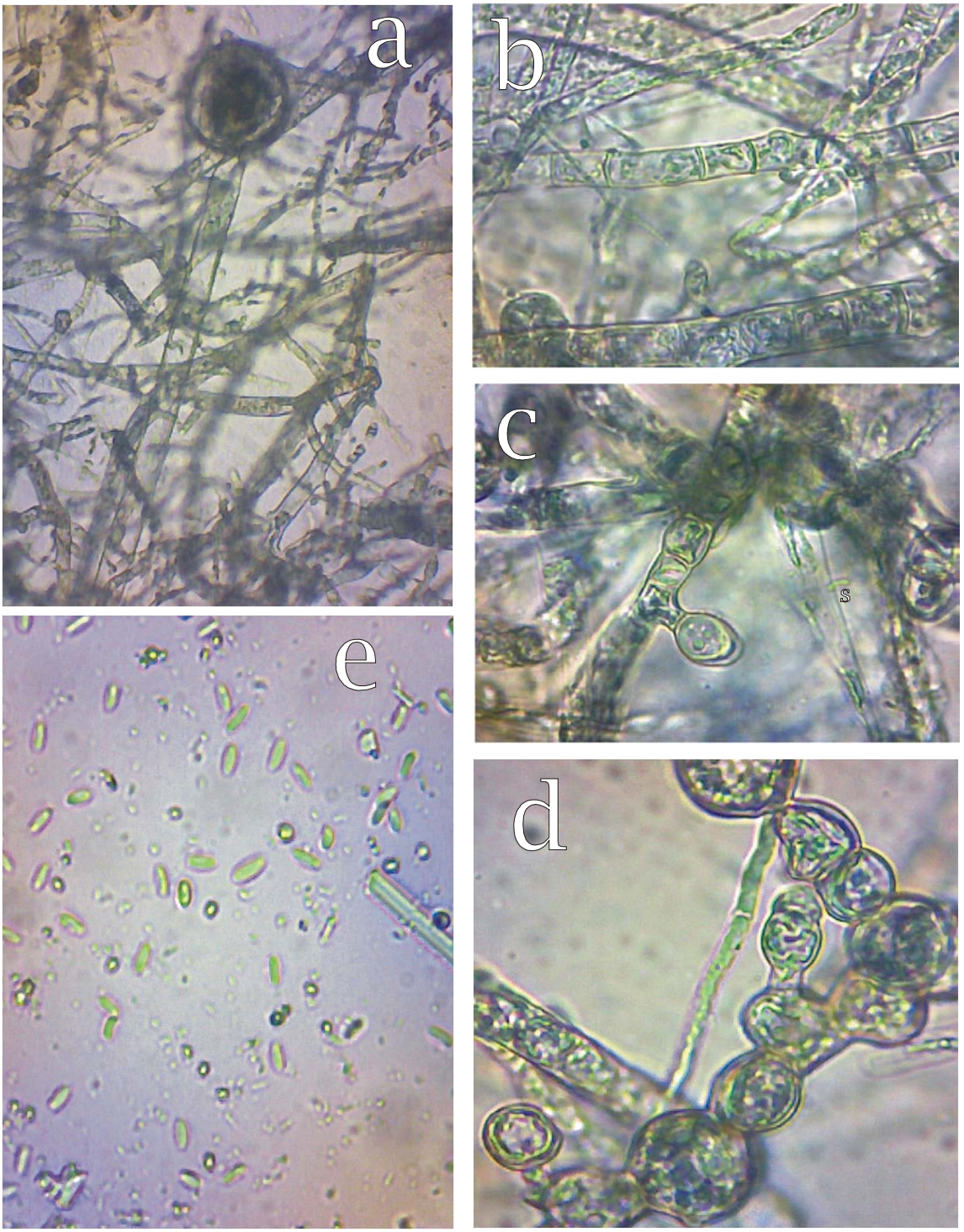

Figure 49 : Characteristics of *Mucor manihotis* after reversion to filamentous growth on termination of experiment; **a**, aerial mycelium showing sporangiophore & sporangium; **b-c**, broth surface mycelia showing septation of filaments; **d**, thallo-arthric growth; **e**, sporangiospores, s; a-d, $(NH_4)_2SO_4$-culture & d, Peptone- culture 9days after inoculation. Magnification, 1000x

Fig. 50 : Lateral morphogenetic transformation of *Mucor manihotis* in minimal medium as observed in this study

13.Cytodifferentiation of Mucor species

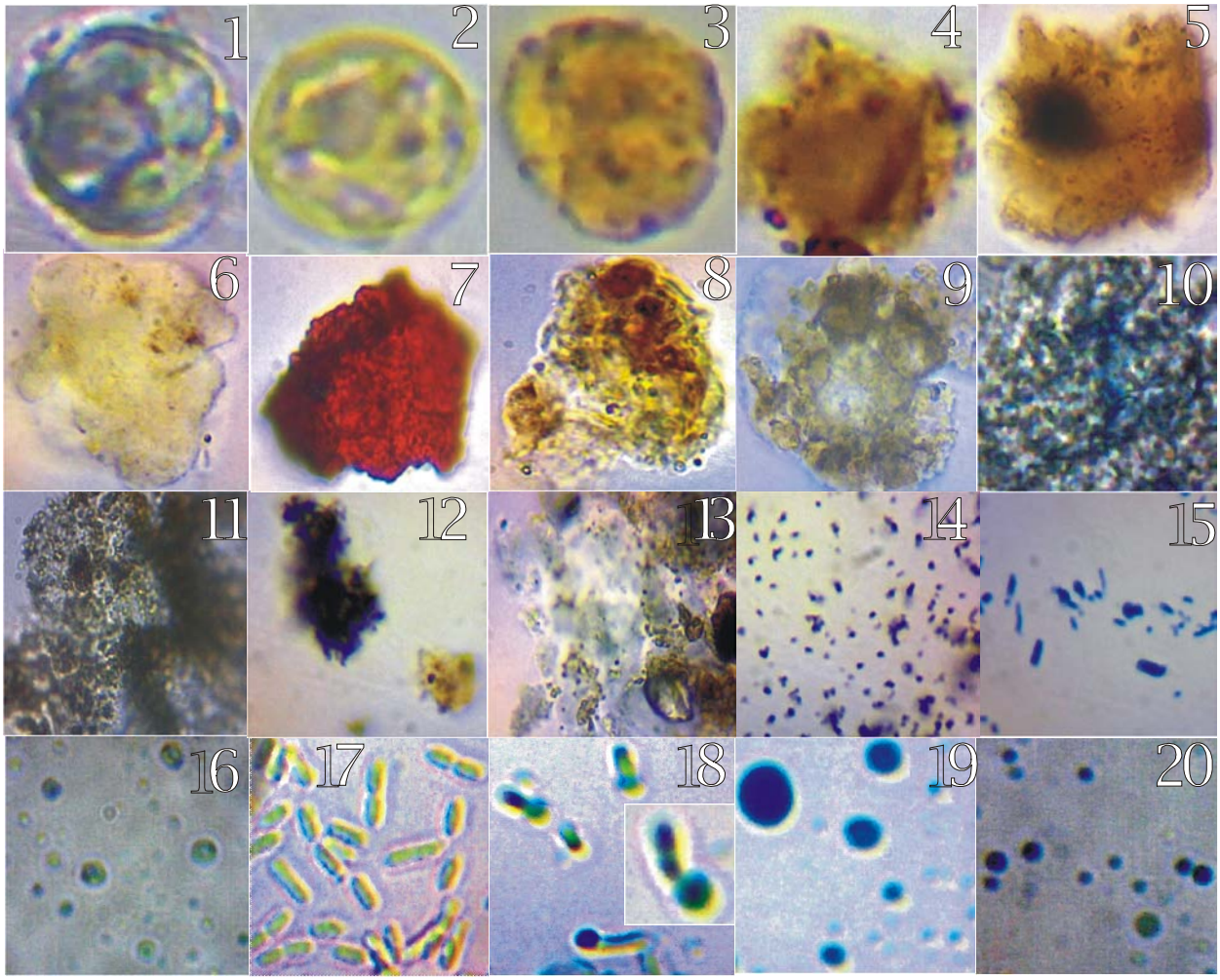

Figure 51 : Cytodifferentition of *Mucor manihotis* as observed in this study. 1, spheroplast; 2, cytoplasm; 3, neoplasm; 4-5, differentiating neoplasm; 6-9, imploding neoplasm; 10, provencal entities; 11, primeval units; 12-13, incipient neoplastic units; 14-15, midmost neoplastic units; 16, ultimate neoplastic units; 17, rod-shaped and binary protoplasts; 18, protoplast generation of nascent yeast initial (inset : optimum size nascent yeast initial); 19, prevegetative cell yeast cells; 20, polar budding yeast cells. Magnification, 2500x

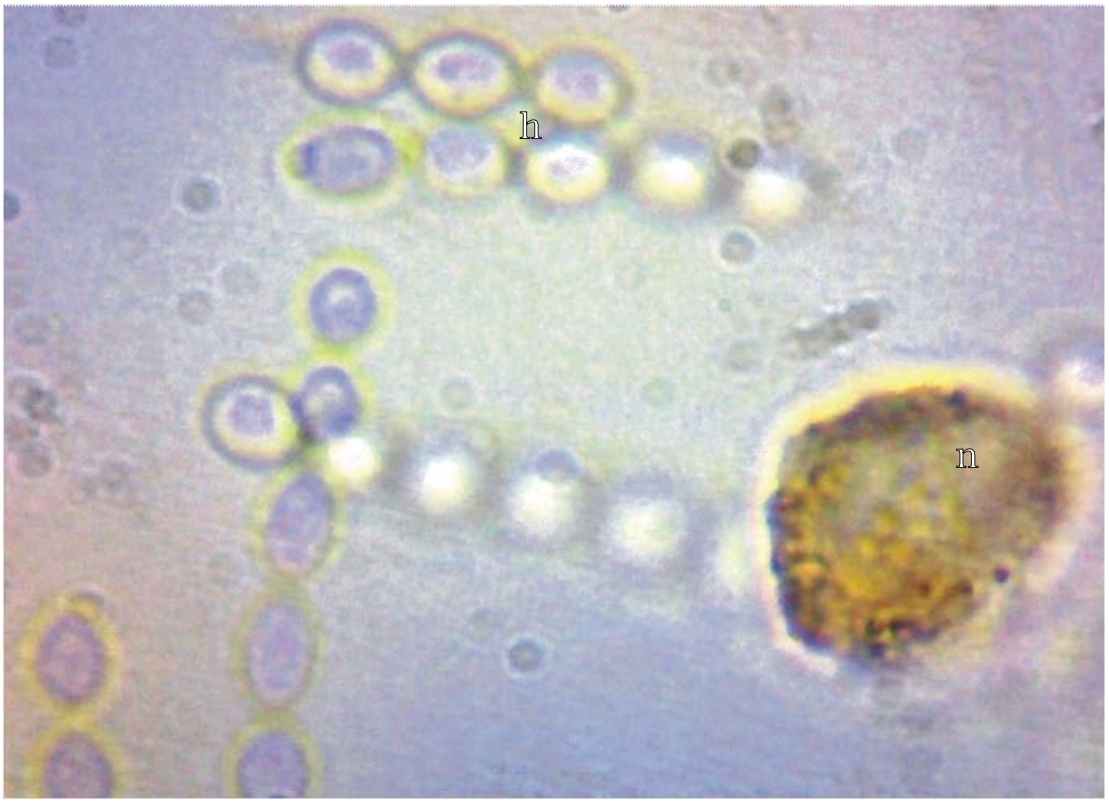

Figure 52 : Induction of neoplasm and young holoblastic conidia of *Mucor manihotis* in Peptone incorporated minimal medium after 6h of cultivation at temp 28°C & pH5.0. Magnification, 2500x. *As this study showed, two pathways exhibit here both leading to the same end-form: 1, when conidia mature cytoplasmic differentiation within each conidium occur but when conidial wall rupture primeval units expose in the medium & these subsequently differentiate to nascent yeasts; 2, when germ cell envelope lyse, priveval units expose in the medium & these subsequently differentiate to nascent yeasts*